Climate Change in Queensland under Enhanced Greenhouse Conditions

Final Report
2002 - 2003

CSIRO Atmospheric Research

Climate Change in Queensland under Enhanced Greenhouse Conditions

Annual Report, 2003

Report on research undertaken for

Queensland Departments of
State Development, Main Roads, Health, Transport, Treasury, Public Works, Primary Industries and Fisheries, Environmental Protection and Natural Resources and Mines, Queensland Rail, SunWater, CS Energy

by

Wenju Cai, Steve Crimp, Kathy McInnes, Barrie Hunt, Ramasamy Suppiah, Mark Collier, Tracy Elliott, Kevin Hennessy, Roger Jones, Cher Page, and Penny Whetton

CSIRO Atmospheric Research
PMB1
Aspendale Vic 3195

T: (03) 9239 4400
F: (03) 9239 4444
E: wenju.cai@csiro.au

Report C/0708 Commercial in confidence 20040501

Important Disclaimer

This report relates to climate change scenarios based on computer modelling. Models involve simplifications of the real physical processes that are not fully understood. Accordingly, no responsibility will be accepted by CSIRO or the QLD government for the accuracy of forecasts or predictions inferred from this report or for any person's interpretations, deductions, conclusions or actions in reliance on this report.

May 2003

Address for correspondence:

Dr Wenju Cai
CSIRO Atmospheric Research
PMB 1
Aspendale Victoria 3195
Telephone: (03) 9239 4419
Fax: (03) 9239 4444
E-mail: Wenju.Cai@csiro.au
World wide web: http://www.dar.csiro.au

For additional copies of this report, contact:

Steven Crimp
Queensland Department of Natural Resources,
80 Meiers Road,
Indooroopilly,
Queensland,
AUSTRALIA, 4068.
Telephone: (07) 3896 9795
Fax: (07) 3896 9843
World wide web: http://www.LongPaddock.qld.gov.au

ISBN 0 643 06649 7

Contents

Acknowledgments

This report summarizes work performed for the first year of a second four-year contract between the Queensland Government and CSIRO Atmospheric Research. The work was performed by CSIRO Atmospheric Research as part of its Earth System Modelling Program under the leadership of Brian Ryan with the support of Queensland Departments of State Development, Main Roads, Health, Transport, Energy, Treasury, Public Works, Primary Industries and Fisheries, Environmental Protection, Natural Resources and Mines, Queensland Rail, CS Energy and SunWater. Support has also been provided by the Commonwealth through the Australian Greenhouse Office, and by CSIRO. Ian Smith reviewed this report.

We acknowledge the support of Ken Brook and Greg McKeon from the Department of Natural Resources.

Climate model experiments reported here were performed by Martin Dix, Bob Cechet and Hal Gordon. The efforts of the CSIRO climate model developers have been indispensable.

Some observational data were supplied by the Bureau of Meteorology, Melbourne. Rainfall data were supplied by the CSIRO Climate Impacts Group and the Queensland Department of Natural Resource Sciences Group. Janice Bathols prepared many of the analyses contained in Section 4 which also incorporates inputs from Debbie Abbs.

The report was formatted by Julie Siedses.

List of Abbreviations and Acronyms

CC50 resolution	CSIRO's Conformal Cubic Atmospheric Model run at 50 km
CCCM	Canadian CentreClimate Model
DAR125 resolution	CSIRO's regional climate model "DARLAM" run at 125km
DKRZ	Deutsches Klimarechenzentrum (German High Performance Computing Centre for Climate- and Earth System Research)
ECHAM4/OPY3	European Climate Model
ENSO	El Niño Southern Oscillation
GCM	General Circulation Model – also Global Climate Model
GFDL	Geophysical Fluid Dynamics Laboratory
HadCM3	Hadley Centre Coupled Atmosphere/Ocean General Circulation Model
MSLP	Mean Sea Level Pressure
NCAR	National Center for Atmospheric Research
NCEP	National Center for Environment Prediction
OLR	Outgoing Radiation-Longwave
RCM	Regional Climate Model
SOI	Southern Oscillation Index
SRES	Special Research Emission Scenarios
SST	Sea Surface Temperature
TAR	Third Assessment Report (IPCC)

Summary for Policy Makers

This report summarises the work of the first year of a second four-year project examining the impacts of climate change in Queensland. The initial focus of the contract was to obtain a definitive sign and/or narrower range for projected rainfall changes over Queensland using both the improved CSIRO Mark 3 coupled climate model and the application of a multi-model consensus technique. A series of milestones were determined as part of the contract agreement. All aspects of the work associated with these milestones have been completed. The following provides a summary.

Task 1
The first task of this contract was to perform a detailed assessment of the climatology for Queensland as simulated by the Mark 3 coupled model for current conditions. This is a necessary task prior to making any assessment of climatic changes under enhanced greenhouse conditions. Comparisons were also made with the climatology from the earlier Mark 2 coupled model in order to illustrate improvements. We find that:

1. There has been a significant improvement in the ability of the model to simulate both realistic ENSO cycles and global ENSO-rainfall teleconnections. The Mark 3 climate model is one of the few in the world that can do so.

2. The model still suffers from a common "cold tongue" problem, in which the cold water zone of the central and eastern equatorial Pacific extends too far west. While this is problem common to almost all coupled models, deficiencies in several fields (e.g. rainfall and evaporation) appear to be associated with this bias. CSIRO is one of several leading modelling groups in the world that are endeavouring to overcome this problem.

3. The model is also able to simulate tropical cyclone events with realistic intensity, spatial scale and frequency. Until now, this has been extremely difficult.

4. The simulated hydrological fields from the model are generally improved but in some fields (soil moisture, runoff) improvements are difficult to demonstrate. This is believed to be due to the fact that the resolution is still unable to resolve the appropriate spatial scales.

Task 2
The second major task was to analyse projected climate change to 2100 AD and beyond from a transient CO_2 simulation that included other forcings such as aerosols. The CO_2 forcing is based on the A2 projection of the Special Research Emission Scenarios (SRES) and follows the observed evolution from 1870 to 2000, then follows the projected CO_2 levels of the A2 scenario from 2001-2100. By 2100, the equivalent CO_2 reaches a level that is more than three times the level of 1870 (concentration ppm). Thereafter, both the CO_2 and aerosol levels are held constant and the model integrated for another 150 years. This simulation was then contrasted with a control simulation, in which the CO_2 and aerosols were kept at 1870 levels. The focus of the

analysis has been the response of hydrological processes at regional scales, an assessment of the influence of multi-decadal variability, and the response of simulated ENSO events. We find that:

1. The model produces distinctively different surface temperature responses in different catchment areas, with a small warming rate in coastal areas increasing toward inland regions.

2. From early in the 21st century, the model produces a decreasing rainfall trend in all catchment areas (in the range of 5-20% by 2100 for summer season). This is particularly clear after interannual signals are removed. The decrease in rainfall is associated with the development of an El Nino-like warming pattern in the equatorial Pacific Ocean. This result is consistent with those previously found in an ensemble of results from the previous Mark 2 model.

3. Alongside the rainfall decrease, actual evaporation, soil moisture and runoff all exhibit decreasing trends. It is important to differentiate potential and actual evaporation. Potential evaporation increases with temperature at a rate of between 2-8% per degree warming in global mean temperature.

4. The results suggest a tendency for a more variable climate, with more extreme flood and drought events, and hence stronger variations in soil moisture and runoff. They also imply that the impacts of drought events will be more severe, being exacerbated by the increased temperature and evaporation.

5. During summer, the impact of decreased rainfall on soil moisture is disproportionately large compared to winter since temperature represents the major driver of soil moisture retention.

6. Referenced to the present day (control) climate, there is a tendency for slightly increased amplitude of ENSO events.

Task 3

The third major task was to investigate a range of possible climate change outcomes by pooling together the results from the CSIRO model with those of its global peers. The focus was to be on the results for rainfall and other hydrological processes. We find that:

1. From a total of 12 sets of model results, 7 show a decrease in annual mean rainfall. The remainder shows either no change or else a small increase. Eliminating those models which are unable to produce a reasonable seasonal cycle of rainfall over Queensland yields 7 out of 10 showing a decrease.

2. Of the 9 models that provided results, annual mean potential evaporation increases. The increase for the Queensland region is in the range of 2-8% per degree warming in global mean temperature.

3. As a consequence of increased potential evaporation/decreased rainfall, the water balance deficit increases in all 9 models.

Task 4

The fourth major task was to analyse the results from an ensemble of climate change simulations using the same model. The aim here is to better identify the climate change signal above the climatic "noise" or "natural" climate variability. Computational demands made this impractical with the Mark 3 coupled model but achievable using the coarser resolution Mark 2 model. This model was forced by a range of SRES emission scenarios, for a total of 12 experiments. In addition, the Mark 3 *atmosphere-only* model was used to generate an ensemble of 10 sets of results based on forcing by observed sea surface temperatures over the past century. We find that:

1. The ensemble mean result of the 12 SRES experiments shows a decrease in annual mean rainfall, although the trend is weak when compared with the amplitude of interannual and inter-decadal rainfall variability. The decrease is also discernible in the majority of the individual experiments.

2. The decrease in rainfall trend is well "registered" in the response of soil moisture, which shows a corresponding decrease in the mean of the 12 ensemble experiments, and in the majority of the individual experiments.

3. The results from the 10-member ensemble using the Mark 3 atmosphere-only model indicate that the basic features of observed extreme events over recent decades were reproduced in a majority of the experiments.

A significant achievement of the first Consultancy year was the development of more certain rainfall scenarios over Queensland. On average, annual rainfall is projected to decrease under enhanced greenhouse conditions, and this is the case with the majority of other global climate models. This finding represents both opportunities and challenges. It is an opportunity because we can now start to assess its likely impacts. The challenge is to quantify the extent of the reduction on regional scales. This is where regional models of enhanced spatial resolution are required. There is also a need to better define the human-induced climate signal from that due to natural variability. These issues will be addressed during the next phases of the Consultancy agreement.

1 Introduction

This is the first report of a second four-year consultancy (2002-2006) between CSIRO and the Government of Queensland. *The consultancy addresses the following aspects of climate change:*

- a definitive sign (increase or decrease) and/or narrower regional range for projected rainfall changes over Queensland;
- the response of the associated hydrological processes on regional scales;
- possible changes to ENSO characteristics, notably in its amplitude, frequency and the associated ENSO-rainfall relationship;
- possible changes to tropical cyclone frequency, intensity and location;
- climatic impacts across a range of issues, including possible changes in energy demand and supply due to changes in temperature and water availability, and possible changes in air quality;
- risk assessments for selected climate impacts, especially those hydrological related, including possible influence on the environmental flow in selected catchment region.

In this report we detail the achievements of the first year of the consultancy against the agreed milestones of the contract:

Milestone (1) Perform a detailed assessment of the climatology of the Mark 3 coupled climate model for current climate conditions over Queensland involving temperature, rainfall, water availability, runoff, mean sea level pressure,, etc. Appropriate comparisons with the Mark 2 coupled climate model will also be made to illustrate improvements.

- The Mark 3 control run has been extended to cover a period of 260 years for this assessment, and is reported in section 2 and section 4, where the performance is assessed in the context of other international models.

Milestone (2) Analyse projected climatic changes over Queensland using a transient CO_2 simulation with the Mark 3 coupled model to 2100 AD. This analysis will primarily investigate changes in rainfall and hydrologic processes on a regional basis. Decadal variability will be investigated by modifying future projections for known historical decadal variations. The decadal variability simulated by the Mark 3 coupled model will also be assessed. The impact of possible changes in ENSO variability will also be assessed, by examining any changes in the Mark 3 simulation of ENSO and its impact on hydrologic processes.

- A Mark 3 warming simulation has been performed, which includes a 100-year period after CO_2 and aerosols are held at a constant level. Detailed responses are examined in section 3.

Milestone (3) Investigate outcomes in terms of rainfall changes based on results from international models comparable to Mark 3. An assessment of their results for current climate will be made, and any model performing poorly in simulating Queensland climate will be eliminated. Transient CO_2 simulations from the remaining models will then be analysed as regards their rainfall changes over Queensland, to obtain a consensus projection. Where differences occur an attempt will be made to identify the possible causes with a view to improving the consensus projections.

- Results from 12 international models (including CSIRO models) have been analysed. Two models that did not simulate a reasonable rainfall climatology over Queensland were eliminated. Detailed outcomes of this milestone are reported in section 4.

Milestone (4) An ensemble of greenhouse runs made with the CSIRO Mark 2 model will be used to estimate climatic variability over Queensland. Secondly, an ensemble of simulations using the Mark 3 *atmosphere-only* model (completed on the CINRS CRAY supercomputer as part of an informal collaboration between the Queensland Department of Natural Resources and Mines and CSIRO) and forced by observed SSTs for the period 1949-1998 will also be analysed. The outputs from these runs will be used to assess the projected greenhouse-induced impacts.

- Outputs from an ensemble of 12 Mark 2 coupled model experiments and an ensemble of 10 atmospheric-only experiments were analysed and are reported in section 5.

Milestone (5) A workshop will be held to focus on subsequent impact studies (to be conducted in Year 2), to ensure that these studies are oriented towards relevant outcomes.

- A workshop was held in Brisbane on 2nd June 2003, and a workshop report was produced (See Cai *et al*., 2003).

2 Mark 3 model assessment

The major new scientific tool CSIRO is bringing to this contract is its Mark 3 coupled climate model. This is a vastly improved model compared with earlier versions, and is at the forefront of international models. Explicit aims of this project are a definitive determination of the sign of rainfall change in Queensland and the use of this information, along with projected changes in other climate variables, in order to allow a greater range of climate impact studies to be undertaken in order to facilitate the use to inform policy options.

The first task of this contract work, as defined in the milestones, is to perform a detailed assessment of the climatology of the Mark 3 coupled model for current climate conditions over Queensland involving temperature, rainfall, precipitation minus evaporation, runoff, mean sea level pressure, outgoing long wave radiation, etc. This is a necessary task prior to making any assessment of climatic changes under enhanced greenhouse conditions. NCEP reanalysis data, regarded as the best representation of the observed present day climate system, were used to benchmark the model outputs. Appropriate comparisons with the Mark 2 coupled model are made to illustrate improvements.

2.1 Winter season simulation

The Mark 3 model produces a reasonably realistic climatology. We first focus on the winter season.

In terms of annual rainfall, winter rainfall represents only a small fraction, since the majority falls in summer. However, an important part of the model evaluation, is to examine the performance at capturing the seasonal cycle. In the 2002 report (Walsh et al. 2002, Cai *et a*l., 2003) it was shown that the seasonal cycle was successfully simulated, in terms of a large area average Moreover, the teleconnection with ENSO for each season was also simulated, particularly for the rainfall intensive summer time. Here we focus on the spatial pattern.

Figure 2.1 shows the averaged surface temperature (^{o}C) for the June July August (JJA) season. We see that the model results resemble very well the observed in terms of the spatial pattern. There is marked improvement of the Mark 3 results over the Mark 2, in particular, along the coast, where the error is much smaller in the Mark 3 than in the Mark 2, reflecting the higher resolution of the Mark 3 model. Nevertheless, model performance in the coastal areas continues to require attention. The temperature over Northern Queensland and coastal water is generally too cold, in both the Mark 2 and Mark 3 models. With the northern part of Queensland, this is partially associated with the model "cold tongue" problem, in which the cold water zone of the central and eastern equatorial Pacific extends too far west to the western Pacific. This is a common problem suffered by all climate models, and CSIRO Atmospheric Research is actively involved in the international effort to rectify the problem. In the Southern Ocean, especially immediately off the southeastern coast, the low temperature in Mark 3 is in part associated with a residual drift that takes place as a result of no flux-adjustment, which is an unphysical means used to correct model errors. The CSIRO Mark 3 model is able to operate without it.

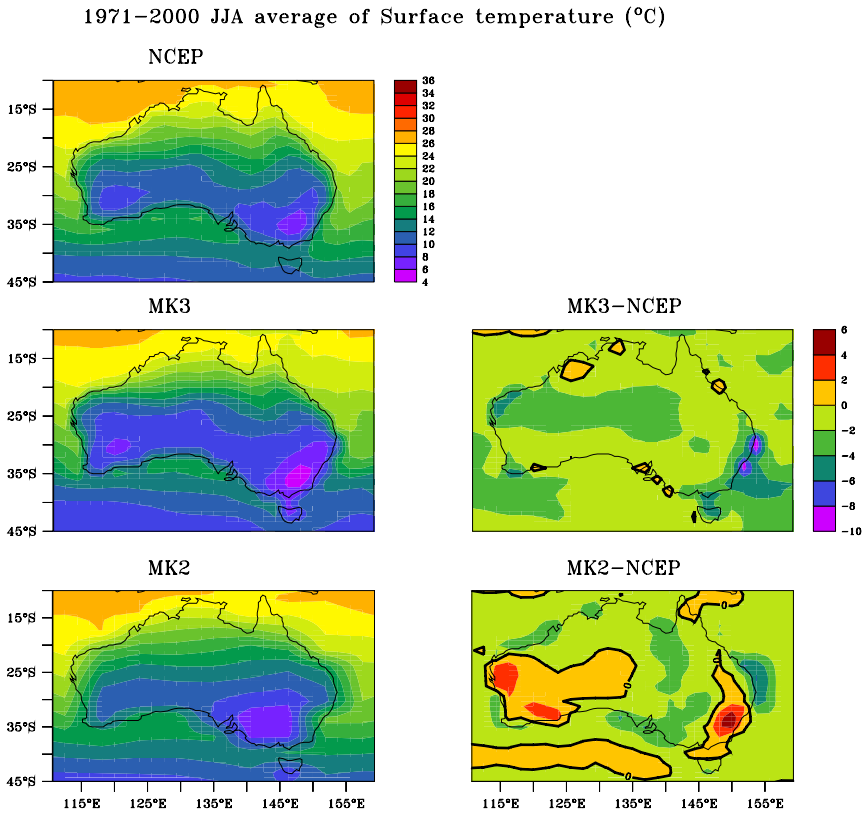

Figure 2.1: *Winter season surface temperature (in ^{o}C). Anti-clockwise from top left: climatology from NCEP reanalysis data, climatology from the Mark 3 control run, climatology from the Mark 2 control run, the difference between the Mark 3 and NCEPclimatologies, and the difference between between the Mark 2 and NCEPclimatologies.*

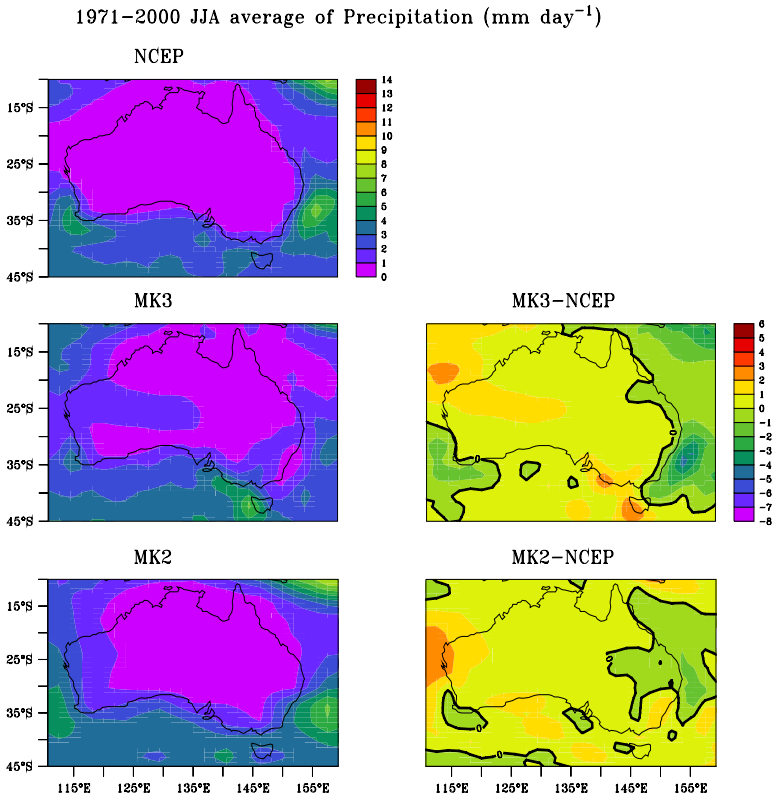

Figure 2.2: *As in Figure 2.1, but for winter season rainfall.*

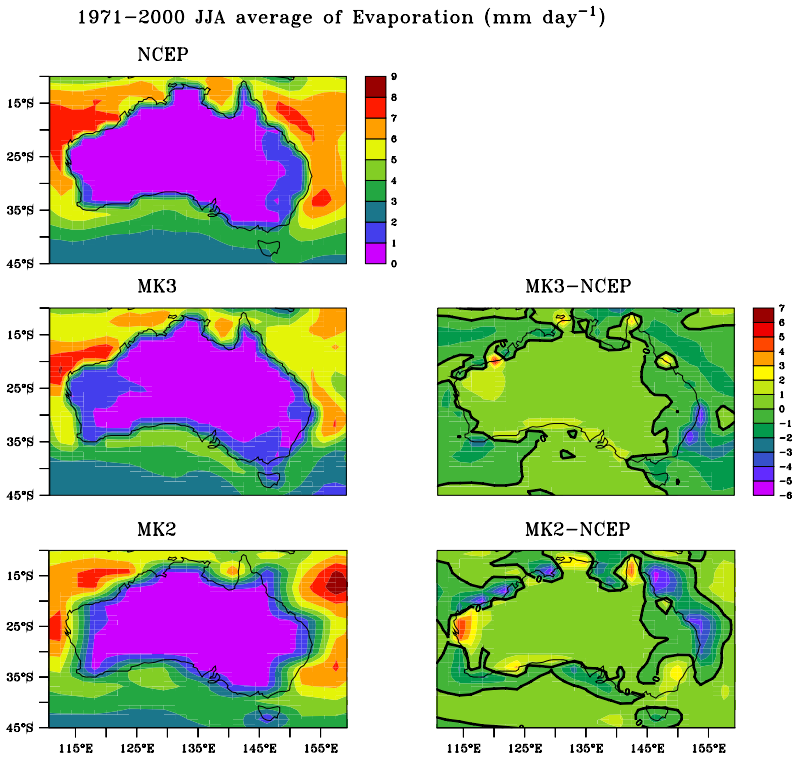

Figure 2.3*: As in Figure 2.1 but for winter season actual evaporation.*

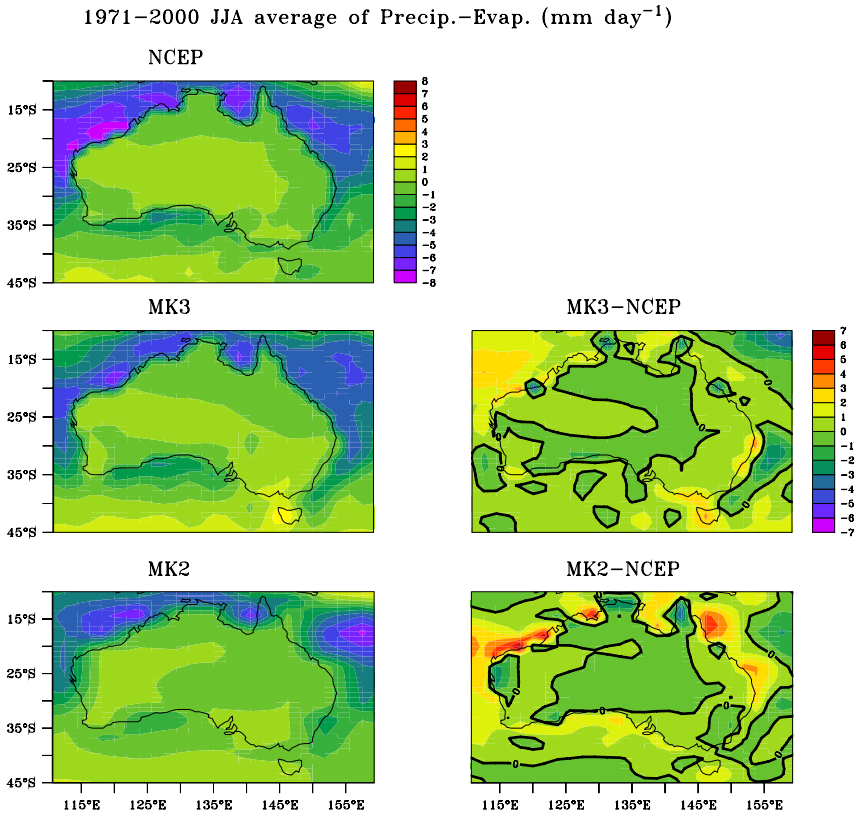

***Figure 2.4**: As in Figure 2.1, but for winter season precipitation minus evaporation.*

Both the Mark 3 and Mark 2 simulate the winter rainfall reasonably well (Figure 2.2). This is partially because winter rainfall in Queensland accounts for only a small percentage of the annual total rainfall. Coarse resolution models generally behave reasonably well in low rainfall seasons. The small difference between the Mark 3 and Mark 2 (in terms of absolute value) may be a reflection of this feature. Off the northeast coast, however, due to the cold tongue problem discussed above, rainfall in Mark 3 is too low as the low temperature there suppresses convection. The low temperature off the southeastern coast also suppresses the rainfall there.

Over the southeastern region, where rainfall is too low, actual evaporation also reduces (Figure 2.3). The relationship between rainfall and actual evaporation will be discussed in sections 3. Despite this, there is significant improvement in the simulation of actual evaporation. Along the Queensland coast, the errors are generally smaller in the Mark 3 than in the Mark 2. The improvement carries over to the precipitation minus evaporation (Figure 2.4); the errors along the coast have been greatly reduced.

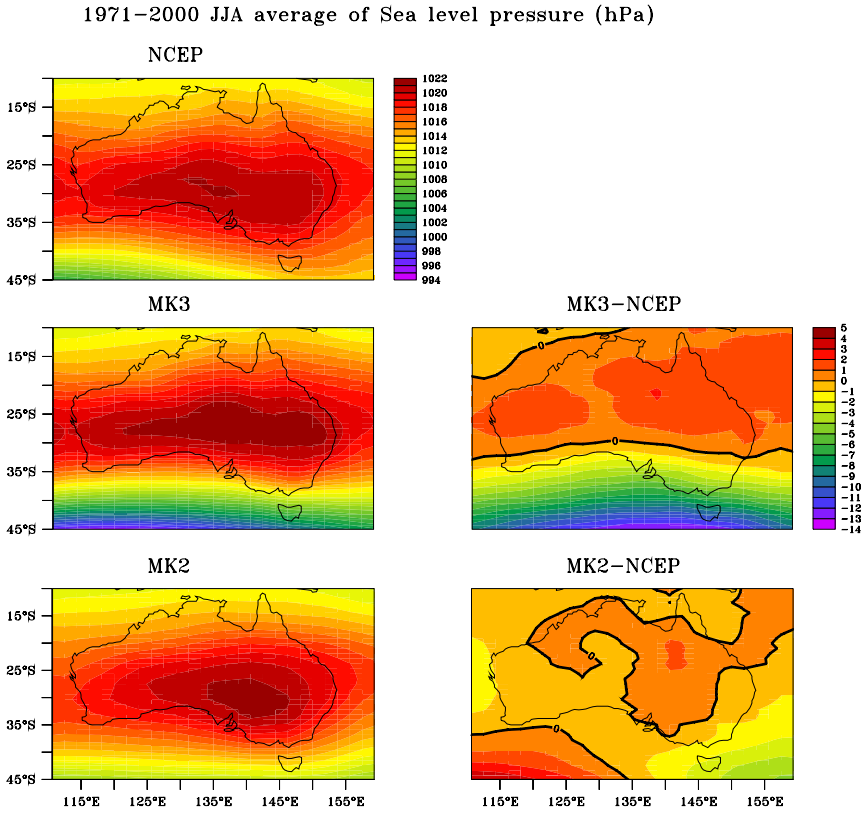

***Figure 2.5**: As in Figure 2.1, but for winter season mean sea level pressure.*

In terms of MSLP (Figure 2.5), the improvement of the Mark 3 over the Mark 2, is however less clear, particularly over Queensland, and over the Southern Ocean. Again this is associated with the problem identified above in association with temperature, which is too cold in the Southern Ocean. As a consequence, in the southern subtropics, MSLP in Mark 3 is too high, compared with the observation or the Mark 2 results

The cold tongue problem also affects the simulation of the outgoing long wave simulation, more so in the Mark 3 (Figure 2.6). The suppression of convection by the cold temperature in the western Pacific has resulted in a climatological mean over the Queensland region that is too low in both the Mark 3 and the Mark 2.

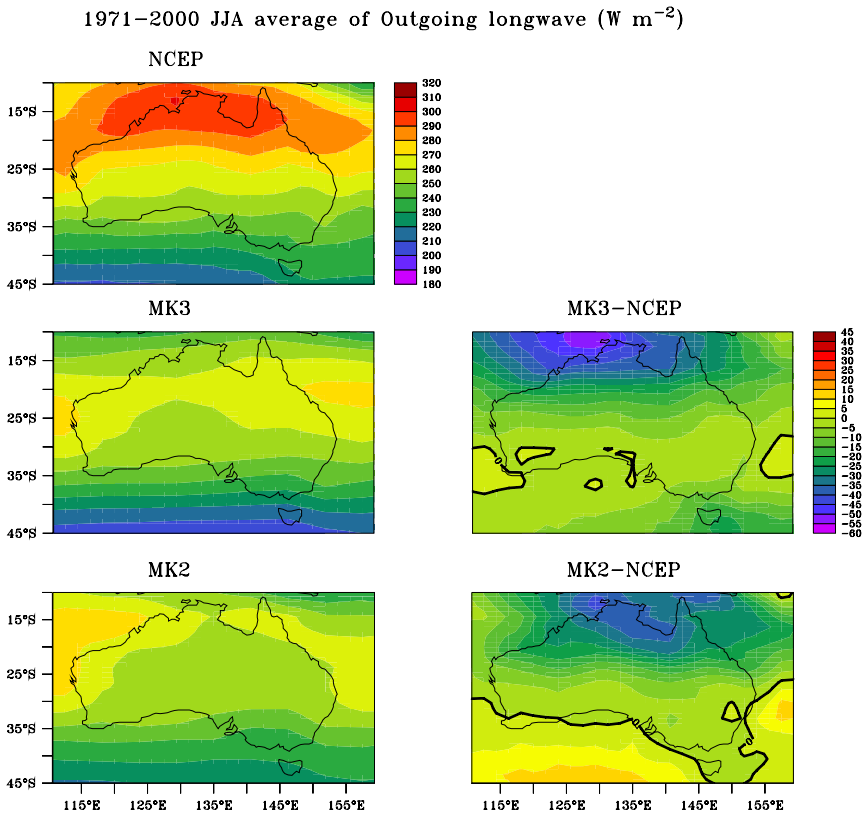

Figure 2.6: *As in Figure 2.1, except for winter season outgoing long wave radiation.*

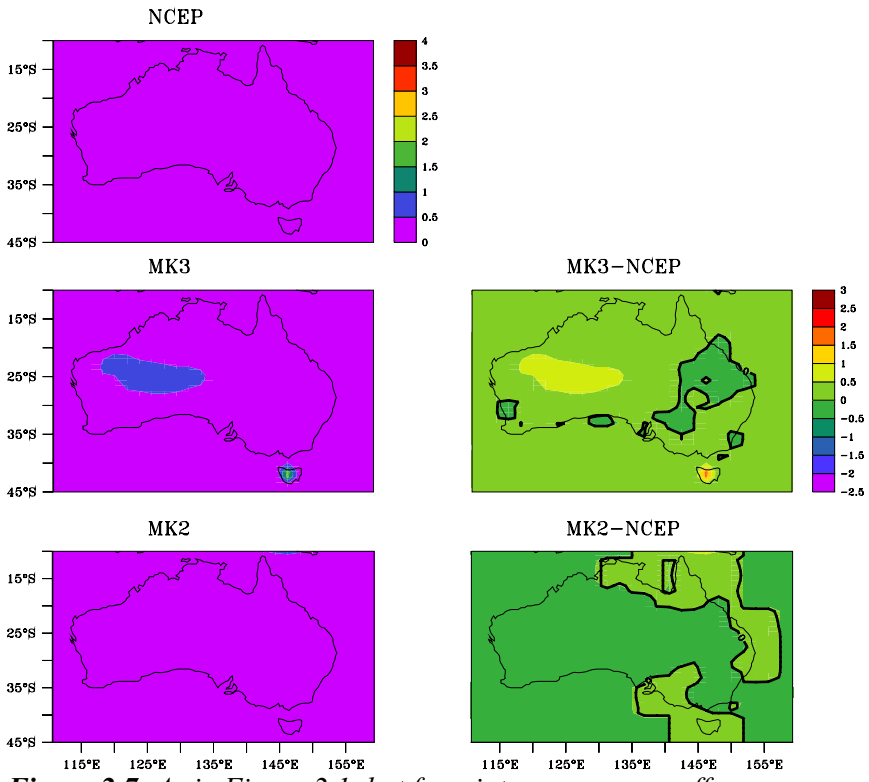

Figure 2.7*: As in Figure 2.1 but for winter season runoff.*

Coming to the runoff (Figure 2.7), the errors of the Mark 3 are generally much smaller than those of Mark 2, particularly along the Queensland coast. It is worth mentioning that a proper representation of run off in climate models, including models used for NCEP reanalysis, requires an employment of much more sophisticated hydrological sub-models. Further, runoff is a scarcely observed field, and the values in the NCEP reanalysis are mainly derived from their model outputs, therefore the quality of this field may be questionable.

2.2 Summer season simulation

The hydrological outputs for the DJF season again show general improvement in terms of most hydrological fields (Figures 2.8-2.14). The improvements in terms of surface temperature (Figure 2.8), rainfall (Figure 2.9), P-E (Figure 2.11), MSLP (Figure 2.12) are particularly conspicuous. However, in terms of actual evaporation (Figure 2.10) the improvement is minimal. For outgoing radiation at the top of the atmosphere (Figure 2.13) and runoff (Figure 2.14), the errors are actually bigger in the Mark 3 than in the Mark 2. This difference is mainly due to a different cloud parameterization used in the Mark 3.

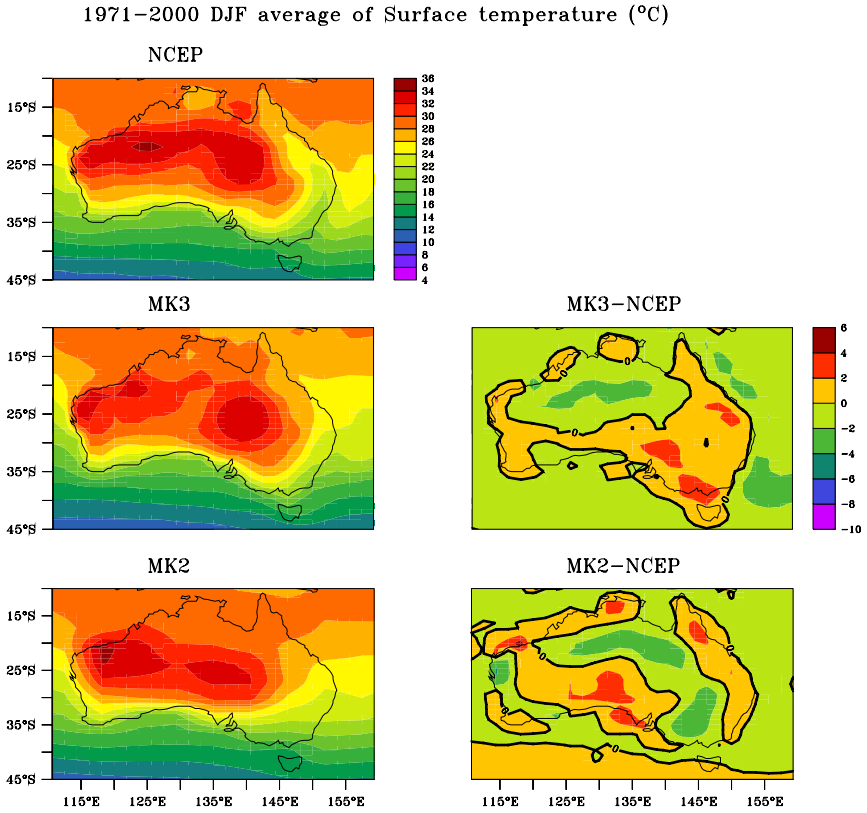

***Figure 2.8**: As in Figure 2.1, but for the summer season.*

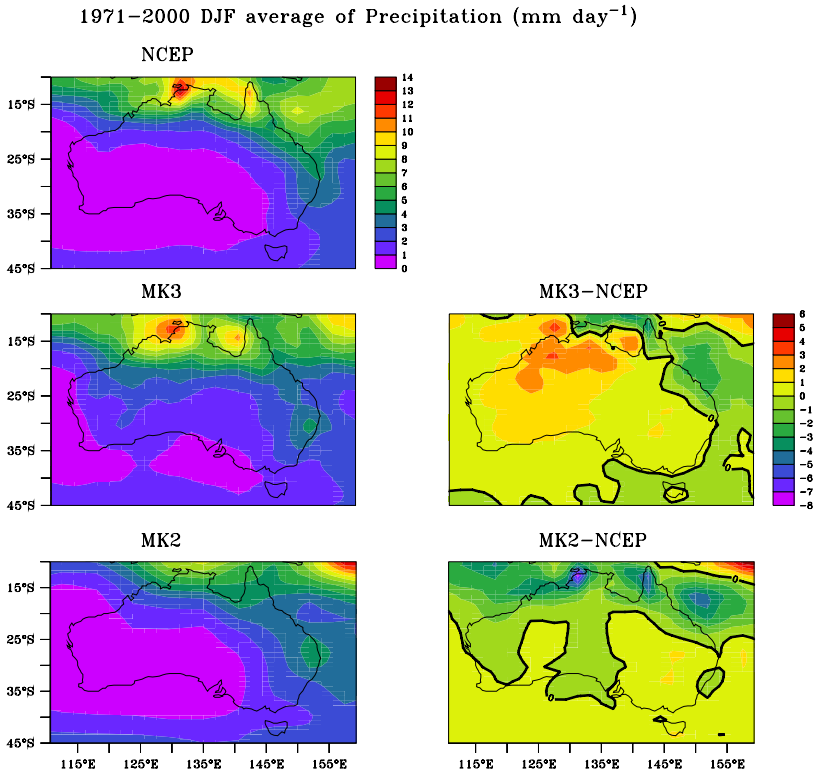

***Figure 2.9**: As in Figure 2.2, but for the summer season.*

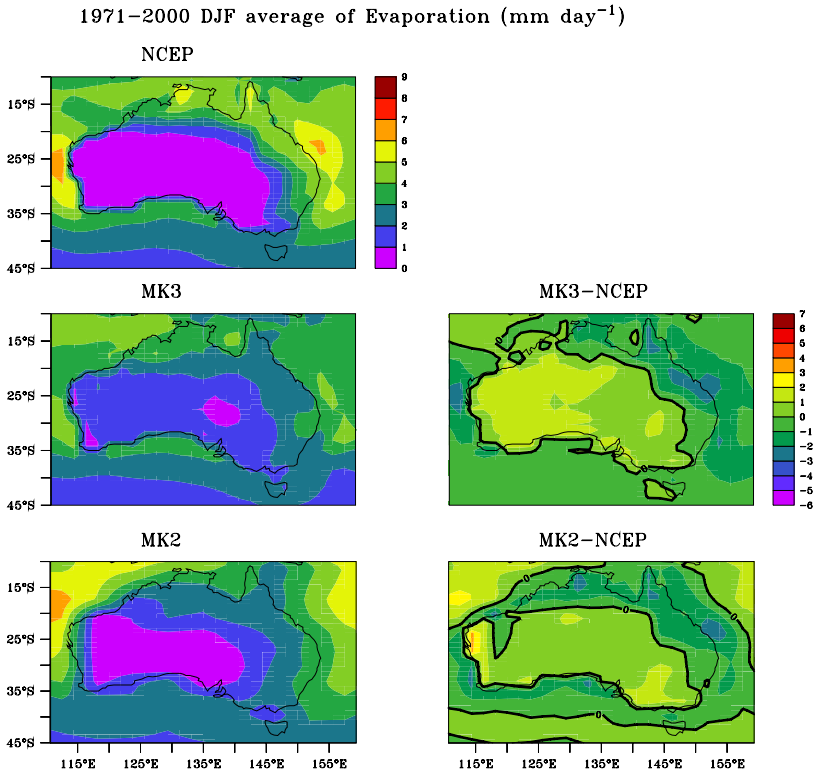

***Figure 2.10:** As in Figure 2.3, but for the summer season.*

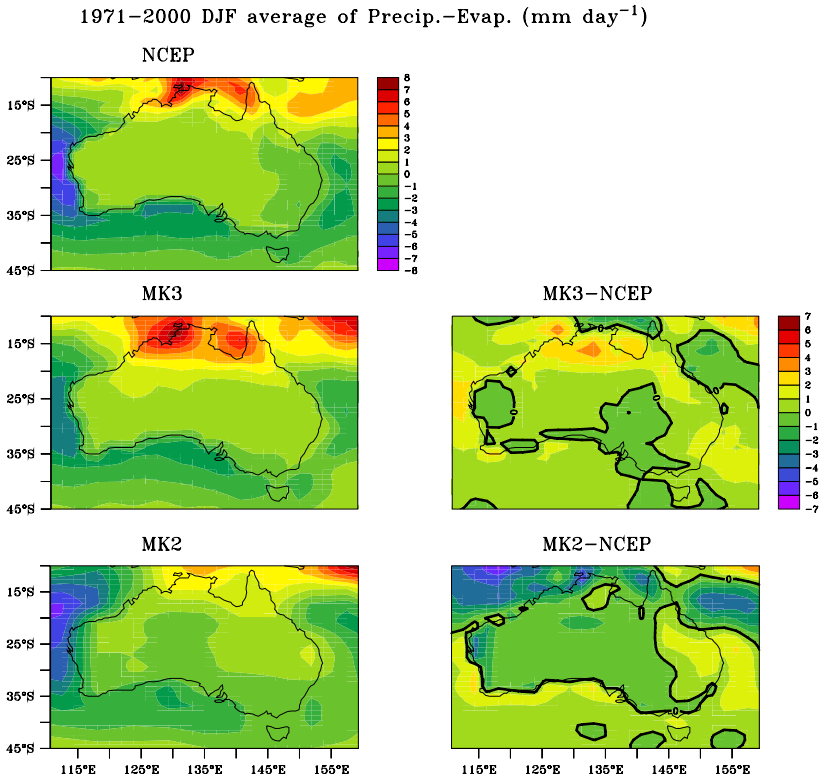

***Figure 2.11**: As in Figure 2.4, but for the summer season.*

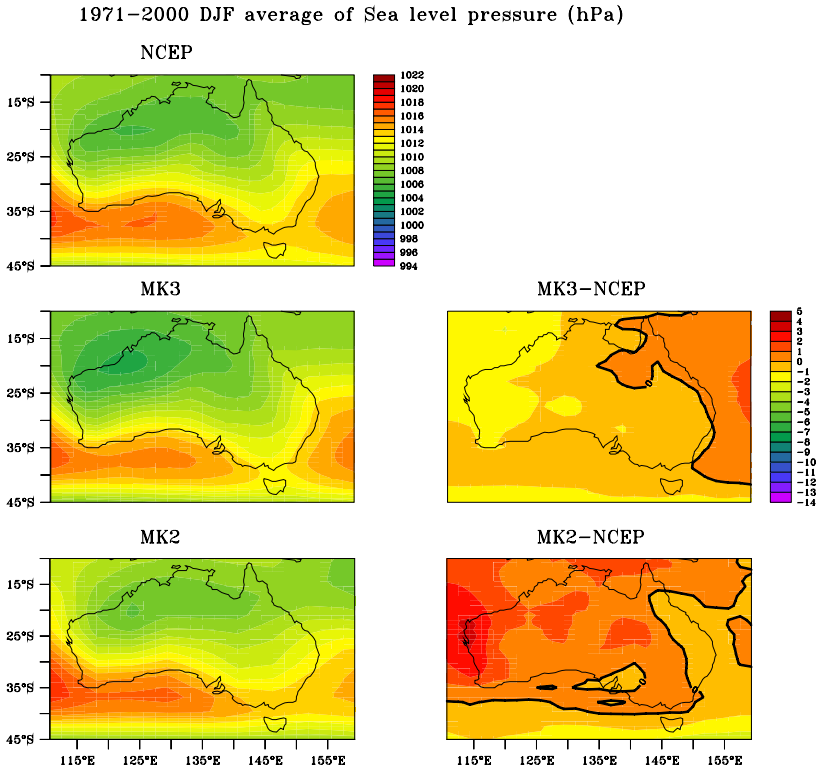

***Figure 2.12**: As in Figure 2.5, but for the summer season.*

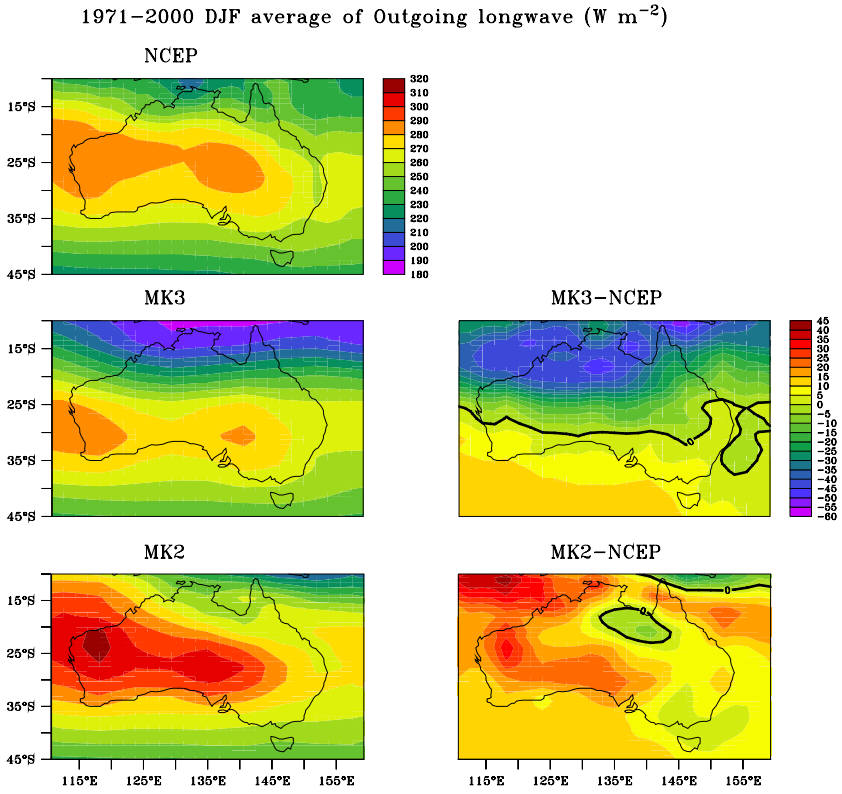

***Figure 2.13**: As in Figure 2.6, but for the summer season.*

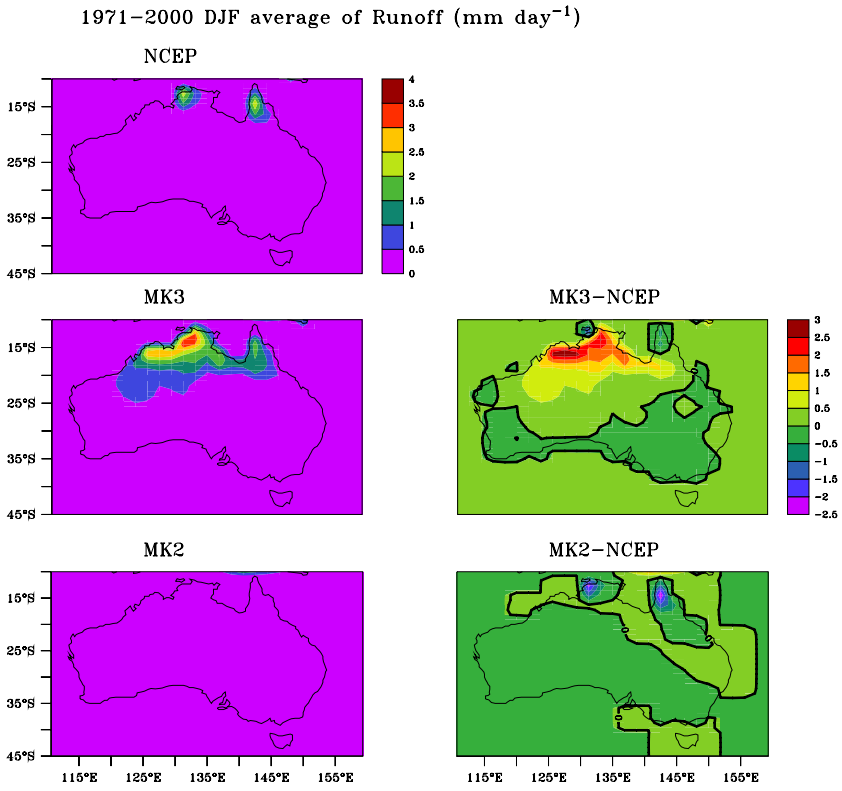

***Figure 2.14**: As in Figure 2.7, but for the summer season.*

To a large extent, the spatial distribution of the summer season errors in both Mark 2 and Mark 3 is very similar. Take for example, the summer rainfall and evaporation (Figures 2.9 and 2.10), both have large errors to the Northeast Coast of Australia. This is because they both are caused by a similar cold tongue problem in both versions of the model. The difference lies in that for some fields, for example, the outgoing longwave radiation, the cold tongue problem appears to produce a much more excessive response to the cold temperature in the western Pacific in Mark 3 than in that in the Mark 2.

In summary, the hydrological outputs from the Mark 3 show general improvement over the Mark 2. In some fields, such improvement is not clear, but some are scarcely observed and a detailed assessment is not possible at this stage. The model suffers from a common "cold tongue" problem. The cold tongue extends too far west to the western Pacific, and many model deficiencies appear to be associated with this problem.

3 Response to greenhouse warming

Milestone 2 aims at analysis of projected climate change over Queensland due to CO_2 increases and other forcings such as aerosols obtained with the Mark 3 coupled model from the present day to 2100AD. The experiment follows the A2 projection of SRES. The time-varying forcing consists of atmospheric CO_2 equivalent and direct aerosols. The CO_2 follows the observed evolution from 1870 to 2000, and uses the projected CO_2 of the A2 scenario from 2001-2100. By 2100, the equivalent CO_2 reaches a level that more than tripled the level of 1870. Thereafter, both aerosols and CO_2 are held at a constant level and the model integration continues for another 150 years, for further identifying any trend in the response. The warming simulation is contrasted with a control simulation, in which the CO_2 and aerosols are kept at a constant 1870 level.

3.1 The relationship between hydrological parameters

3.1.1 Temperature and rainfall, actual evaporation and temperature

In order to elucidate the response of hydrological processes to global warming, we first examine the basic relationship between surface temperature and rainfall in the control run. We will compare it with that in the warming run. Figure 3.1a plots the relationship between rainfall (actual evaporation) and surface temperature using model outputs up to the stage before CO_2 is held constant (year 2100). Plotted are the monthly anomalies from a long-term mean of the control run climatology (model 1961-2000) averaged over the model Queensland region. To explore the relationship more thoroughly, a linear regression is conducted separately in the positive and negative temperature quadrants, and the slope in each quadrant is also plotted. The relationship shows that when it rains, because there is more cloud, less heat penetrated to the surface, therefore surface temperature decreases (while actual evaporation increases), as is observed. It is interesting to see that for a unit of decrease or increase in rainfall, the change in surface temperature is comparable; that is, the slope in the positive and negative quadrants is comparable, or nearly symmetric.

Figure 3.1b is the equivalent of Figures 3.1a for the warming experiment. Plotted are monthly changes from monthly climatologies of the control experiment. It shows that under greenhouse conditions, the relationship seen in the control run continues but

because of the underlying warming trend, when rainfall is anomalously low, a per-unit change of rainfall is associated with a greater amount of warming, with a smaller slope in the positive temperature quadrant. There is also a slight but significant increase in the slope in the negative temperature quadrant, indicating that temperature does not go as low as otherwise without greenhouse warming. Together, we see that greenhouse warming causes a strong asymmetry in the slopes in the positive and negative temperature quadrants. The asymmetry represents an unfavourable condition for soil to hold moisture, with potentially serious implication for farming and other agricultural activities. This point is illustrated in Figures 3.2, which shows that when it does rain, the warmer temperature increases the evaporation rate (Figure 3.2b).

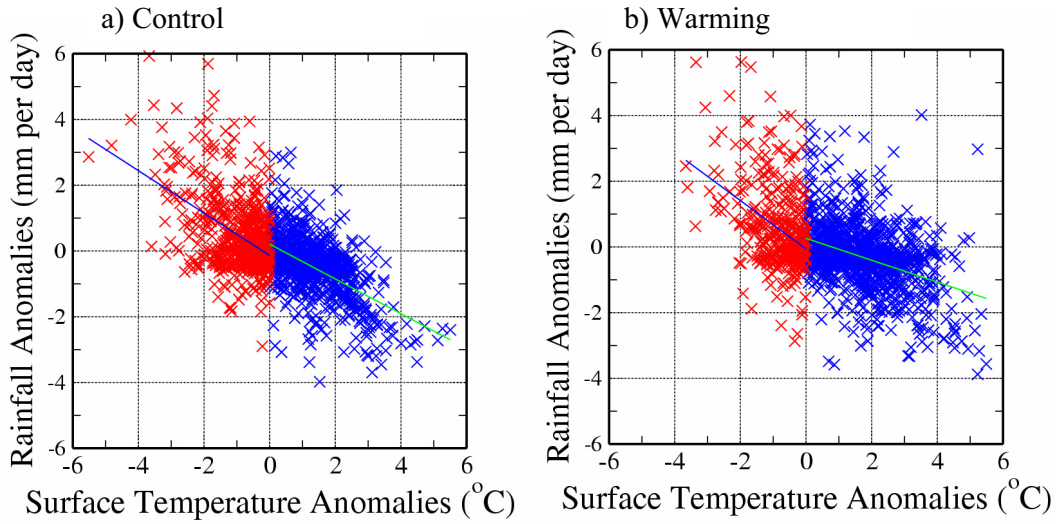

Figure 3.1*: The relationship between rainfall and surface temperature in (a) the Mark 3 control run and (b) the transient climate change run at 2100AD.*

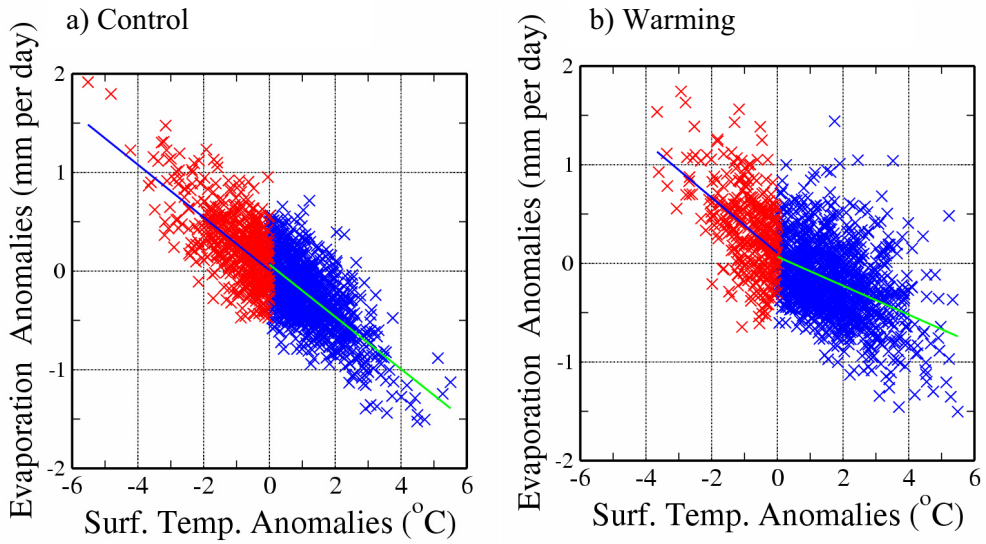

Figure 3.2: *The same as Figure 3.1 but for the relationship between surface temperature and actual evaporation.*

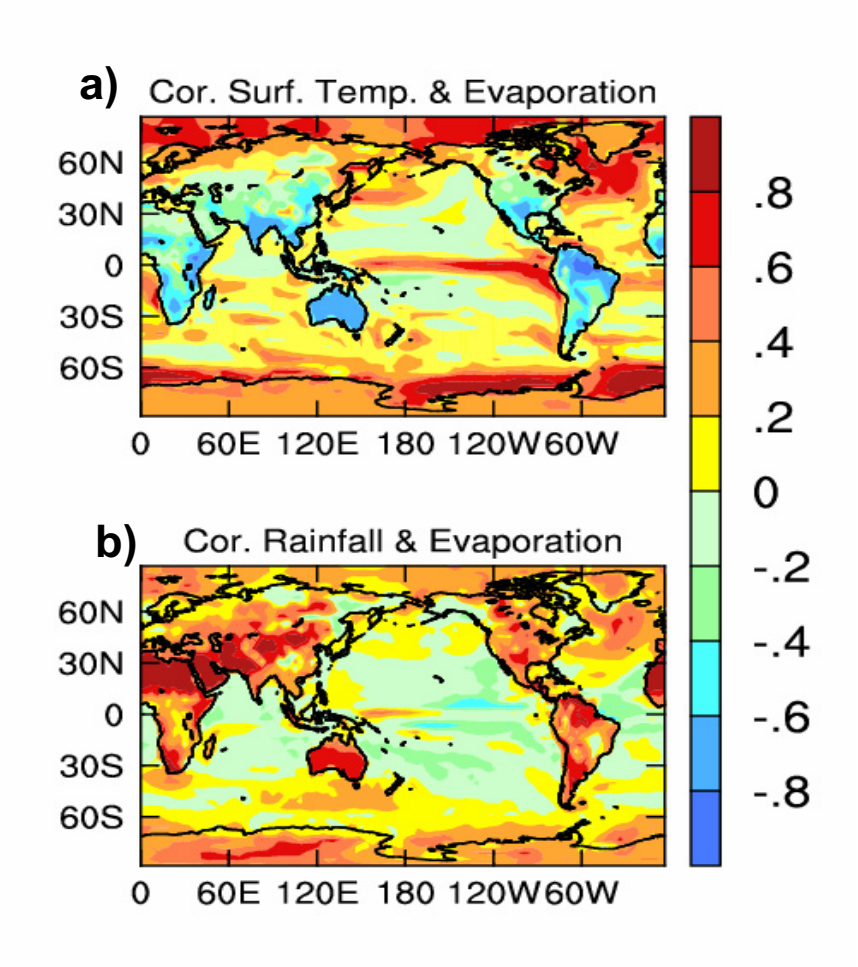

***Figure 3.3**: Point to point correlation a) between temperature and actual evaporation and b) between rainfall and actual evaporation.*

3.1.2 Actual, Pan and Potential Evaporation

Before we address the possible change in evaporation, it is necessary to differentiate the three different terms that climate scientists use. Pan evaporation is used to measure the evaporation at a location where the pan is. Pan evaporation is somewhat similar to potential evaporation in that both allow an unlimited water source.

Actual evaporation and surface temperature over land are both predominantly controlled by rainfall, which provides the water source. This is demonstrated in Figures 3.3a and 3.3b. Figure 3.3a confirms what has been shown in Figure 3.1a. Figure 3.3b shows the correlation between anomalies of rainfall at each location and evaporation at the same location from the control run. We see that over land actual evaporation increases with rainfall (Figure 3.3b). But there is a sharp contrast between land and ocean. Over ocean, water availability is not a problem and the relationship between rainfall and evaporation is weak. In the equatorial Pacific the relationship is opposite to that seen over land. There, water is always available for evaporation, and as the ocean warms up, actual evaporation increases.

The availability of water for actual evaporation is usually indicated in the soil moisture content. The relationship between soil moisture and rainfall and that between actual evaporation and rainfall are similar, in that both soil moisture and actual evaporation are predominantly controlled by rainfall.

Understanding these relationships is necessary for understanding the response of many hydrological processes in the warming run. Under greenhouse conditions, if rainfall decreases, one expects that actual evaporation and soil moisture to decrease and this is indeed the case for most parts of Queensland.

In a recent paper, Roderick & Farquhar (2002) reported that over the last 50 years there has been a general decreasing trend in Pan evaporation. Over Australia, potential evaporations calculated using meteorological parameters at Pan sites all display an upward trend. It is not clear if the trends in Pan evaporation reflect the trend in potential evaporation. All climate models predict an increase in potential evaporation under greenhouse conditions, including the Mark 3 model, as will be discussed in the upcoming sections.

3.2 Response of hydrological processes to global warming

The response is obtained through differences of averages over a 30-year (2071-2100) period between the warming and the control simulation. The result for the December January and February (DJF) season is plotted in Figure 3.4. For most of the Queensland coastal area, the warming in DJF is in the range of 2.5-5.5 ^{o}C, increasing toward inland area, where the maximum warming reaches 5.5 ^{o}C. Rainfall generally decreases (by up to 0.5 mm day^{-1}, about 5-20% from northern Queensland to Southeast Queensland). In association, OLR at the top of the atmosphere increases over most of the Queensland, indicating a reduction in convective activities, although there is little change in MSLP. As expected from the hydrological relationship discussed above, actual evaporation decreases, by up to 15% as rainfall decreases. However, precipitation minus evaporation (P-E) also decreases, indicating that the reduction in rainfall is greater than the reduction in evaporation. As P-E decreases, runoff and soil moisture also decrease.

The response in June, July and August (JJA) season is qualitatively similar (Figure 3.5). Rainfall in JJA decreases, up to 60%. Consistently, OLR increases. In general, actual evaporation, P-E, runoff, and soil moisture all decrease in response. For the MAM and SON, the response similarly features a decrease in rainfall, giving rise to a decrease in actual evaporation, P-E, soil moisture and other parameters of hydrological processes. In Section 3.4, we show that these trends persist even after CO_2 and sulphate aerosols stabilise.

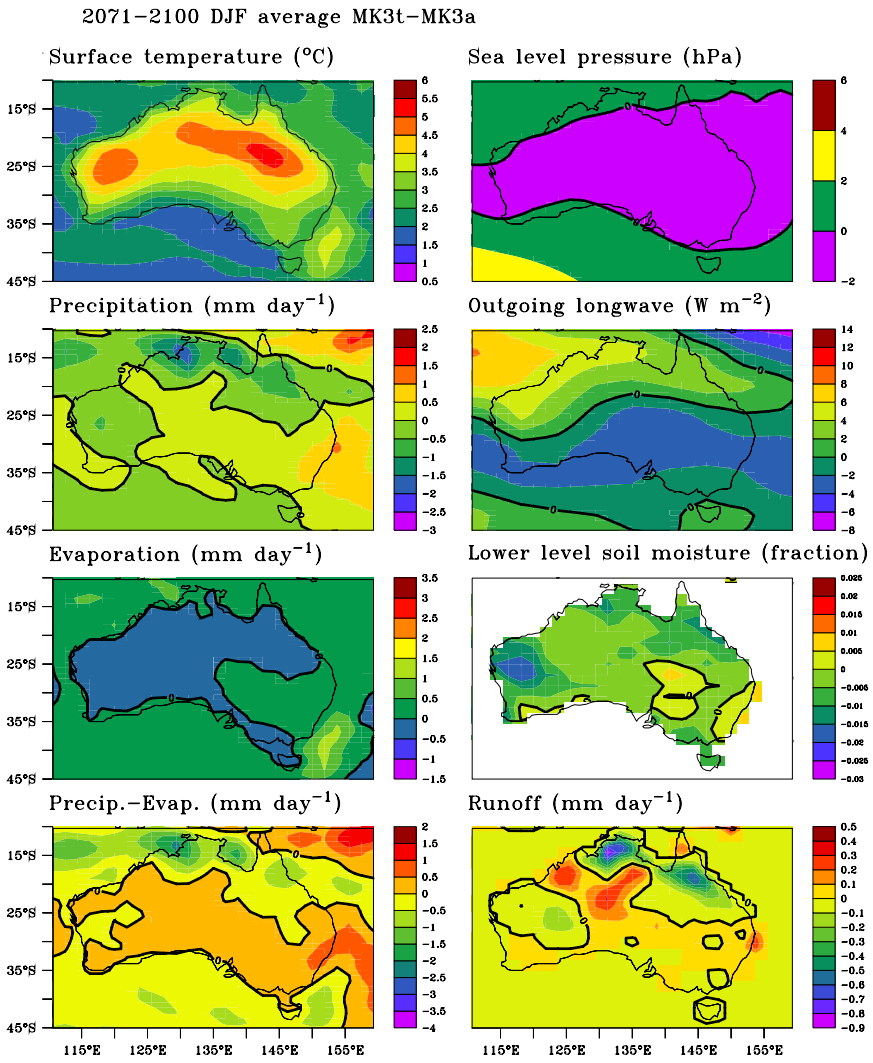

***Figure 3.4**: Change of hydrological processes due to greenhouse warming. The change is obtained as the difference between the DJF average over a 30-year epoch (years 2071-2100) of the warming run and a 30-year average of the same season of the control run. Clockwise from top left: Surface temperature, sea level pressure, outgoing long-wave radiation, lower level soil moisture, runoff, P-E (precipitation minus evaporation, evaporation, and precipitation.*

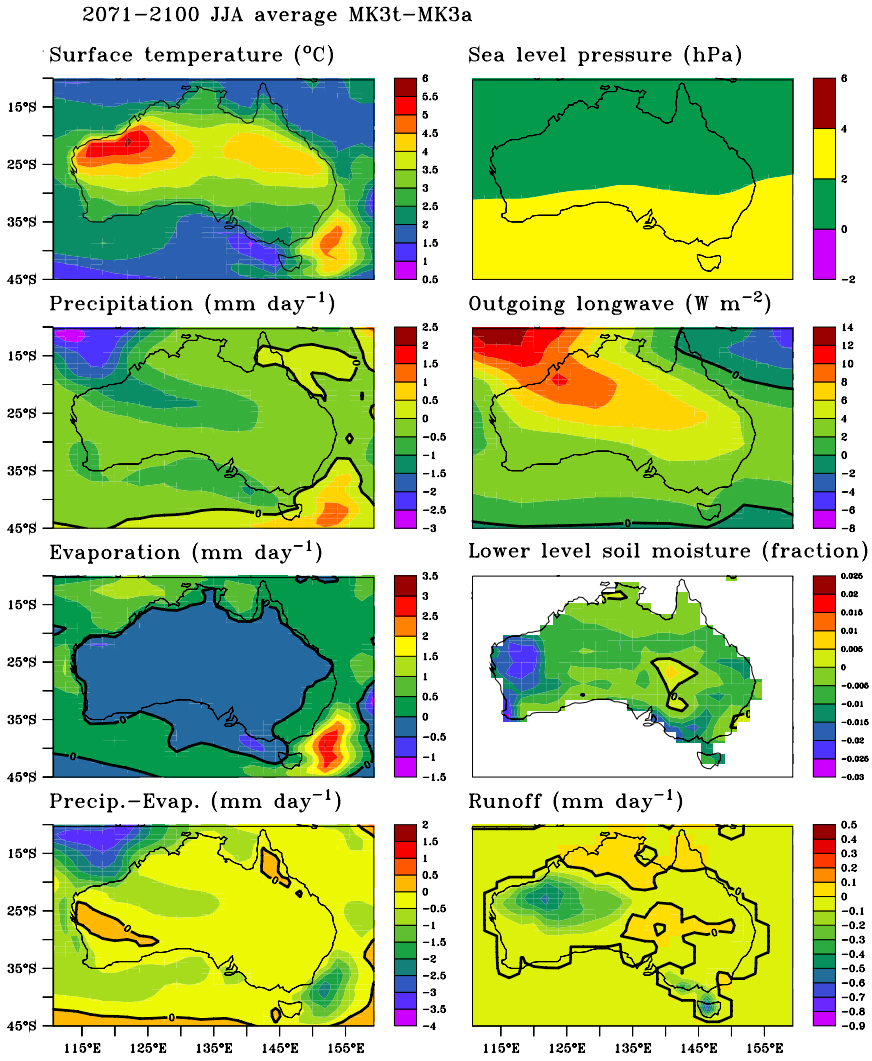

***Figure 3.5**: The same as Figure 3.4 but for JJA season.*

3.3 Response of potential evaporation to global warming

So far, we have not addressed the response of potential evaporation. As discussed above, potential evaporation over land assumes an unlimited water source, in contrast to actual evaporation, which is to a large extent determined by the availability of water. This latter feature determines that the response of actual evaporation to global warming follows the response of rainfall. By contrast, an increase in temperature does contribute to an increase in potential evaporation.

The upper four panels of Figure 3.6 show the climatological mean for each season from the control run. Potential evaporation is strongest in summer and spring. The former is very much controlled by the high temperature in the summer season while the latter is determined by a large radiation and strong winds in the spring season. The lower four panels show the changes for each season attributable to global

warming. There is a general increase, the increase being largest in summer and spring season in terms of absolute values.

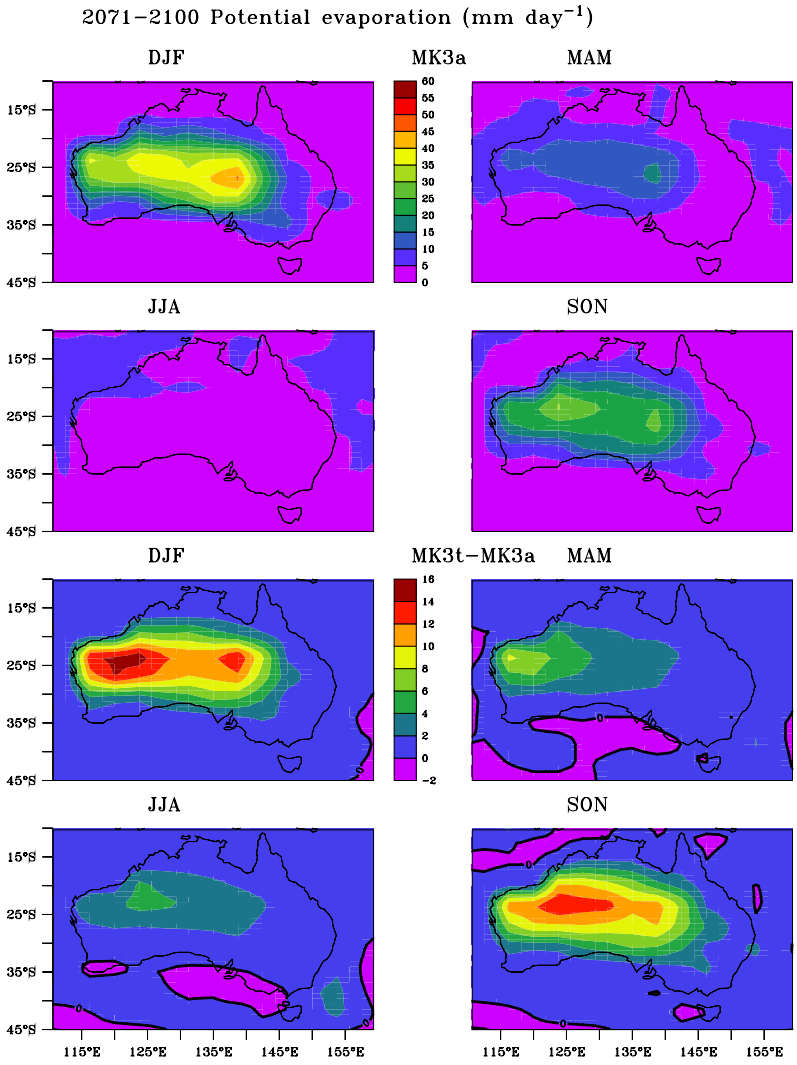

Figure 3.6: *Potential evaporation (mm per day). Top four panels, clockwise from top left seasonal climatologies from the control run: DJF, MAM, SON and JJA. Bottom four panels, changes of seasonal climatologies from the control run (years 2170-2100).*

3.4 Regional response

Given that Queensland is a vast area within which hydrological processes and their response to climate change may vary significantly from one region to another, it is necessary to investigate this possibility. This is carried out in this section.

Queensland is divided into 5 catchment regions as shown in Figure 3.7 according to the geographycal information provided by Queensland Department of Natural Resources and Mines. Clockwise, region 1 (R1) represents the northern Queensland, R2 the coastal area, and through to R5 the central south Queensland region.

Figure 3.8 shows monthly surface temperature change (departure from the mean climatological values of the control run averaged over 1961 –1990), filtered to remove interannual time scales. A clear feature is that there are significant fluctuations on decadal and multi-decadal time scales and these fluctuations are of a similar magnitude from one region to another, suggesting that they be driven by same mechanisms. In all regions surface temperature rises, as expected, although the rise is modulated by decadal and multi-decadal fluctuations.

However, regional differences emerge from about year 2050. The coastal region (R2) and the North Queensland (R1) warm less, when compared with R3, R4 and R5, and warming in the R5 region is the strongest. Most of these regional differences are the consequence of a well-known feature, that is, under greenhouse conditions, the warming rate over land is greater than that over ocean, because of the far greater inertia of the ocean that makes it harder to warm. Modulation by the slow ocean warming is also the cause of the slower warming in the coastal area, relative to R5, and the slower warming in R3 relative to R4. In R1, its proximity to the western Pacific warm pool, where any additional warming is offset by a greater increase in evaporative heat loss, may also contribute to the small warming.

Figures 3.9, 3.10 and 3.11 show the equivalent plot for rainfall, evaporation and P-E. Like surface temperature, there exist significant fluctuations on decadal and inter-decadal time scales in all three hydrological parameters. For rainfall, although the initial trend shows a slight increase, a discernible decreasing trend is conspicuous since the beginning of 21th century. This temporal behaviour is seen in all regions, the decrease being most obvious in the North Queensland region (R1). For actual evaporation, the temporal behaviour in R3, R4 and R5 is generally similar to that of rainfall with an initial increase prior to year 1990, and a discernible decreasing since mid-21th century.

The decrease in actual evaporation in the North Queensland (R1) and coastal Queensland (R2) regions is not as large as in R3, R4, and R5. As a result, in terms of P-E, there is a substantial reduction in the coastal and North Queensland regions, particularly since about 2000. The decreasing trend in these parameters is consistent with the development of an El Nino-like warming pattern, which also develops in the Mark 3. This El Nino-like warming pattern has been discussed extensively in the previous studies (Cai and Whetton 2000, 2001), which develops as a result of transmission of a subtropical warming via the Pacific Oceanic pathway to the equatorial Pacific (Gu and Philander 1997, Deser 1997).

Soil moisture is one of the most relevant hydrological parameters. Its response indicates the extent to which climate change affects farming practice and agriculture land usage. Figure 3.12 shows that in all catchment areas, soil moisture decreases, and that the magnitude of the decrease is similar in all catchment areas.

The temporal fluctuations (Figure 3.13) in runoff generally follow those of rainfall. As in the rainfall response, a decreasing trend is evident in all seasons. Note that the model runoff parameterisation is still crude, and most of the model Queensland runoff is located in north Queensland, hence the decrease in R1 is large.

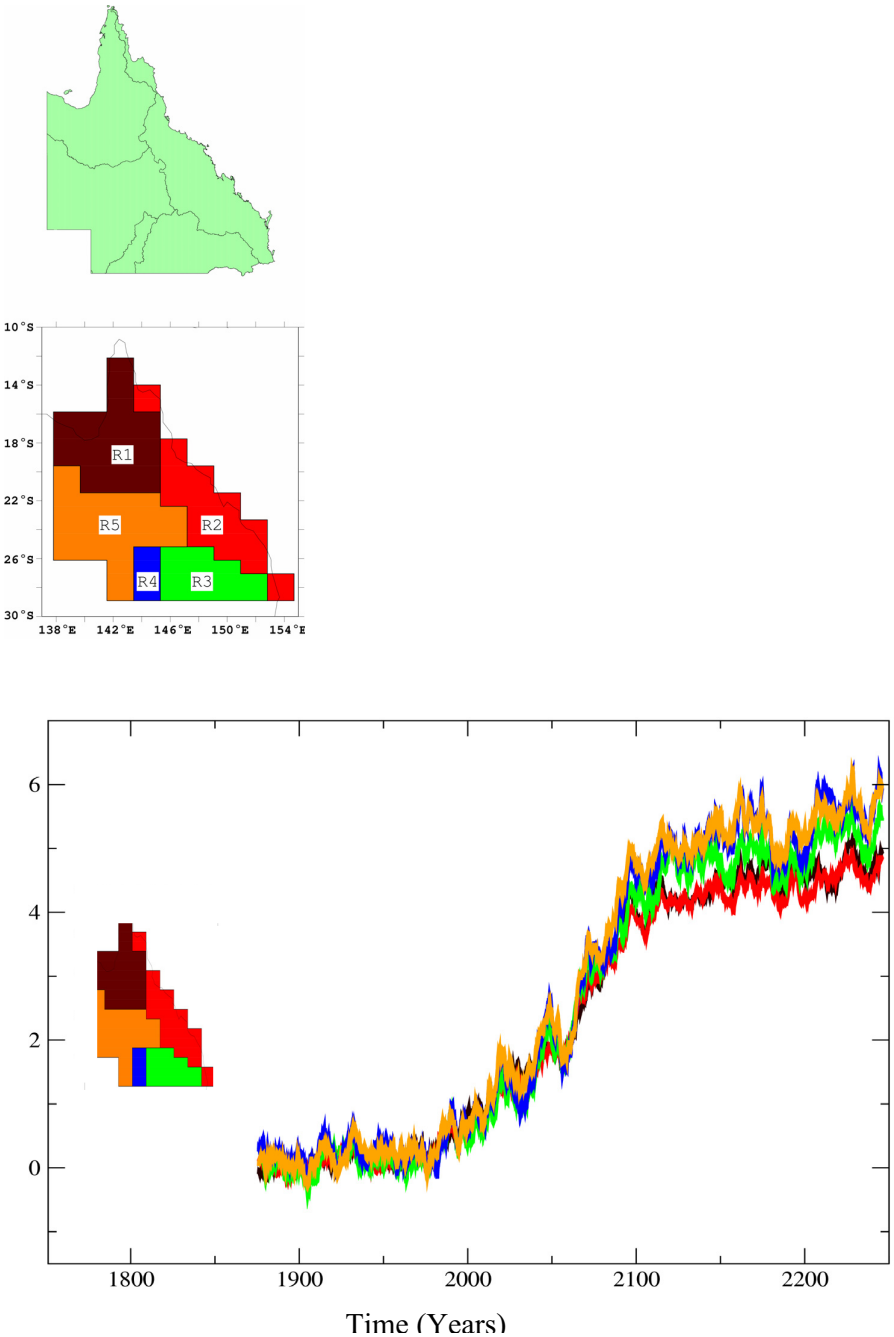

Figure 3.8: *Queensland major rivers (top panel), major catchment areas on the model grid (middle panel) and response of surface temperature (in °C) from each area (lower panel). The colour of each curve matches that of the catchment areas.*

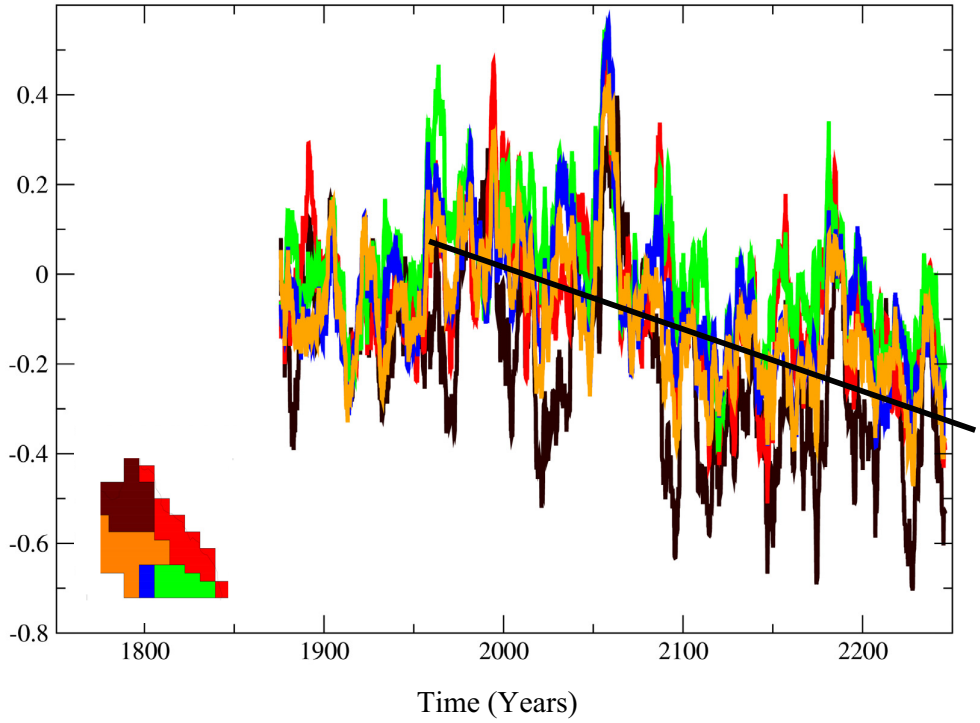

Figure 3.9: *The same as Figure 3.8, but for rainfall (mm per day) response.*

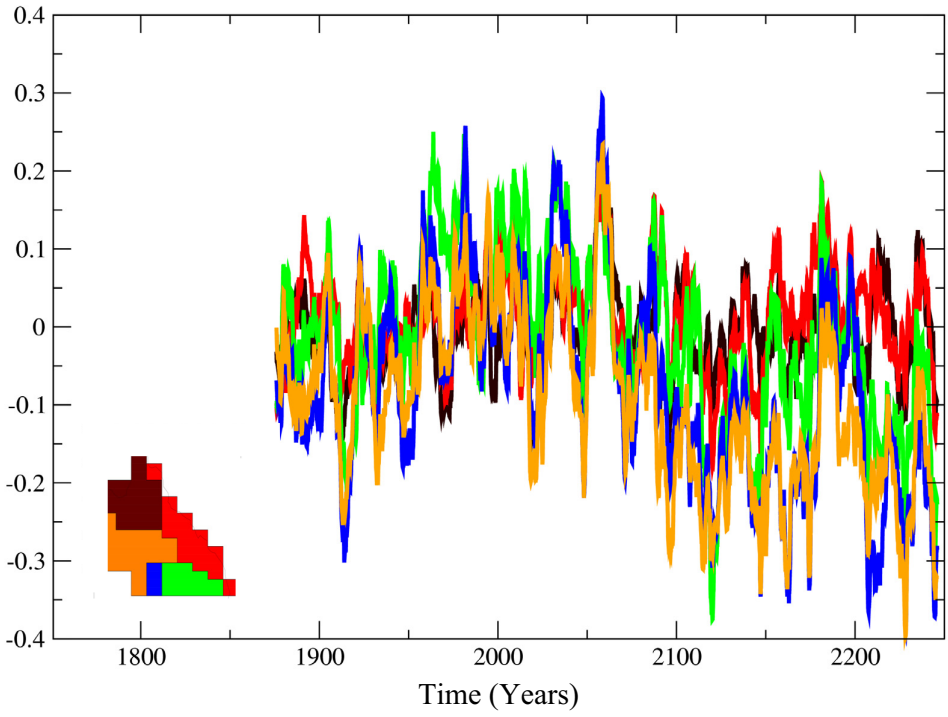

Figure 3.10*: The same as for Figure 3.8 but for (actual) evaporation (in mm per day).*

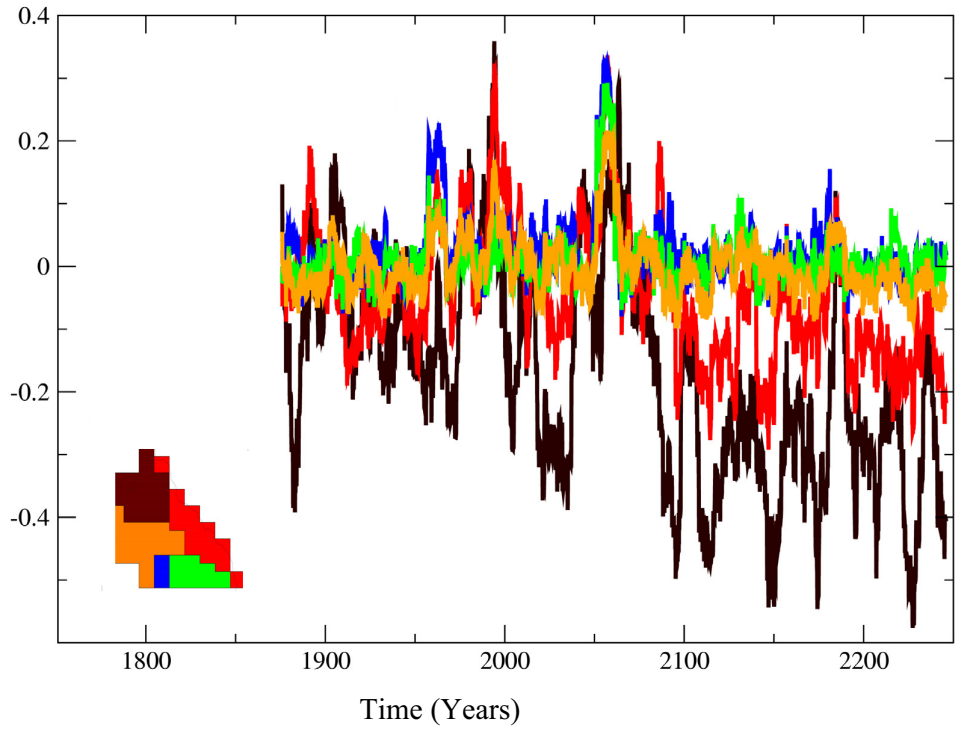

Figure 3.11**:** *The same as for Figure 3.8, but for precipitation minus evaporation (P-E, in mm per day).*

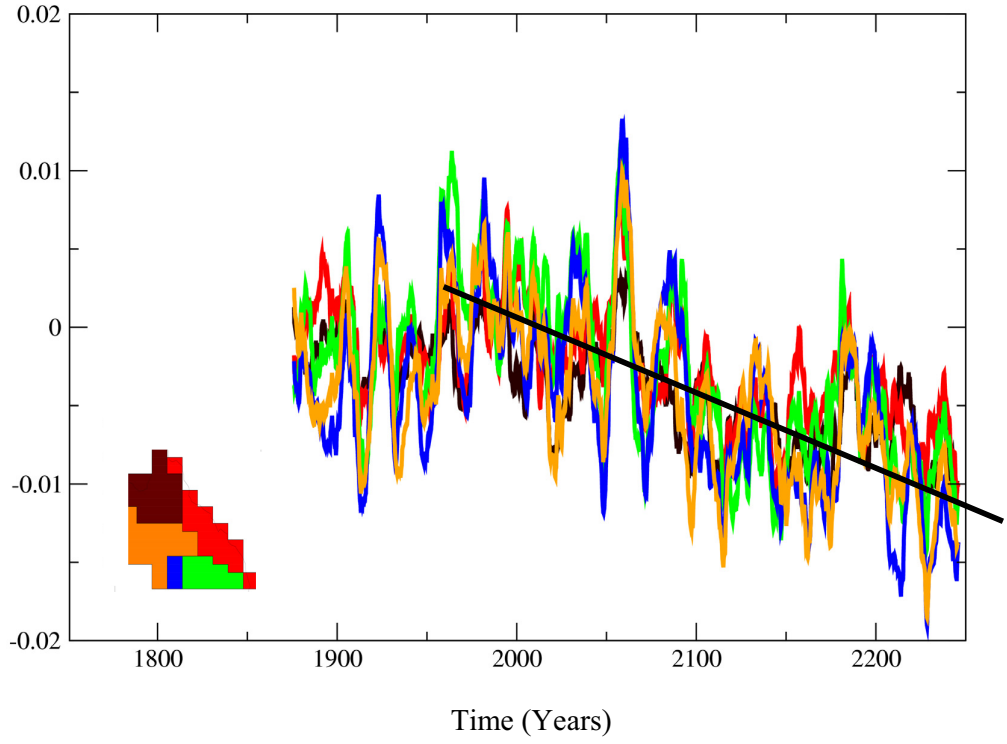

Figure 3.12*: The same as Figure 3.8 but for soil moisture (in fraction).*

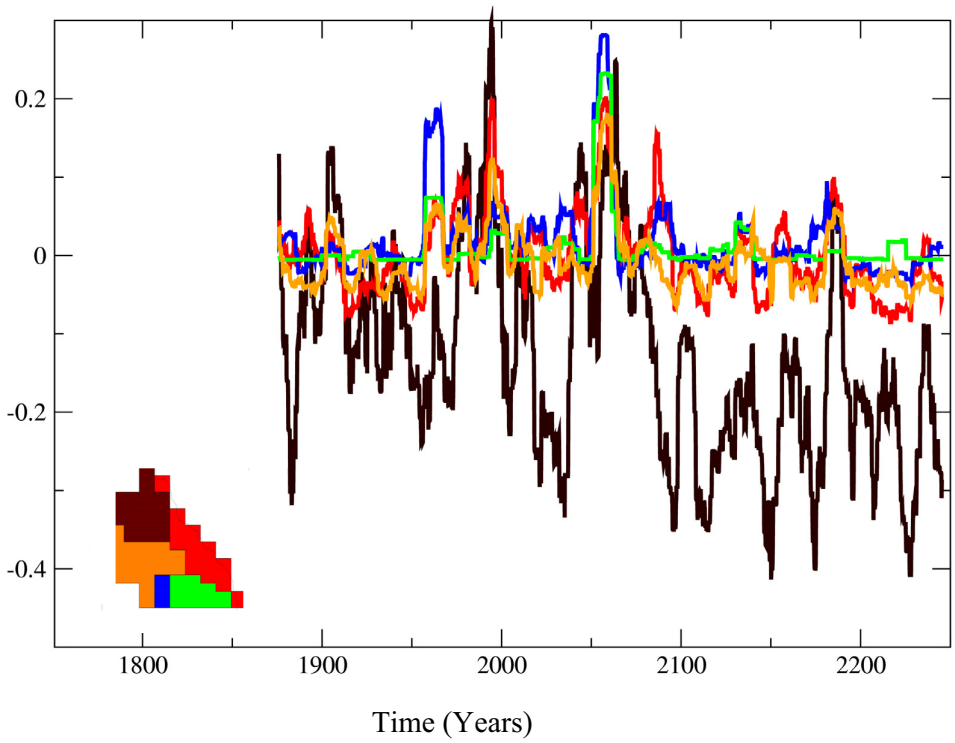

Figure 3.13: *The same as for Figure 3.8 but for runoff (mm per day).*

3.5 Multi-decadal signals and secular trends of rainfall

Rainfall in Queensland experiences significant variations on multi-decadal time scales. The extent to which future rainfall variability may be modified by global warming and by the superimposing effect of a secular trend and a multi-decadal-scale dry or wet period needs to be investigated. For example, it is highly likely that given the decreasing trend noticed above, the impact will be exacerbated by a multi-decadal scale dry period.

Since we focus on low frequency oscillations, results will be presented using filtered data. All four seasons and five sub-regions of the State are considered. The summer, autumn, winter and spring seasons are considered as December-February, March-May, June-August and September-November, respectively. The five regions have already been shown in Figure 3.7. The variability is investigated using the so-called Coefficient of Variation (CV), which measures the amplitude of variability relative to the climatology. To identify any trend, a 31-year sliding window is used. The 31-year sliding window is used so that there is a sizeable statistical sample. The CV is computed based on the following equation:

$$CV = (\sigma/\chi)\times 100.0,$$

where σ is the standard deviation and χ is the climatological mean. For comparison, both the modelled and the observed are calculated. Figures 3.14 to 3.18 show the results for each catchment area and stratified into four seasons. Also plotted in these figures are the 30-year running mean of the rainfall time series.

The observed data set covers the period from 1901 to 2000 and the control and transient experiments are from 1752 to 2120 and from 1872 to 2250, respectively. Disappointingly, the model produces more summer rainfall in Regions 3, 4 and 5, but less rainfall in Region 2, when compared to the observed. This is despite the fact that when averaged over the entire Queensland region, the modelled and the observed show considerably good agreement. This highlights the difficulty in getting the rainfall climatology right in individual catchment areas, and the need to use CCAM to simulate regional rainfall and the associated response to global warming.

Despite the discrepancy in the climatology, the modelled amplitude of the multi-decadal fluctuation is generally comparable to that of the observed. Thus it is suitable for examining the superimposing effect of the multi-decadal fluctuations and the global warming-induced trend. In all regions and in all seasons, the rainfall-decreasing trend has taken rainfall to levels that are lower than those troughs seen in the control run. Thus greenhouse warming is seen to enhance the severity of a multi-decadal-long drying period.

In terms of variability, there are larger swings in the warming run than in the control run, indicating more extreme events, partially as a result of a decreasing climatology. The amplitude, in terms of CV calculated for a 31-year period, also undergoes multi-decadal-scale fluctuations. Power et al. (1999) and Cai and Whetton (2001) have suggested that these fluctuations could be a result of modulation by multi-decadal variability in the Pacific Ocean. In the model, despite the fact that overall the drift is small, the drift in the mid- and high-latitude Pacific Ocean has prevented a proper examination of the possible influence by the Pacific Ocean multi-decadal Oscillation.

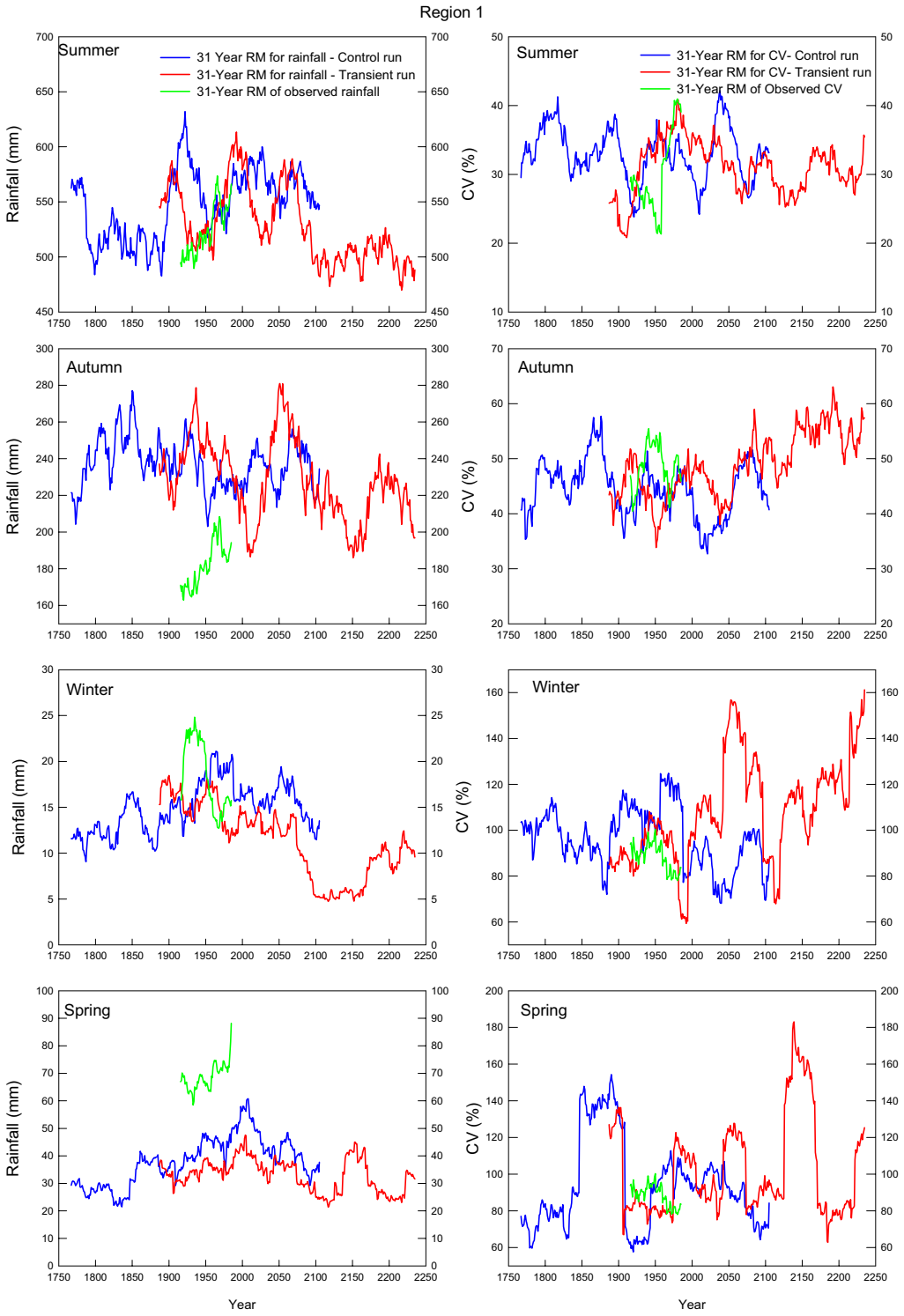

Figure 3.14. *Observed and simulated variations of seasonal rainfall Region 1. From top to bottom, summer, autumn, winter and spring. Left panels show 31-year running averages of seasonal totals, right panels show 31-year running averages of the Coefficient of Variation (CV). Blue curves show results from the control run, red curves show results from the transient run and green curves show observations.*

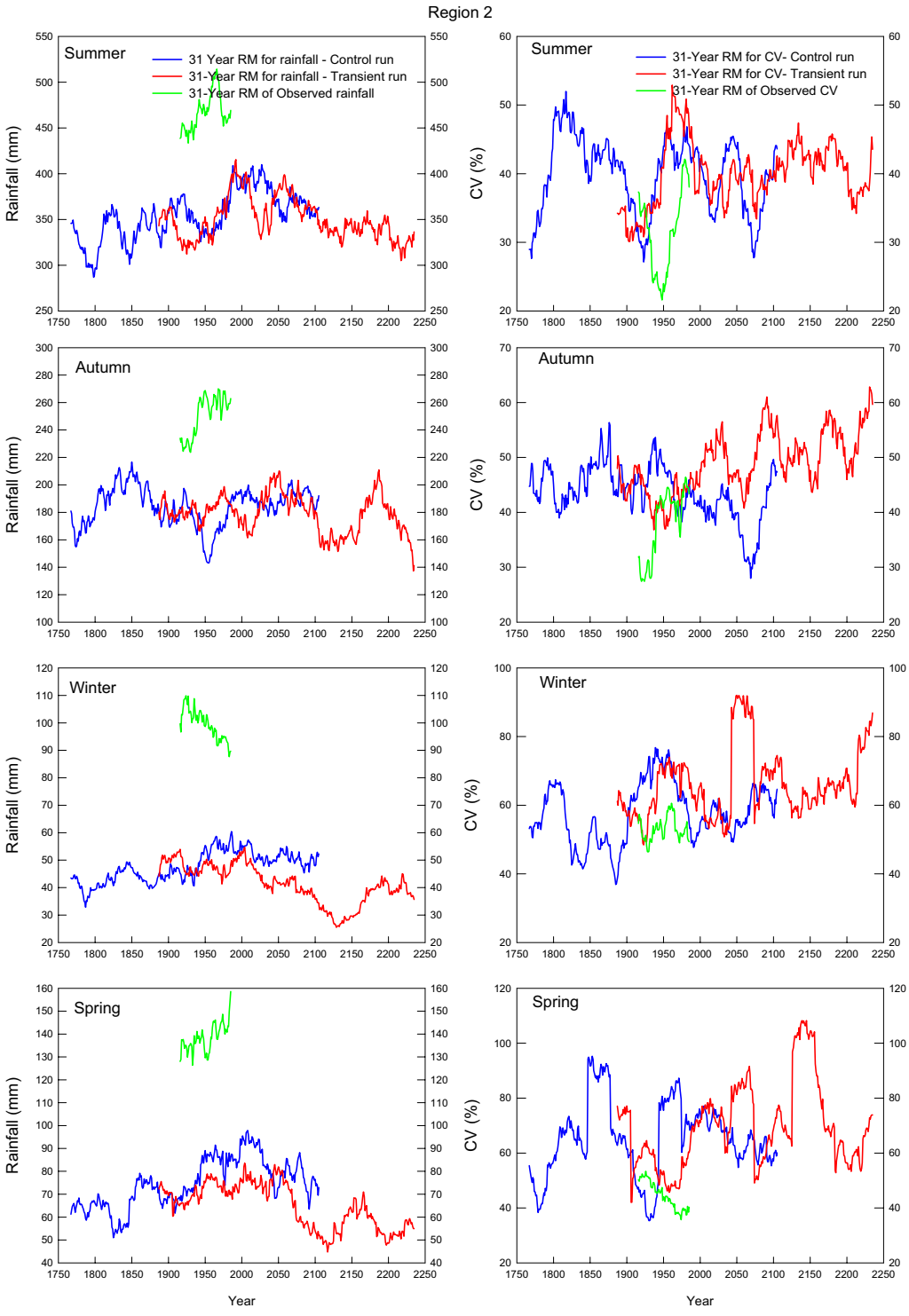

***Figure 3.15**: The same as in Figure 3.14, but for Region 2.*

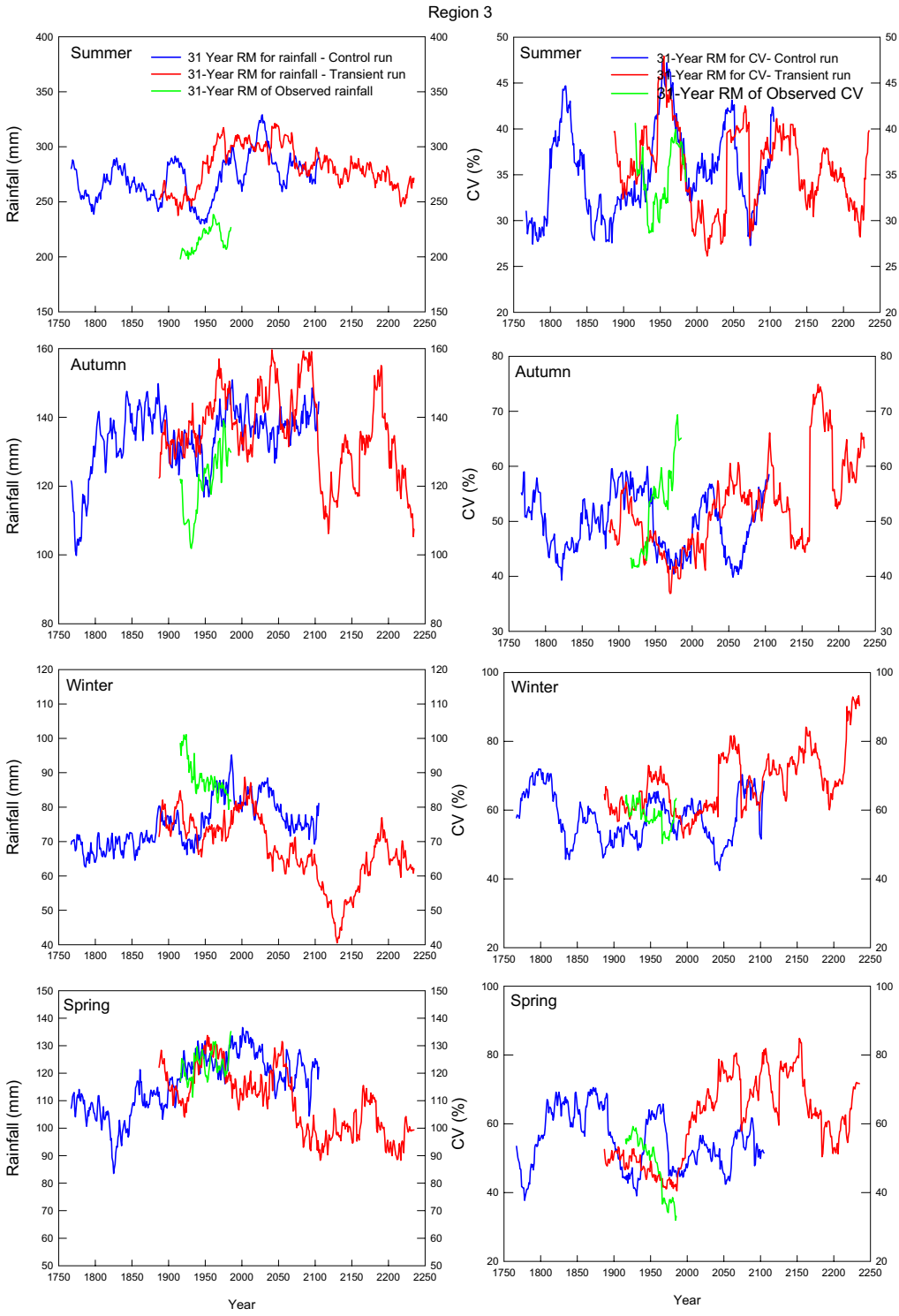

Figure 3.16: *Same as in Figure 3.14, but for Region 3.*

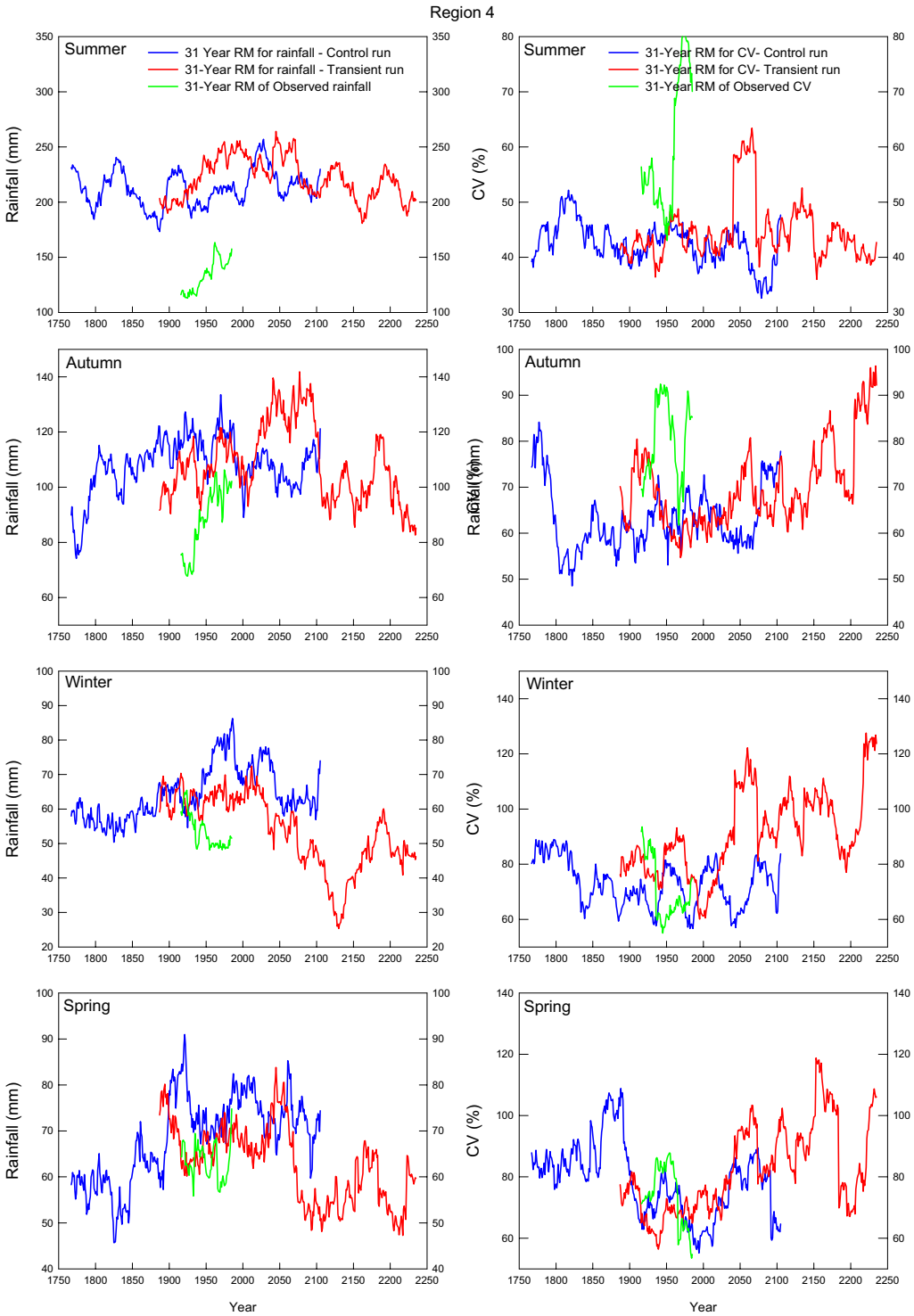

Figure 3.17: *Same as in Figure 3.14, but for Region 4.*

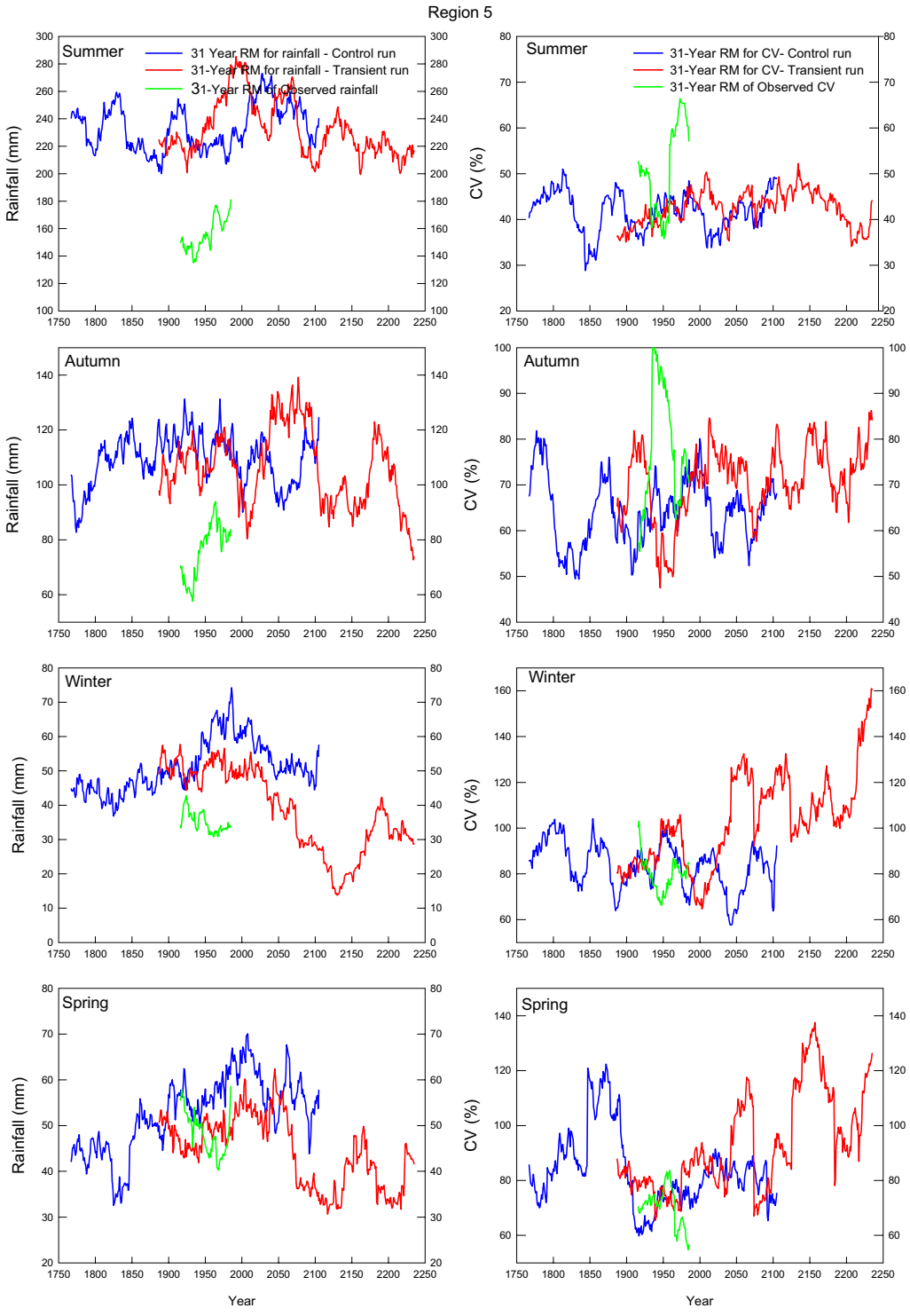

Figure 3.18: *Same as in Figure 3.14, but for Region 5.*

The most impressive feature is that in all regions and seasons, the CV in the warming run has at least one peak that has gone beyond the fluctuating range of the control run. Further, there is a general increase (compare the blue and red dotted curve) in all areas

and this general increase is most evident in winter season, indicating a particularly large range of fluctuations in this season.

Because of the discrepancy between the modelled and observed regional climatology, we return to the rainfall climatology averaged over the entire state to assess the super-imposing effect of multi-decadal variability and the rainfall decreasing trend. Upper panel of Figure 3.19 shows the fluctuations of summer rainfall. The three curves are for the control experiment, the observed, and the warming experiment, respectively. Two features that have been noticed before reappear. First, the amplitude of fluctuations in the control run is comparable to the observed, and the graph shows that it is in the range of –10% to +10%. Second, the global warming has caused a decrease, bringing the lower end of the range to about -16%.

The lower panel of Figure 3.19 shows that for soil moisture averaged over Queensland. For this field, there is no observation for comparison. Like rainfall, soil moisture also varies within the range of –10% to +10%. However, the reduction of rainfall from a trough of -10 % to -16% has caused an incommensurate reduction in soil moisture bringing the low end of the range from –10% to -25%, reinforcing the nonlinear influence of a decreasing rainfall on soil moisture.

Figure 3.20 shows the equivalent of Figure 3.19 but for the winter season. Rainfall in this season is low, and is more variable, in the range of –20% to + 20%. Greenhouse warming has brought the low end of the range to –80%. One the other hand, because it is cold, the evaporation is at its annual minimum and fluctuates within a small range (–10% to 10% against a rainfall range of -20% to +20%). Consistently, in the warming run, despite a maximum decrease of rainfall of up to 80%, soil moisture decreases only some 30%.

Overall, the model simulation with global warming forcing produces a greater agreement with observations in terms of rainfall change, which shows a decrease since 1950s. This supports the view that recent rainfall trends have a strong greenhouse–induced signal. In section 4, we demonstrate that majority of global climate models produce a drying trend into year 2030 and beyond.

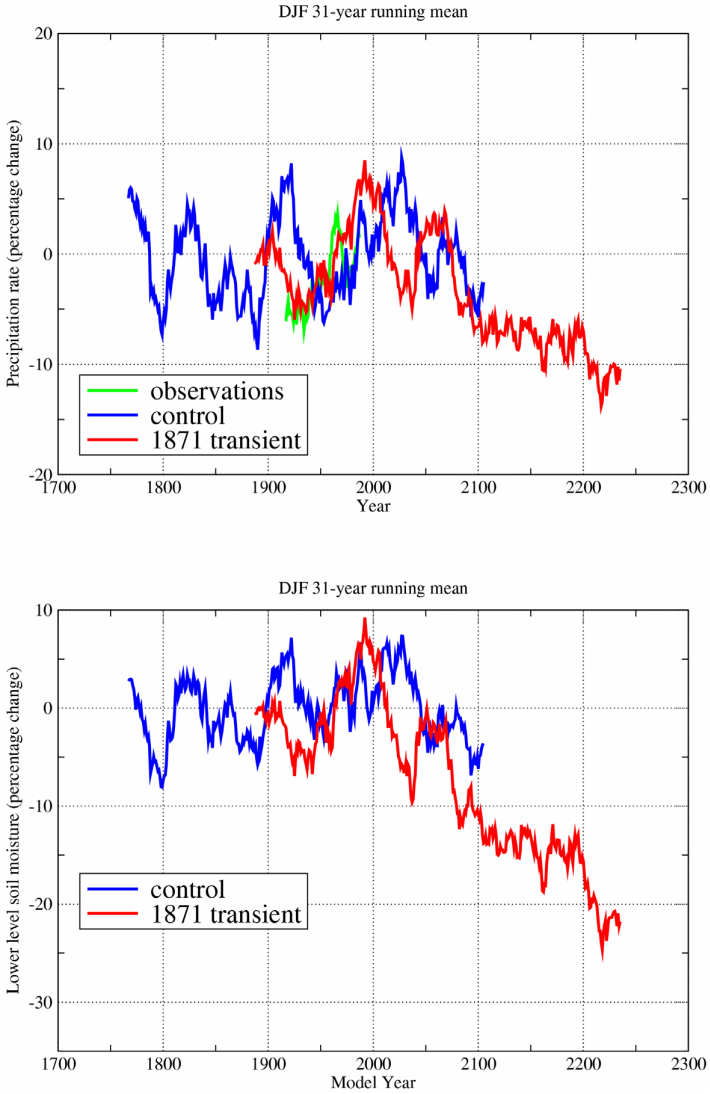

***Figure 3.19**: Upper panel, time series of multi-decadal-scale summer season rainfall fluctuations averaged over the entire Queensland region and expressed as the percentage of summer season climatology for the observed, the control run, and the warming run. Lower panel, the same as the upper panel but for summer season soil moisture 30 m below the surface. No observations of this field are available*

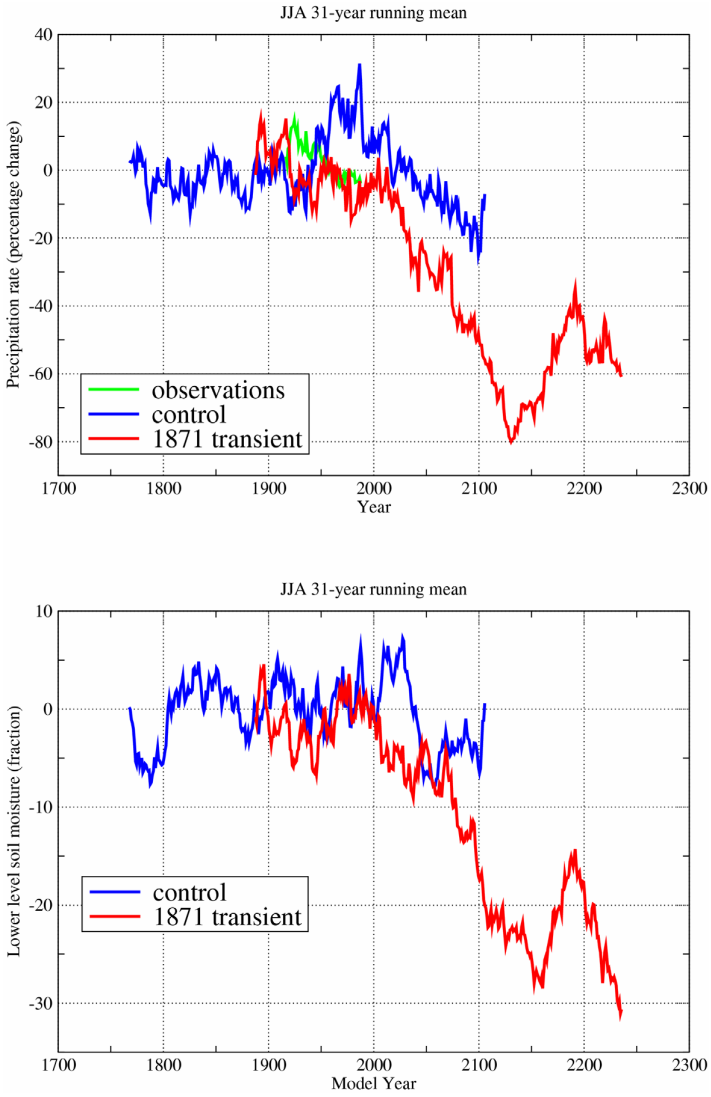

Figure 3.20: *Same as Figure 3.19, but for winter season.*

3.6 The response of ENSO amplitude to global warming

In the 2002 report (Walsh 2002), we used outputs of an early warming run (forced from 1961 onward) to address the response of ENSO frequency to global warming. At the time outputs of 80-year data were used, it was concluded that there is little change in terms of ENSO frequency.

Since then, the control run has been extended to 260 model years, and a new warming experiment (which is the basis of this report), in which the CO_2 forcing starts at year 1871, has been run for 360 years. The output over the longer period provides an

opportunity to re-address this issue. Figure 3.21 shows the spectral distribution of both the control (Figure 3.21a) and the warming run (Figure 3.21b). In both panels spectral peaks are seen, each representing a frequency at which ENSO cycles take place. The peak corresponding to 2-year cycle and 50-month (60-month) are highlighted. While the 60-month peak in the control climate seems to be replaced by a 50-month peak in the warmed climate, there is generally no definite change in the distribution, confirming that ENSO will be a robust mode of climate variability under a warmer climate.

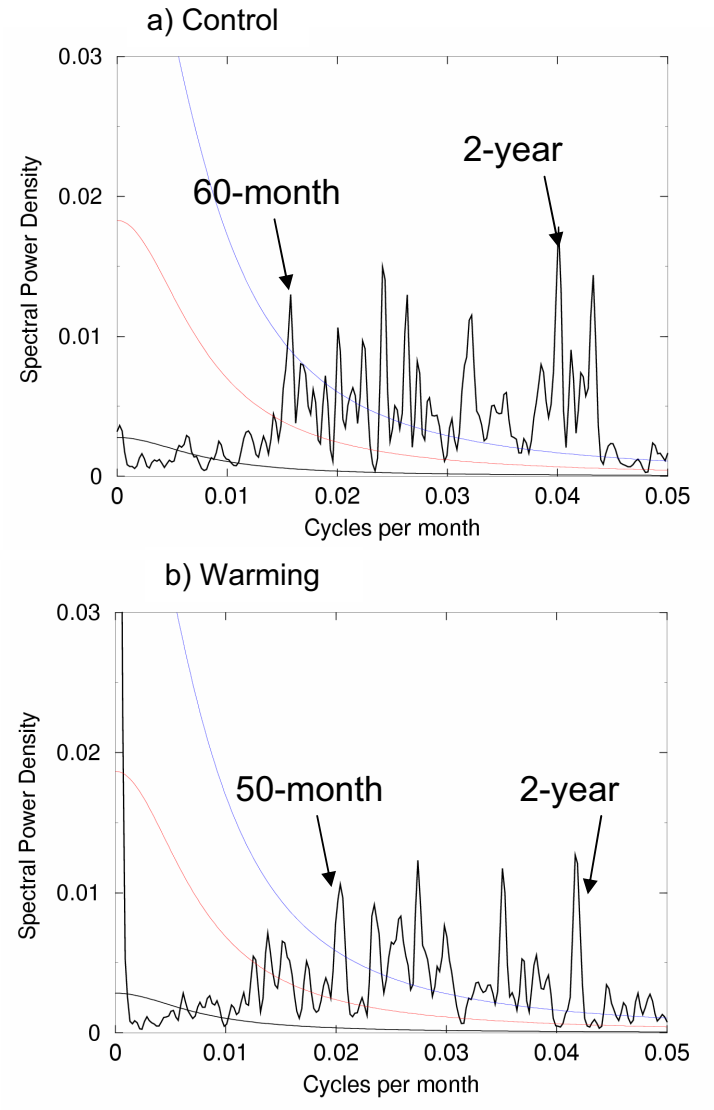

Figure 3.21: *Power spectrum of the Nino 3.4 index in (a) the control and (b) the warming run.*

However, there is a tendency for the low frequency signals to be suppressed (Figure 3.21b). It is not clear whether this change in the frequency distribution is significant as this is obtained from only one experiment. If it is robust, it may indicate that ENSO may be more frequent as the occurrence of low frequency cycles reduces.

These multi-century-long experiments also allow us to examine the possible changes in ENSO amplitude. This however needs to be addressed in the context of a mean state. In Cai and Whetton (2000, 2001) it was found that, in our model run forced by the IS92a emission scenario, since 1970s mean state change in temperature shows an El Nino-like pattern. Such an El Nino-like warming pattern is also obtained in the warming run using the Mark 3 coupled model.

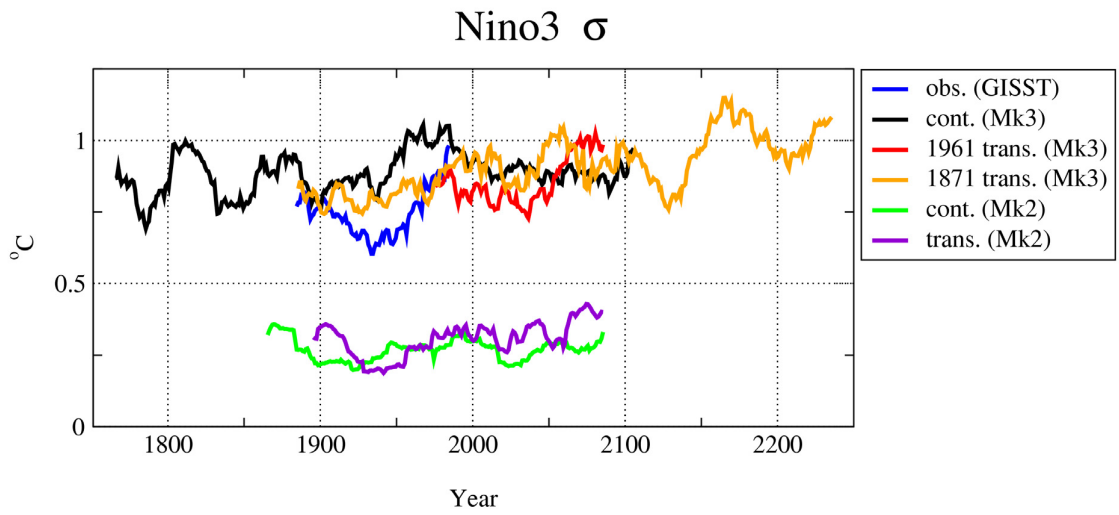

Figure 3.22: *31-year average of the Nino3.4 SST index. Blue curve shows observations, black curve shows the results from the Mark 3 control run, red curve shows the results from the Mark3 transient run started in 1961, yellow curve shows the results from the transient run started in 1871, green curve shows the results from the Mark 2 control run, and the purple curve shows the results from the Mark 2 transient run.*

Time series of standard deviation of Nino3.4 index using a 31-year sliding window for various experiments, including two using the Mark 2 model are plotted in Figure 3.22. Because all the model time series are referenced to a control run climatology.

As already explained, the amplitude in the Mark 2 (purple and green curves) is much weaker. The warming experiment used for this report (orange curve) shows a slight upward trend suggesting that the El Nino-like warming pattern in the mean state will make El Nino events a bit stronger

4 Assessment of Climate Models' ability to simulate Queensland rainfall

The development of climate change projections on a regional scale relies on the analysis of as many GCMs and RCMs as feasible to ensure that uncertainty due to the climate sensitivity inherent in different models is captured. A prerequisite for the inclusion of a GCM into the climate projections is that it adequately simulates present climate conditions. In this chapter, an assessment is made of the ability of the range of available climate models to simulate current climate based upon the climate

variables of MSLP, average temperature and rainfall. Table 4.1 presents some key details pertaining to the simulations and data availability of the models considered.

Table 4.1: *Climate model simulations analysed in this report. Further information about the non-CSIRO simulations may be found at the IPCC Data Distribution Centre (http://ipcc-ddc.cru.uea.ac.uk/). Note that DAR125 and CC50 are Regional Climate Models.*

Centre	Model	Emission Scenarios post-1990 (historical forcing prior to 1990)	Years	Horizontal resolution (km)	Temporal resolution available
CSIRO, Australia	Mark2	IS92a, SRES A2 (four simulations), SRES B2	1881–2100*	~400	daily
CSIRO, Australia	DAR125 (RCM)	Nested in Mk2 with IS92a	1961-2100	125	daily
CSIRO, Australia	CC50 (RCM)	Nested in Mk2 with SRES A2	1961-2100	50	daily
CSIRO, Australia	Mark3	SRES A2	1961-2100	~200	daily
Canadian CCCM	CCCM1	1% increase in CO_2 p.a.	1900–2100	~400	monthly
Canadian CCCM	CCCM2	IS92a	1961-2100	~400	monthly
DKRZ, Germany	ECHAM3/LSG	IS92a	1880-2085	~600	monthly
GFDL	GFDL	1% increase in CO_2 p.a.	1958–2057	~500	monthly
Hadley Centre, UK	HadCM2	1% increase in CO_2 p.a. (four simulations)	1861–2100	~400	monthly
Hadley Centre, UK	HadCM3	IS92a	1861-2099	~400	monthly
DKRZ, Germany	ECHAM4/OPYC3	IS92a	1860–2099	~300	monthly
NCAR	NCAR	IS92a	1960-2099	~500	monthly

* pre-1990 period common to the SRES simulations

4.1 Average patterns of temperature, precipitation and MSLP

Statistical methods have been employed to objectively and efficiently test the performance of each model's present day climate. Observed and simulated patterns for 1961-1990 were compared for their pattern similarity using the pattern correlation coefficient, and for magnitude differences using the root mean square error (RMS). A pattern correlation coefficient of 1.0 indicates a perfect match between observed and simulated spatial patterns while an RMS error of 0.0 indicates a perfect match between observed and simulated magnitudes. For MSLP, NCEP analyses are used as a basis for comparison while Bureau of Meteorology gridded data is used for temperature and rainfall.

A domain encompassing Australia bounded by 110-160ºE and 10-45ºS was used to test MSLP and the results are presented in Figure 4.1. In these figures, the better the model performance, the closer to the top left hand corner of each diagram the result will lie. The correlation coefficient of most models is above 0.8 indicating that the models simulate the observed pattern of MSLP over the Australian region reasonably well. Most models simulate the pressure magnitudes well in summer and autumn with

the exception of GFDL in both seasons and ECHAM3 in summer. During winter and spring however, RMS error values are larger, particularly for some of the lower resolution GCMs such as ECHAM3, CCM1, CCM2 GFDL and NCAR although the Mark 3 also produces a RMS error greater than 2 hPa.

Figure 4.2 compares the spatial pattern of MSLP in two of the better performing models, DAR125 and HADCM3 and two of the poorer performing models GFDL and ECHAM3 with observations. Clearly DAR125 most closely resembles the observations in terms of both the spatial pattern and magnitudes. HADCM3, while reproducing the patterns well, is biased towards lower pressure across the region. The ECHAM3 is also biased towards lower pressure, particularly in summer and spring, while in the GFDL model, it is higher than the observed.

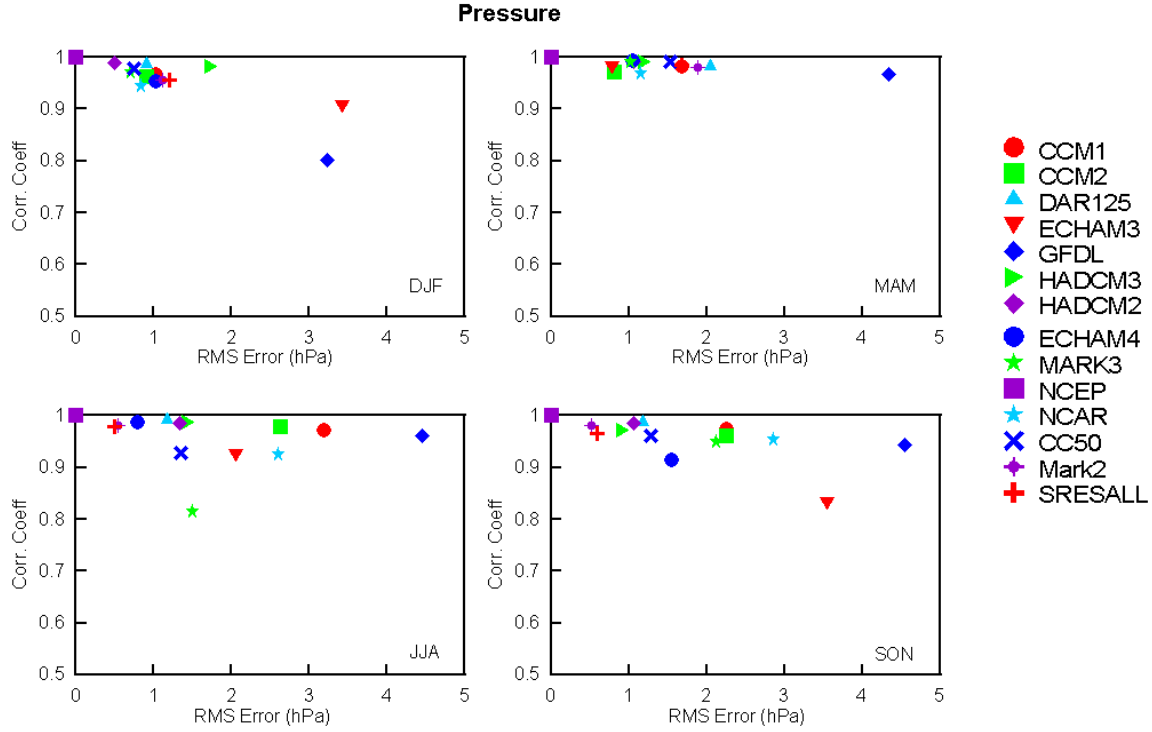

Figure 4.1: *Pattern correlation versus RMS error for mean sea level pressure for each of the models listed in Table 1. Clockwise from top left: summer, autumn, spring and winter.*

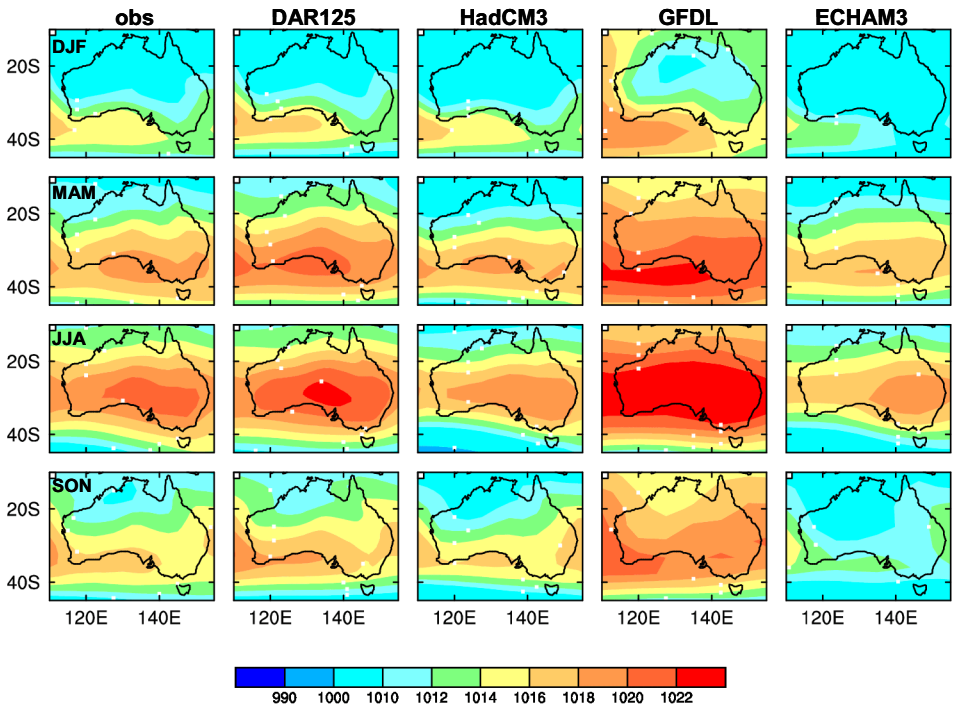

Figure 4.2: *Observed and simulated mean sea level pressure (mb). Top row to bottom row: summer, autumn, winter and spring. Left column to right column: observed, simulated by DAR125, HadCM3, GFDL and ECHAM3 for the period 1961-1990.*

Pattern correlations and RMS errors for temperature are calculated over an area covering Queensland and are shown in Figure 4.3. Note that the agreement between the NCEP analyses and the Bureau of Meteorology analyses are also compared, and indicate that while temperature patterns are generally well represented by NCEP over Queensland, the RMS error is of the order of 1°C in all seasons. Agreement between observed and modelled spatial patterns is poorest in summer when seven of the simulations produce a correlation pattern lower than 0.8. Pattern correlation is generally well captured by all models in the other seasons. RMS errors are largest during winter and spring with the poorest performers being ECHAM3, ECHAM4 and GFDL. The best performers for temperature in all seasons and on both skill scores are HadCM2, HadCM3 and DAR125.

Spatial patterns of observed and modelled temperatures are compared in Figure 4.4 for the same models as in Figure 4.2. The impact of model resolution is well illustrated by this diagram with DAR125 much better able to reproduce the temperature variations influenced by topography.

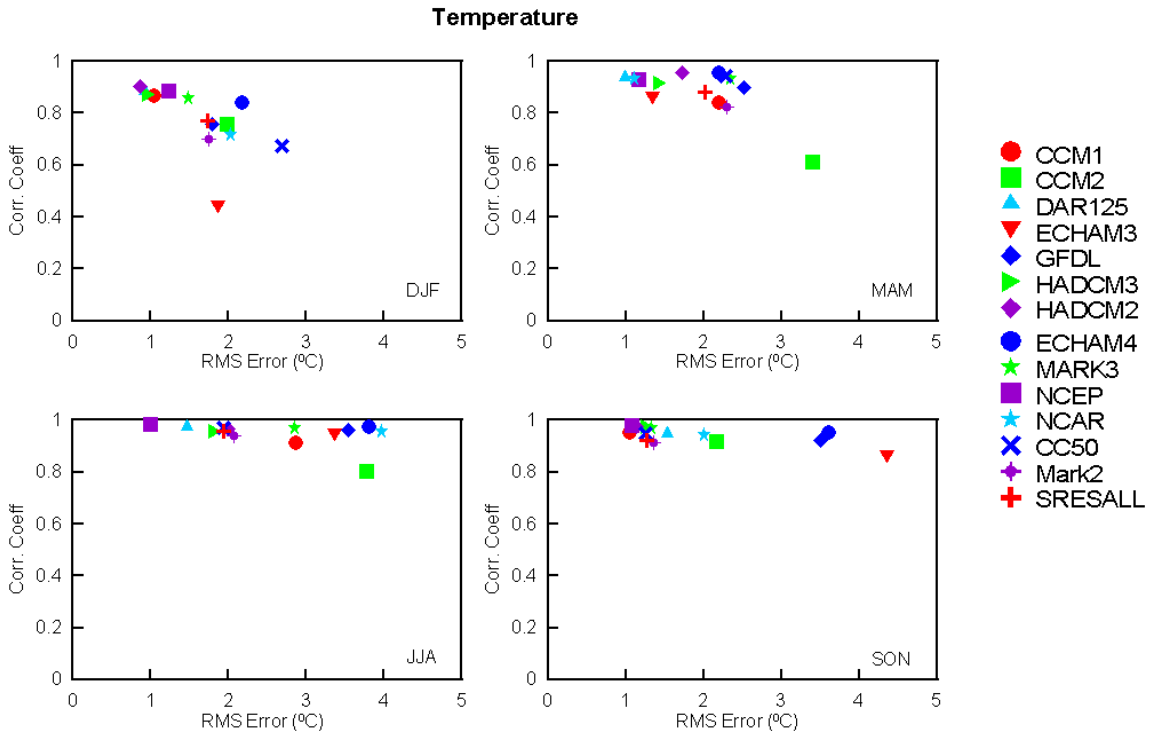

Figure 4.3: As for Figure 4.1 but for temperature.

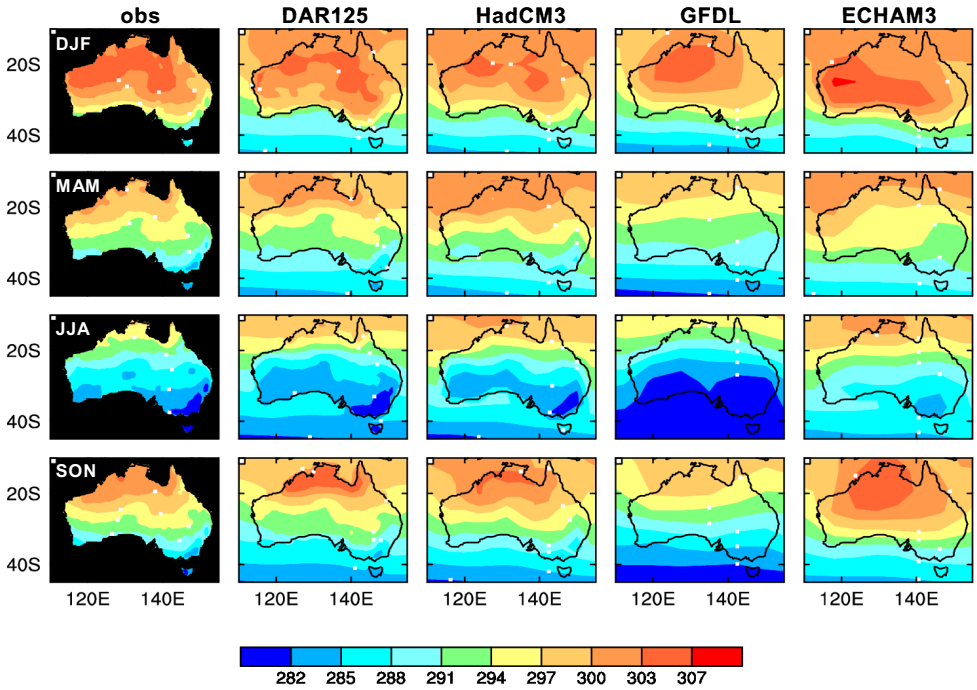

Figure 4.4: *As for Figure 4.2 but for temperature(°K).*

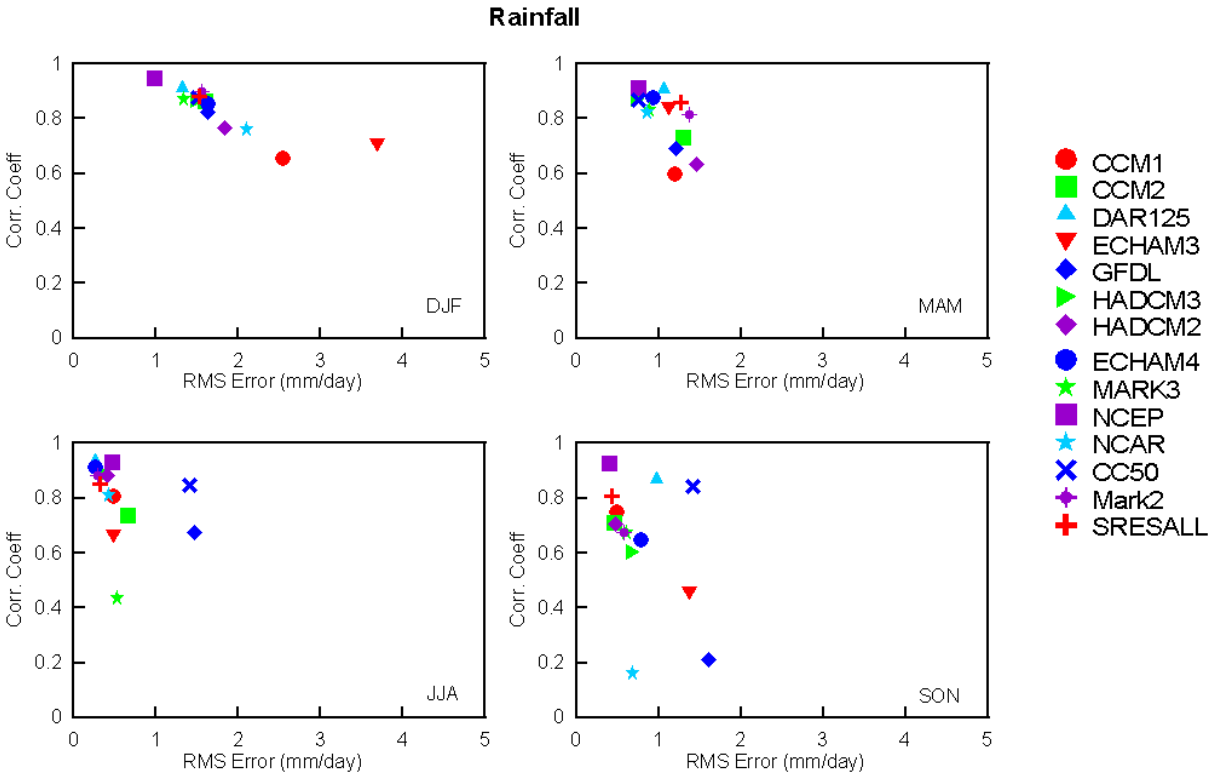

Figure 4.5: *As for Figure 4.1 but for rainfall.*

Figure 4.5 shows the pattern correlations and RMS errors for rainfall. RMS errors are greater in the summer, which is the wettest season of the year with the poorest performing models being NCAR, CCM1 and ECHAM3. For the other seasons, the errors are less than 2 mm day^{-1}. Rainfall patterns, on the other hand, are better captured by the models during the summer with correlations greater than 0.6 and poorest in spring with correlations around 0.2 for GFDL and NCAR. Generally, the lower resolution GCMs do not capture the spatial pattern of rainfall well.

The spatial patterns of rainfall are compared with observations between the two best (DAR125, HADCM3) and two of the poorest performing models in Figure 4.6. While the spatial patterns are well represented in DAR125 and HADCM3, both models are a little too dry in autumn and too moist in spring. GFDL produces too much rainfall across Australia. ECHAM3 shows reasonable agreement to the observations in autumn and winter, but produces too much rain in summer and spring.

These statistics suggest that most models capture the average climatic features reasonably well. However, some models clearly perform better than others. To compare the overall performance of each model, a simple point system based on thresholds was devised. Models with a RMS error greater than 2.0 or with a pattern correlation below 0.8 for MSLP and temperature and 0.6 for rainfall were assigned a point. A maximum of 12 points would indicate failure to achieve these minimum requirements for either pattern or magnitude for each variable in each season. Using this system, the poorest performing models were ECHAM3 and GFDL with scores of eight each. The best performing models were HADCM2, HADCM3, and DAR125

with scores of one and CC50 and Mark2 with scores of two. On the basis of this analysis, it was decided to exclude ECHAM3 and GFDL from the scenario development carried out in the next section.

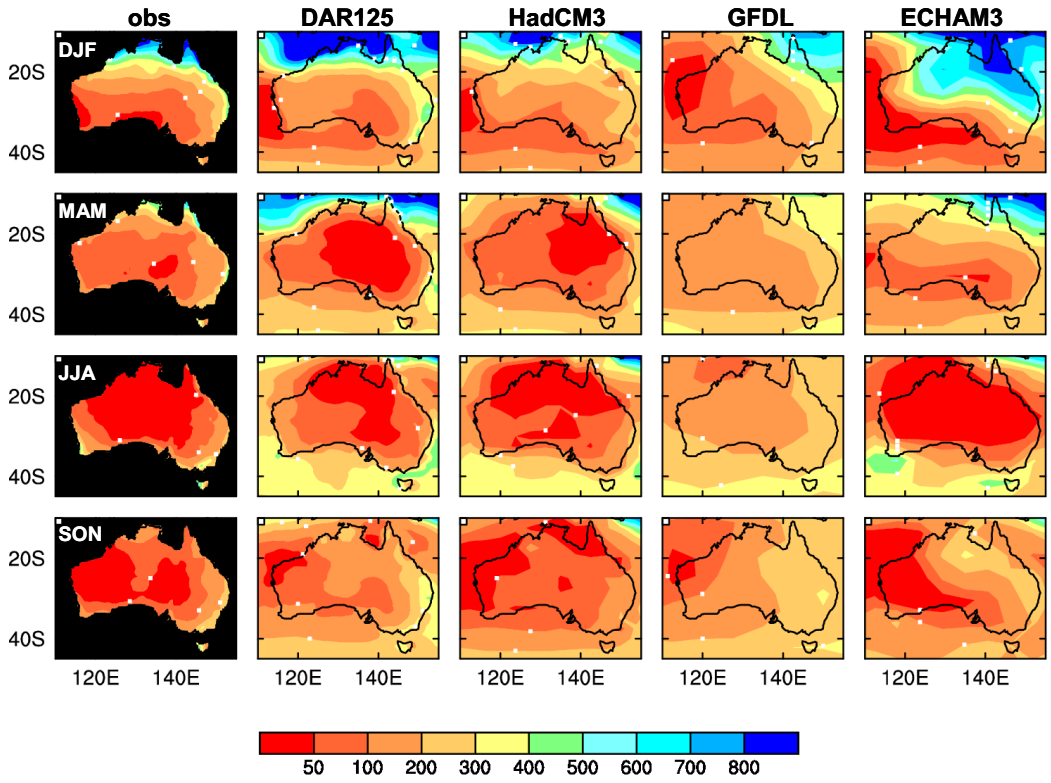

Figure 4.6: *As for Figure 4.2 but for rainfall (mm day^{-1}).*

4.2 Regional average rainfall changes

Uncertainty associated with estimating the sensitivity of rainfall is much higher than it is for temperature. This is for at least three reasons. First, unlike temperature where increases are always indicated, regional rainfall may increase or decrease under enhanced greenhouse conditions. Secondly, the greenhouse signal is much weaker for precipitation than it is for temperature because of the much higher natural variability of precipitation. Finally, the spatial representation of precipitation occurrence by climate models is generally poorer than it is for temperature.

Current GCMs broadly simulate increases in precipitation in mid to high latitudes of both hemispheres and close to the equator and decreases are usually confined to patches in the subtropics of both hemispheres (IPCC, 2001). Figure 4.7 shows the consistency amongst ten current GCMs in the direction of rainfall change across the globe. Note that over Queensland, the models do not portray a clear direction of change with some models indicating rainfall increases and some decreases. Previous

assessments of rainfall change over Australia (e.g. CSIRO, 2001) have all indicated the potential for rainfall decreases, particularly in winter.

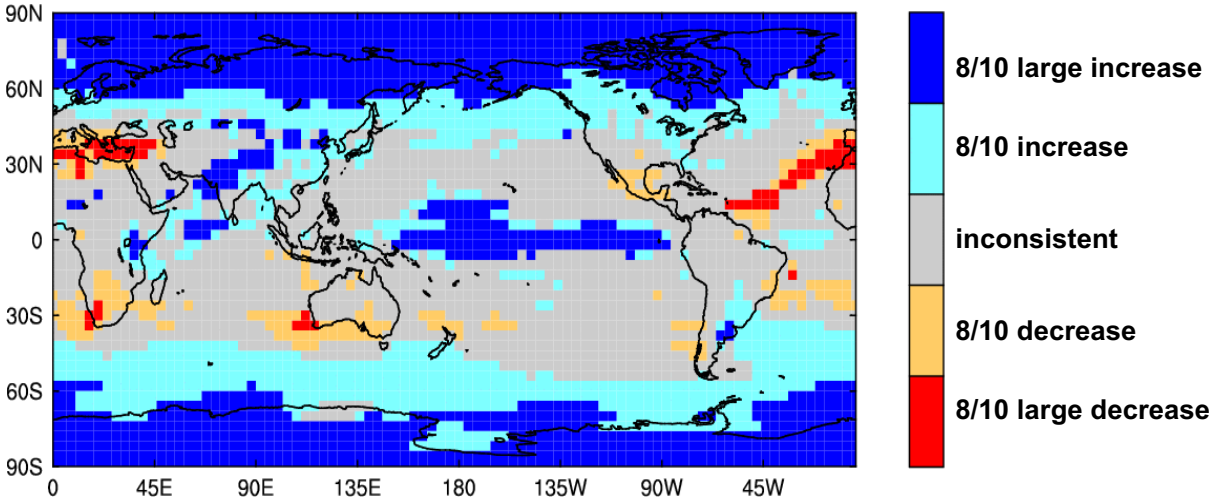

Figure 4.7: *Inter-model consistency in direction of simulated annual rainfall change in ten GCMs (see Table 1). Large changes are where the average change across the models is greater in magnitude than 5% per °C of global warming.*

To explain the patterns of simulated rainfall change, we also examine simulated changes in MSLP. In the annual average, there is broad agreement amongst the models on a pattern of increased pressure in the zone 35-55°S in the Southern Hemisphere (Figure 4.8). The reason for this pattern is not well understood, but there is evidence that the increased pressure is related to the delayed warming in southern high latitudes due to the downward transport of heat by the ocean (see Whetton et al., 1996, Cai et al. 2003). There is also some agreement amongst models on decreased pressure over Australia. Both these features are also present in seasonal analyses, although the increased pressure band extends slightly further north in winter and the decreased pressure over the continent is stronger in summer.

The band of increased pressure to the south of Australia would weaken the westerlies across southern Australia. On the other hand the tendency for lower pressure over the continent may increase rainfall, particularly in summer when this feature is more evident.

Figure 4.8 also shows a tendency for pressure to be decreased over the eastern tropical Pacific and increased in the western tropical Pacific. This pattern may be viewed as the atmospheric response to the El Niño-like warming pattern simulated by most models in the Pacific (see Cai and Whetton 2000, 2001), and based on the analogy of El Nino, rainfall reductions may be expected in the Australian region. However, this feature may be less relevant to Australian rainfall than the analogy would suggest, and other factors such as increase moisture-holding capacity of the atmosphere is also at work. Further, unlike the pattern of change during an El Nino event, the area of pressure increase does not extend far enough to the west to affect the Australian continent.

Finally, it should be noted that the discussion above assumes that atmospheric circulation and rainfall are realistically simulated in current GCMs. Although, the

analysis presented section 4.1 indicated that this was broadly true, it was also noted that some models showed some unusual features.

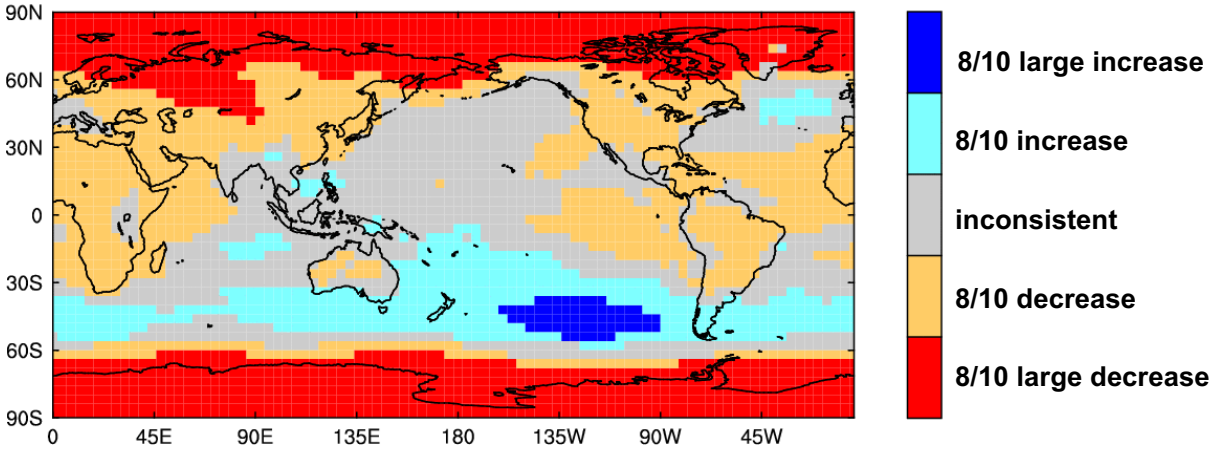

Figure 4.8: *As for Figure 4.7 but for annual mean sea level pressure.*

A useful way to compare the various models' simulation of rainfall due to global warming is to calculate the rainfall change relative to the global warming. This is achieved by linearly regressing the local rainfall against smoothed global average temperatures. The annual changes in rainfall, presented as a percentage change per degree C of global warming for the twelve models, are shown in Figure 4.9. There is considerable model-to-model variation in the direction of change with some models indicating an increase in rainfall of up to 10 % (e.g. GFDL, ECHAM3, ECHAM4 and DAR125) while the other tend towards decreases of up to 10 % over Queensland. CC50 shows the strongest decreases reaching 20% in the west of the state.

A seasonal breakdown of rainfall change per degree C of global warming is shown in Figure 4.10. Summer and autumn show similar variation between models as the annual rainfall changes in the previous figure. In winter, ECHAM3 shows a reversal in trend from the previous two seasons to decreasing rainfall while NCAR, on the other hand, reverses from decreasing rainfall in spring and autumn to increasing rainfall in winter. In spring, all models indicate a trend towards decreasing rainfall over much of Queensland.

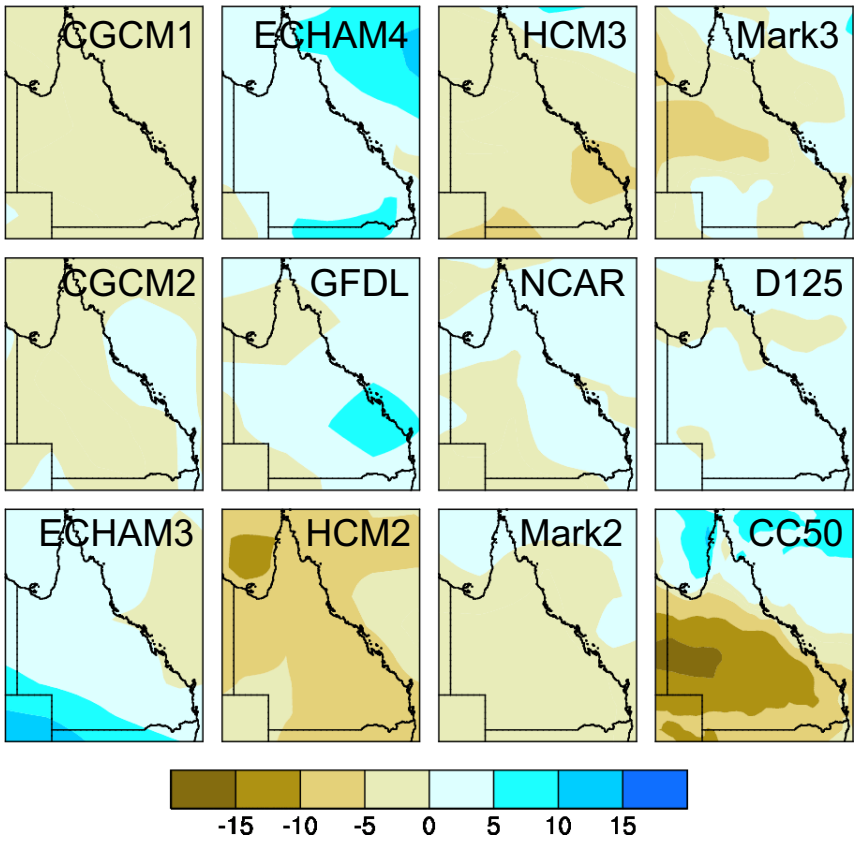

Figure 4.9: *Pattern of annual rainfall change in twelve climate models in percent change per degree of global warming for each season.*

4.3 Projected changes in average rainfall for Queensland

In this section, projections of future rainfall changes in Queensland are presented based on ten of the twelve models shown in the previous section, two models were removed from the suit of twelve due to poor performance. These models were ECHAM 3 and GFDL.

The projections are expressed as a range of change in rainfall. These ranges incorporate the quantifiable uncertainties associated with the range of future emission scenarios, the range of global responses of climate models, and model to model differences in the regional pattern of climate change that were discussed in the previous section.

Figure 4.11 presents the results as colour-coded maps for the changes in average climate conditions by around 2030 and 2070 relative to 1990. These selected dates illustrate changes in average climate that may be expected in the next few decades and the larger changes that may occur towards the end of the century. The conditions of any particular year will continue to be strongly affected by natural climate variability, which cannot be predicted.

Projected annual average ranges tend toward decrease over much of the state by up to 13% by 2030 and up to 40% by 2070. The Cape York Peninsula and a small region in

the south-west of the state indicate that increases or decreases of around 7% are possible by 2030. By 2070, this range increases to 20%.

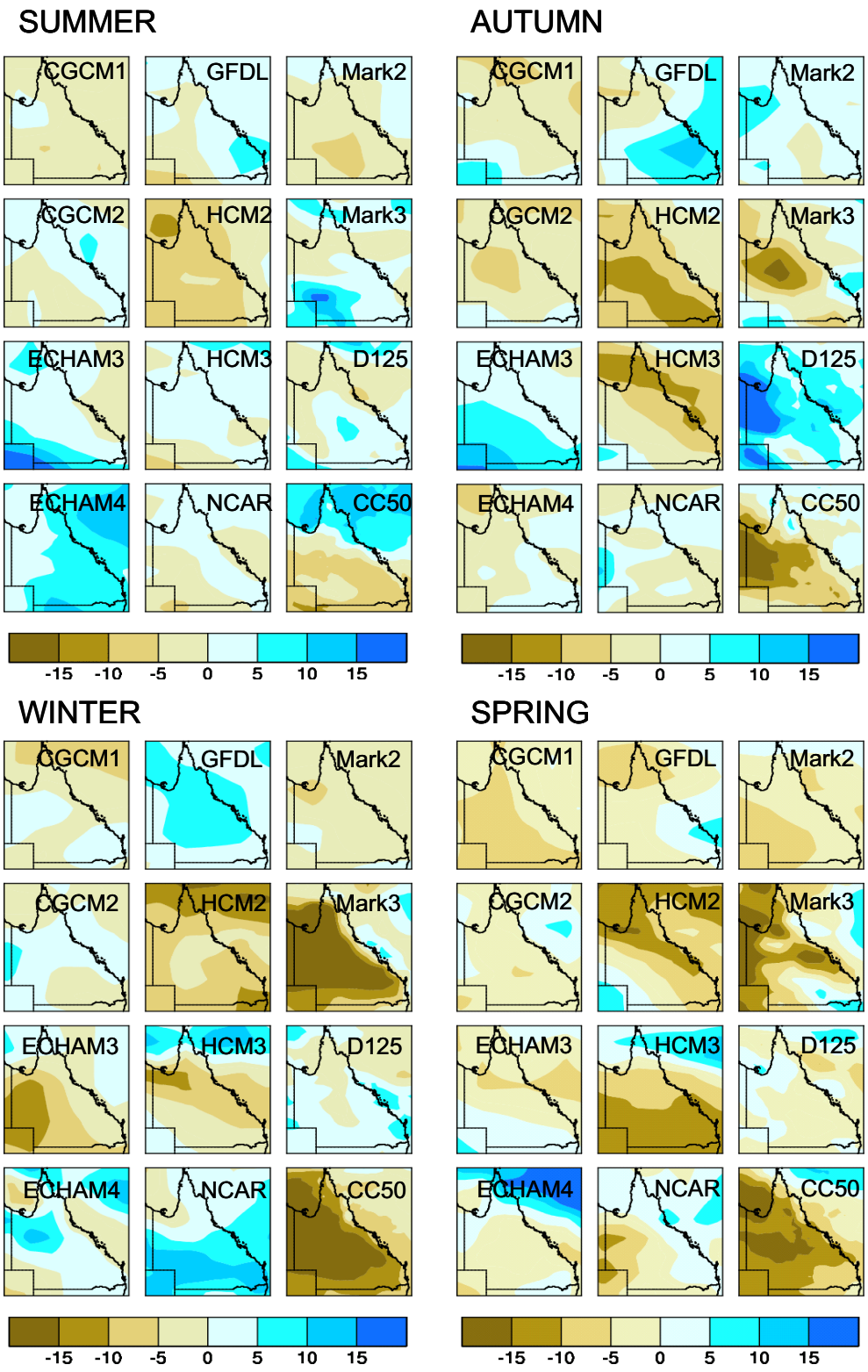

Figure 4.10: *As for Figure 4.9 but for each season.*

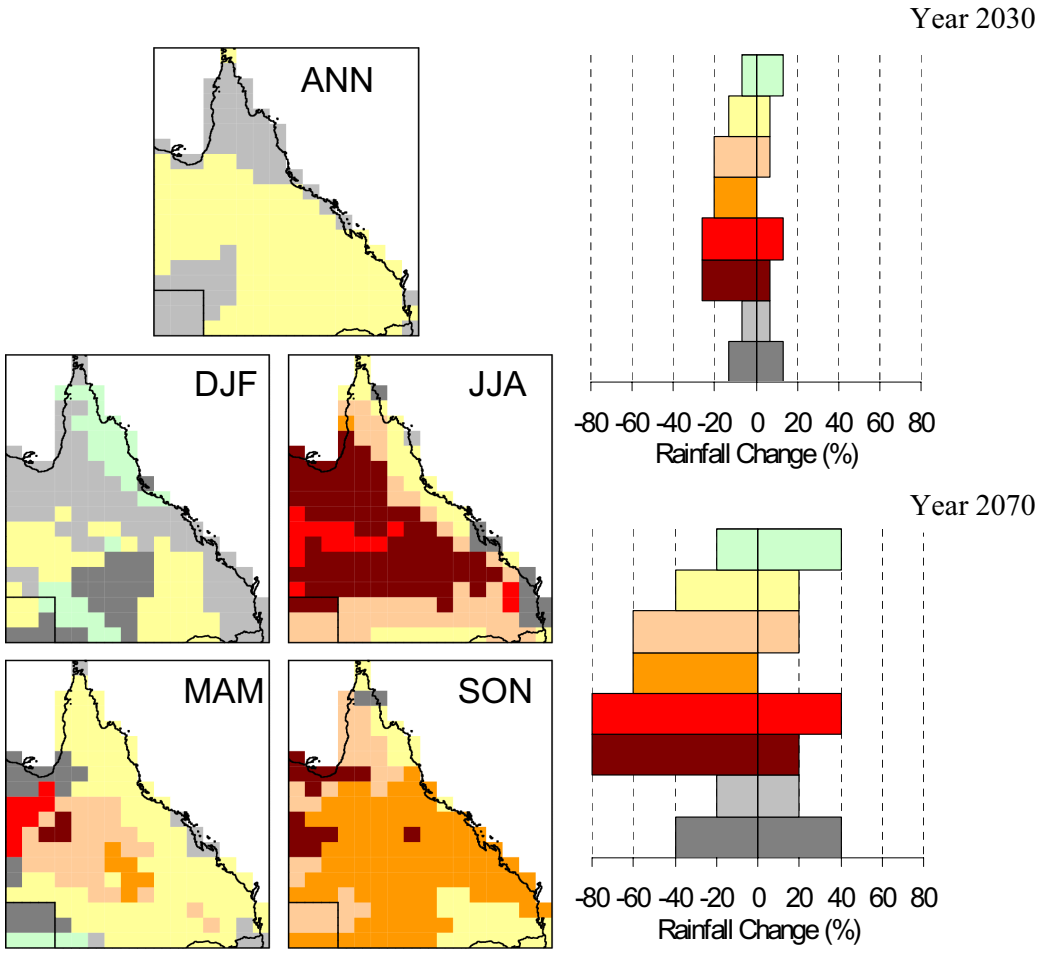

Figure 4.11: *Ranges of average annual and seasonal rainfall change (%) in ten climate models relative to 1990. The colour bars show ranges of change for areas with corresponding colours in the maps.*

In summer, increases or decreases of equal magnitude are possible over much of the state except for the eastern side of the Cape York Peninsula and the south-west of the state where the range of −7% to +13% by 2030 and -20% to +40% by 2070 indicates that there is a greater tendency towards rainfall increases initially, but then the situation reverses. In autumn, there is a tendency toward rainfall decreases over much of the southern and eastern parts of the state in the range of −13% to +7% by 2030, and −40% to +20% by 2070. In the centre of the state, stronger decreases of up to 20% are possible by 2030 and these decreases could be up to 80% by 2070. The strongest possible decreases in rainfall are projected for winter with most of the inland regions projected to change in the range of −27% to +7% by 2030 and −80% to +20% by 2070. Given the low rainfall base in autumn and winter the percentage change in real terms may not be that great and may be surpassed by summer and spring declines, even though the reported percentage change may be smaller. The ranges of change are narrower in the south of the state and along the coastal regions in the east. Over much of the state in spring, rainfall is projected to decrease from 0% to −20% by 2030 and by up to 80% by 2070.

Even though some models show an increase in rainfall, it should be noted that all models for which potential evaporation is available show a significant increase in this parameter over Queensland. Figure 4.12 presents the results for the annual changes in percentage per degree C global warming. The increase is in the range of 2-8% per degree C global warming. Thus even if rainfall does not change, soil moisture will be lower as a result of the increase in potential evaporation.

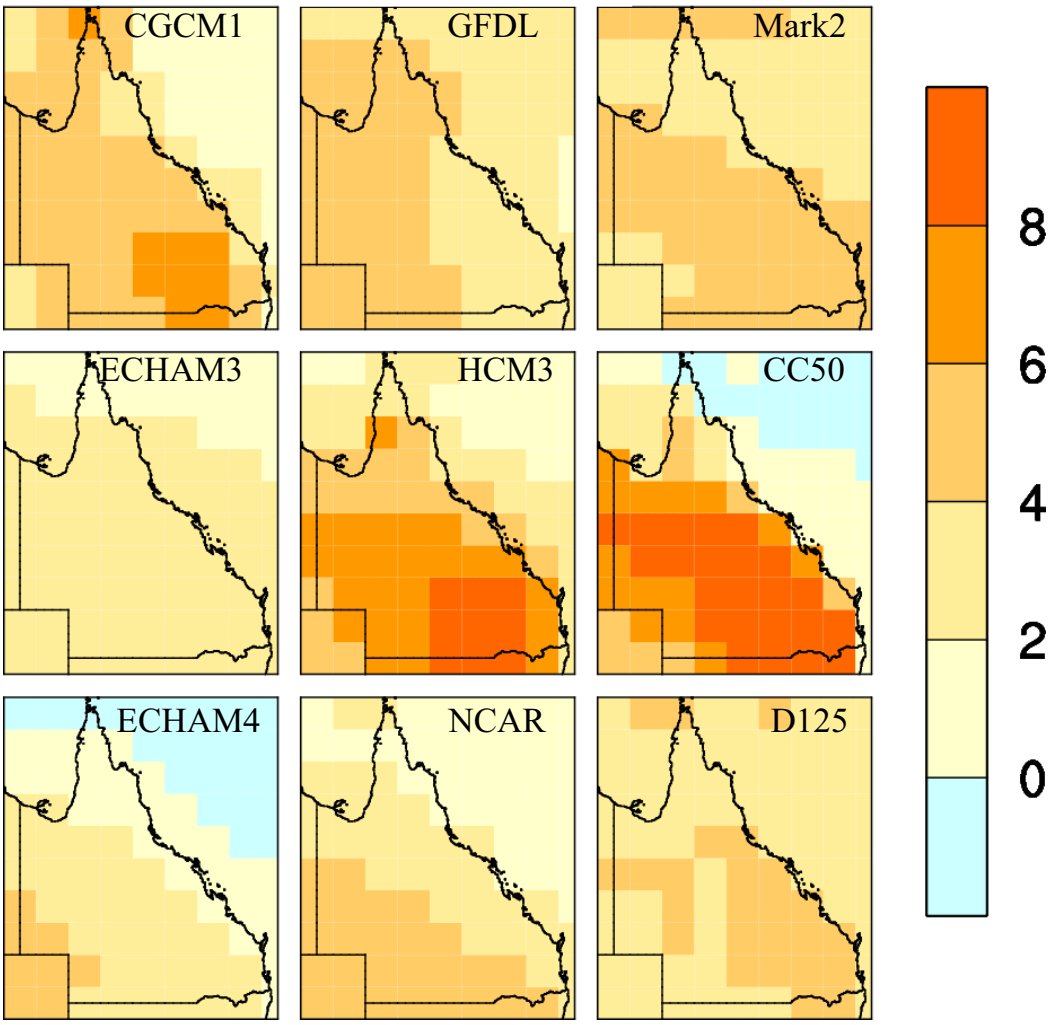

Figure 4.12: *Pattern of annual potential evaporation change in nine climate models expressed in terms of the percentage change per degree of global warming.*

5 Ensemble simulation of greenhouse-induced climatic change over Queensland

5.1 Ensemble results

Two related problems are investigated here: the impact of different CO_2 aerosol scenarios out to 2100 AD, and the impact of chaos within a given CO_2 scenario. This is done using the Mark 2 model, because it is computationally too expensive to use the Mark 3 climate model.

How much the atmospheric CO_2 concentration will increase in the future is unclear, because of the wide range of possible outcomes and controls. For this reason hypothetical CO_2 scenarios have been proposed, known as the SRES.

Four principal scenarios are considered here, A1, A2, B1 and B2, the associated atmospheric CO_2 concentrations are intercompared in Figure 5.1. Each of these scenarios also has a unique atmospheric aerosol concentration, Figure 5.2, which interacts with the model's radiation scheme. Only the direct aerosol effect, in which the aerosol reflects incoming solar radiation, was included in these simulations. No judgment is made here concerning which is the most appropriate and realistic scenario. These scenarios cover a range of the main demographic, economic and technological driving forces of future greenhouse gas and aerosol emissions. For example, the A2 scenario envisions population growth to 15 billion by year 2100 and rather slow economic and technological development. The B2 scenario envisions slower population growth (10.4 billion by year 2100) with a more rapidly evolving economy and more emphasis on environmental protection, producing lower emissions.

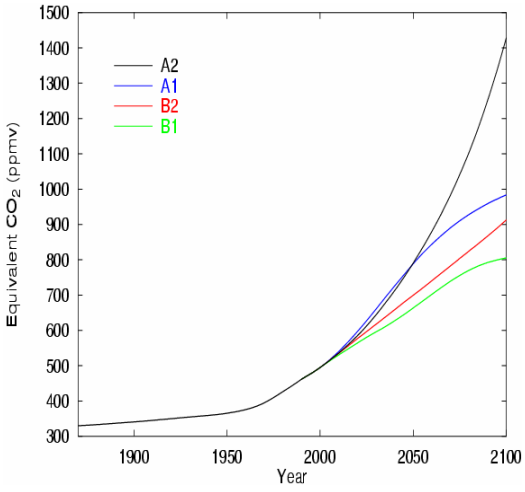

***Figure 5.1**: Equivalent atmospheric CO_2 in the four SRES scenarios.*

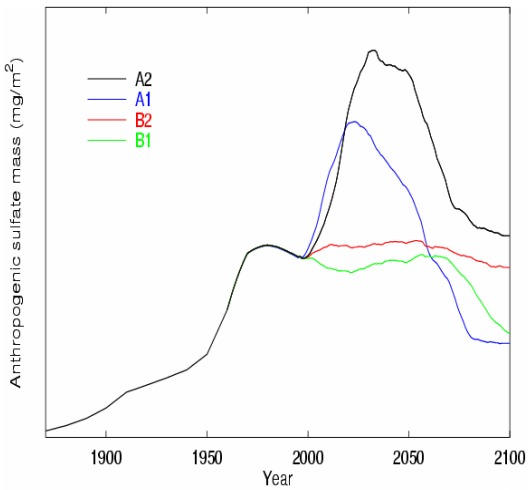

***Figure 5.2**: Annual mean sulphate aerosal burdens for the four SRES scenarios.*

All four scenarios have been used in conjunction with the CSIRO Mark 2 coupled global climatic model to simulate possible climatic changes from 1990 to 2100 AD. These simulations all have a common lead-in period, 1960 to 1990, during which time

observed CO_2 atmospheric concentrations were specified. Two of the scenarios, A2 and B2, have been used to generate 5-member ensembles, which differ only in having different initial conditions specified for 1990.

The response of the SOI, which is a major indicator of interannual climatic variability, is first examined for these SRES scenarios. Figure 5.3 compares the SOI from 1990 to 2100 for all four scenarios, those for A2 and B2 being ensemble mean representations. All four time series are stationary, and there is no obvious response uniquely associated with the greenhouse effect. However, much higher model horizontal resolution is needed to clarify whether the SOI might respond to the greenhouse effect, as the oceanic processes involved are associated with fine spatial scales. Only two sustained, very intense El Niño events are apparent in these results, near year 2043 in the A2 run and near year 2093 in the B1 run. Overall the SOI time series do not suggest a transition to a more drought-dominated Australia under greenhouse conditions (see below). Also, there is no straightforward difference in SOI values which uniquely identifies a behavioural characteristic for any one of the SRES scenarios, despite the widely differing CO_2 growth curves in Figure 5.4. Compared to the observed SOI time series, the greenhouse simulations had less clearly marked transitions between ENSO events. Also the frequency of such events in the CSIRO Mark 2 coupled model is reduced compared with observations.

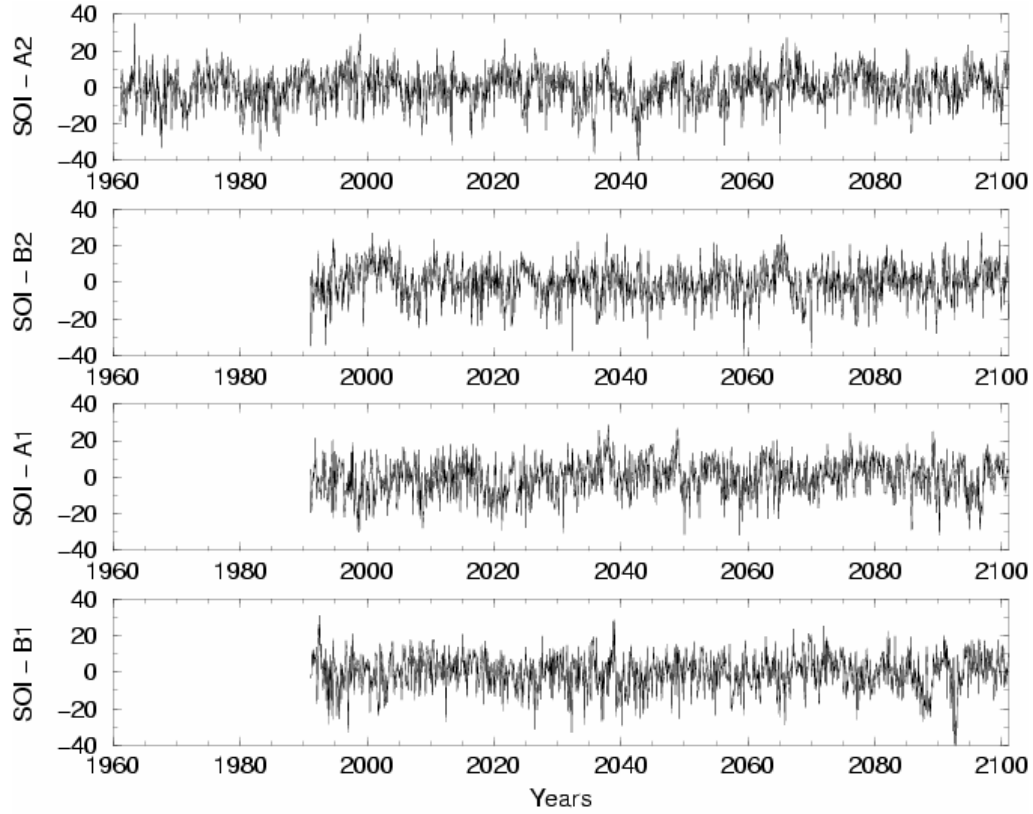

Figure 5.3*: Time series for the simulated Southern Oscillation Index (SOI) from each of four SRES scenario model runs. From top to bottom: A2, B2, A1 and B1. The A2 and B2 results are the means of five-member ensembles simulated with the CSIRO Mark 2 coupled model.*

The influence of chaos on the SOI is demonstrated in Figure 5.4, where the individual members of the A2 ensemble are compared. This figure clearly indicates that in any given year or decade, using a single ensemble member could be misleading.

A broad indication of the rainfall changes associated with the greenhouse effect can be obtained by taking the difference between the means of the last 30 years of the simulation (2071 to 2100) and the 30 year lead-in period (1961 to 1990). The rainfall changes over the Australian region are compared in Figure 5.5 for the four SRES scenarios and the mean of these scenarios. There is an indication in this figure for more widespread rainfall increases across the northwest and centre of Australia. Over Queensland itself, the outcome is for slightly drier conditions.

For a given area over Australia these rainfall changes can vary substantially within a given ensemble. Figure 5.6 contrasts the five members of the A2 scenario, together with the ensemble mean. The difference between the A21 and A22 and A23 ensemble members is quite marked over central Australia. Even over Queensland there are noticeable differences, particularly in the north of the state; compare A21 with A24.

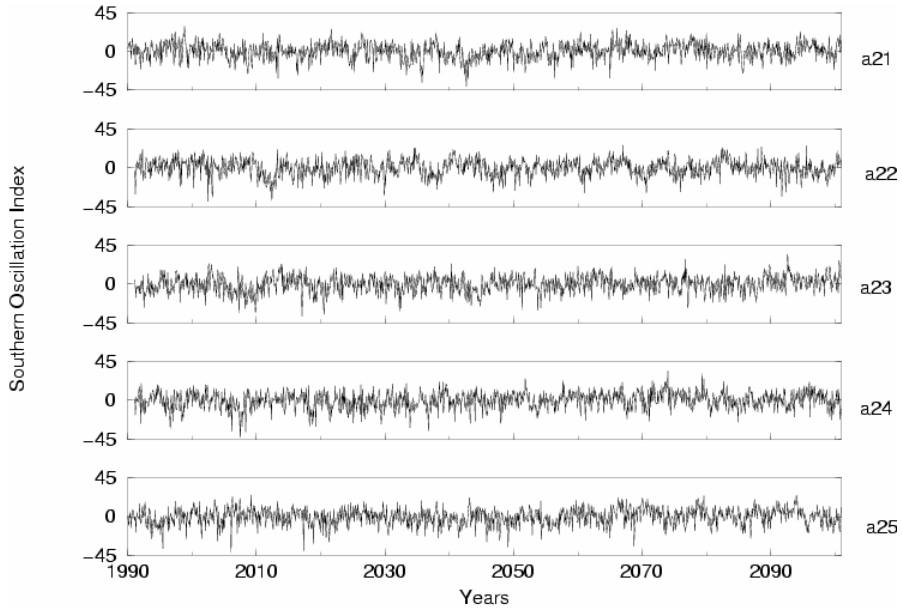

***Figure 5.4**: Time series for the simulated Southern Oscillation Index (SOI) from each of five A2 scenario model runs.*

The soil moisture changes, corresponding to the rainfall changes in Figure 5.5 are shown in Figure 5.8. In general, as expected they reflect the rainfall changes, but overall indicate rather consistent drier conditions in southeast Australia. For Queensland, drier conditions are indicated across all SRES scenarios, particularly B2. Such conditions imply reduced runoff in general.

Examination of soil moisture changes for individual ensemble members for A2 and B2 revealed responses consistent with the rainfall distributions shown in Figure 5.6

and Figure 5.7. Thus substantial increases in soil moisture content across central Australia were indicated for ensemble members A21 and A24, in agreement with the rainfall changes given in Figure 5.6.

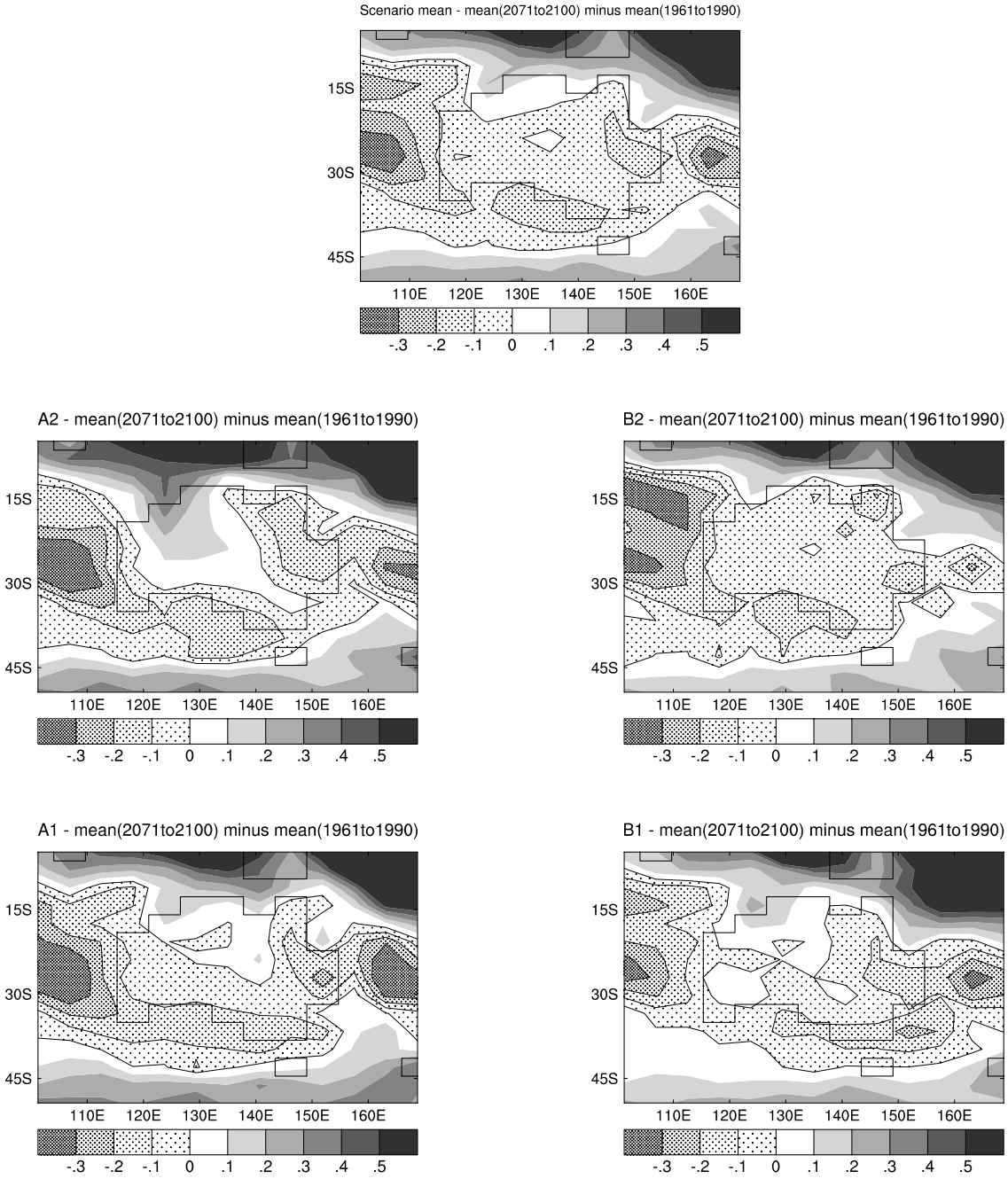

Figure 5.5*: Simulated changes (mm per day) to annual rainfall (2071-2100) relative to (1961-1990).. The bottom four panels show the results from each of 4 SRES scenarios, the top panel shows the ensemble mean result. The A2 and B2 results are means of five-member ensembles.*

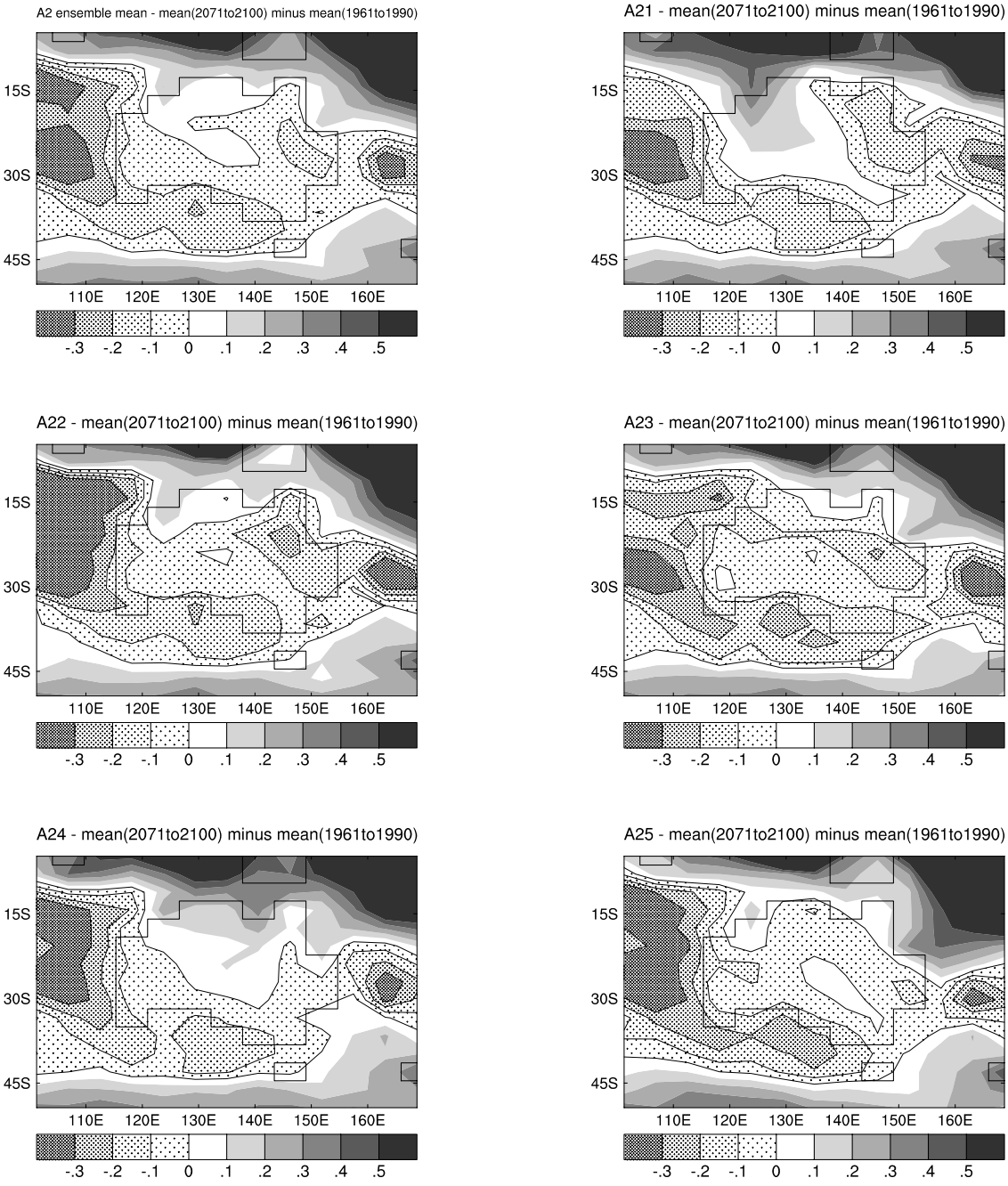

Figure 5.6: *As for Figure 5.5 but for the individual members of the A2 scenario and the ensemble mean.*

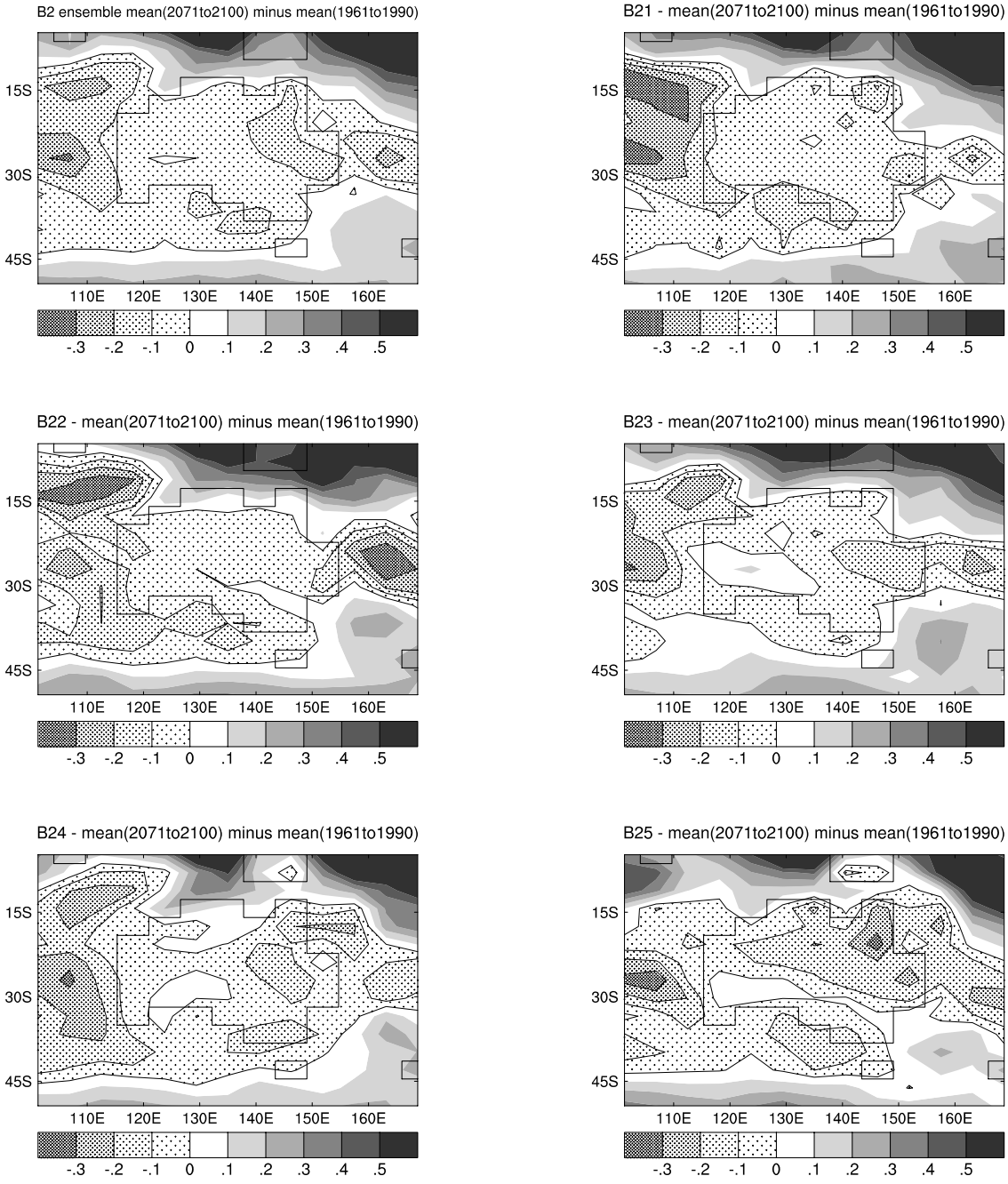

Figure 5.7: *As for Figure 5.6 but for the B2 scenario.*

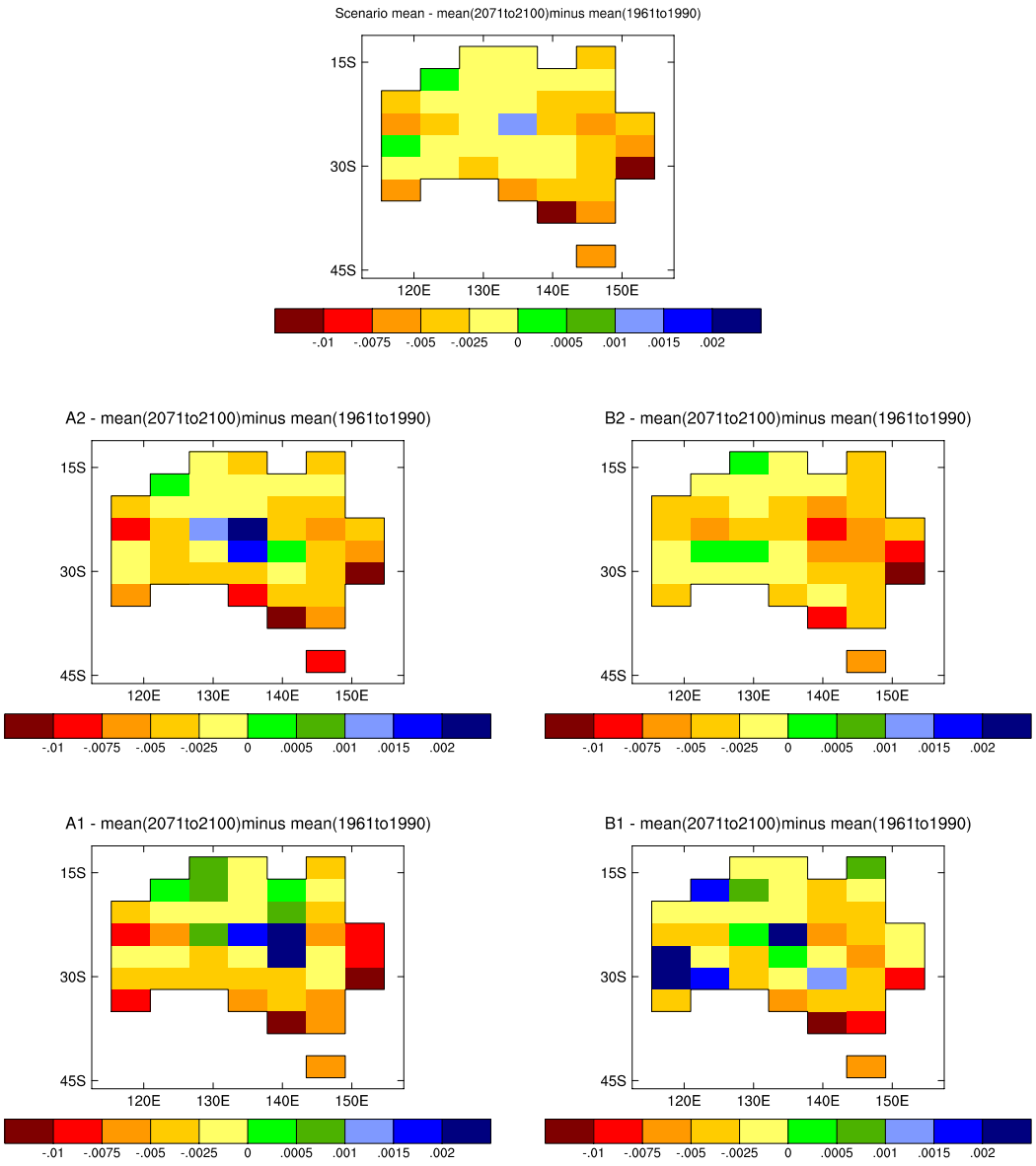

Figure 5.8: *As for Figure 5.5 but for soil moisture (fraction).*

While the preceding figures show an overall drying trend, *in the mean*, over much of Australia associated with the greenhouse effect, the actual situation as regards rainfall variability is far more dynamic than implied in time-mean presentations. This is illustrated in Figure 5.9, where time series of rain averaged over a large region of Queensland (**27°S to 18°S, 140°E to 150°E)** are compared for the four SRES scenarios and the scenario mean. The impression from this figure is one of wide-ranging interannual variability, across all four scenarios. The inter-annual variability for the greenhouse scenario is essentially unchanged from that occurring for 'normal' conditions. The time series for the individual scenarios is shown in Figure 5.9. All show years when rainfall minima (corresponding to droughts) or rainfall maxima (corresponding to enhanced rainfall amounts) occur. Thus from an agricultural

perspective under greenhouse conditions 'good' or 'bad' years can be expected, very much as exist now despite the implied overall drying trend indicated by Figure 5.9. However, from a hydrological perspective some decline in rainfall accumulation might occur despite this interannual variability, because of the increased evaporation rate associated with the higher temperature. This topic needs to be explored in more detail using appropriate catchment models.

Chaotic influences are also important in determining the interannual variability of rainfall within a given SRES scenario. This is illustrated in Figure 5.10, which shows the five individual members of the A2 ensemble plus the ensemble mean for the same Queensland region. In this particular scenario the A22 member exhibited a greater range of interannual variability than the other members. In contrast, the ensemble mean shows limited variability. While the mean is indicative of the overall characteristics, the fluctuations of individual ensemble members are more representative of the likely interannual variability. The problem is that for a given year there is no way of determining what the amplitude of the fluctuation might be. What Figure 5.10 does is provide a sample of the possible range of outcomes available. Similar variability was exhibited by the B2 ensemble.

The differences in rainfall between 'wet' and 'dry' years within a given scenario is shown in Figure 5.11 for scenario A22. For the wet year, 2043, rainfall over most of Queensland was greater than 2 mm per day, ranging up to 4.00 mm per day on Cape York Peninsula. In contrast, in the dry year, 2079, rainfall over most of Queensland was below 1.5 mm/day. The agricultural and water supply situations for such years would be totally different, and effectively this figure highlights the critical, ongoing impact of interannual variability within a greenhouse scenario.

For the selected Queensland region (27°S to 18°S, 140°N to 150°E) the rainfall rate was sampled across all ensemble members on a quarterly basis to determine the most likely rainfall categories. The percentage outcomes for the 500 samples are shown in Figure 5.12, together with observations. For the latter, of course, there is only one sample!

While the simulation reproduces the seasonal variability quite well, the overall comparison with observation is only classified as fair. The model overestimates the rainfall for the highest category in December, January and February, and for the middle categories in March, April and May and also September, October and November. Part of this discrepancy may be attributable to the coarseness of the monthly data. These results are generally better than those obtained from experiments forced by GISST, which will be described in section 5.2.

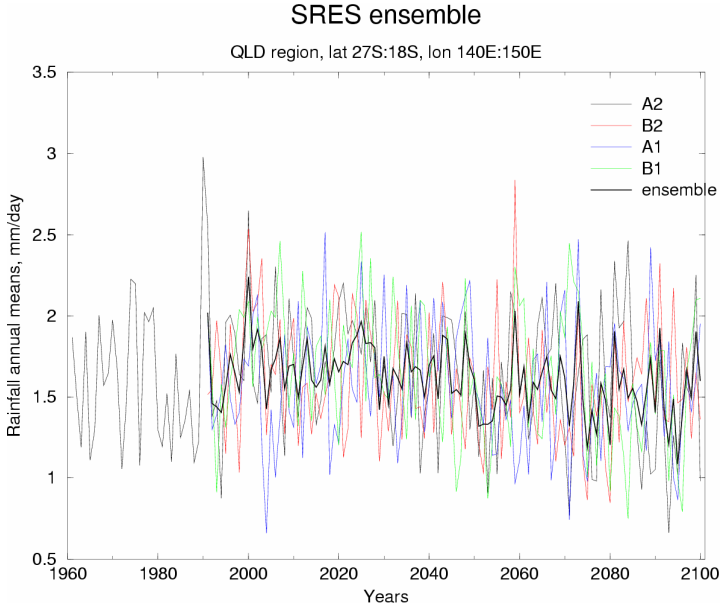

Figure 5.9: *Time series of rainfall for a large region of Queensland for the four SRES scenario members and the ensemble mean.*

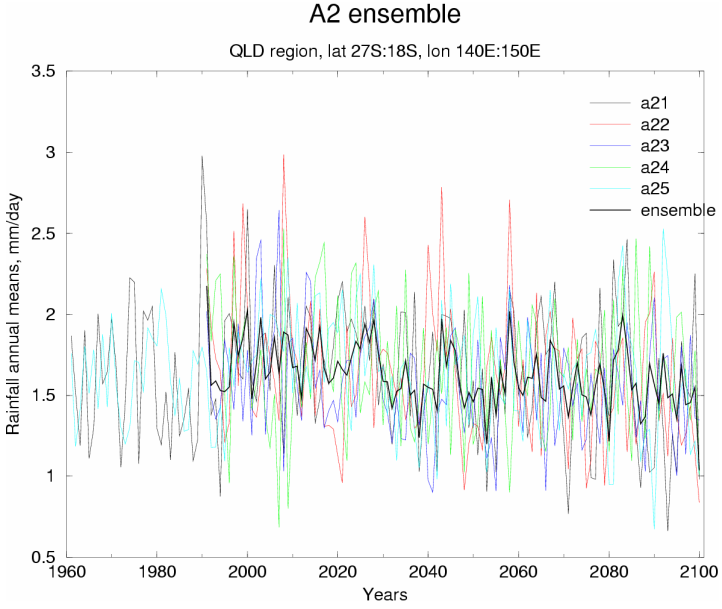

Figure 5.10: *Time series of rainfall for a large region of Queensland for the five members of the A2 ensemble plus the ensemble mean.*

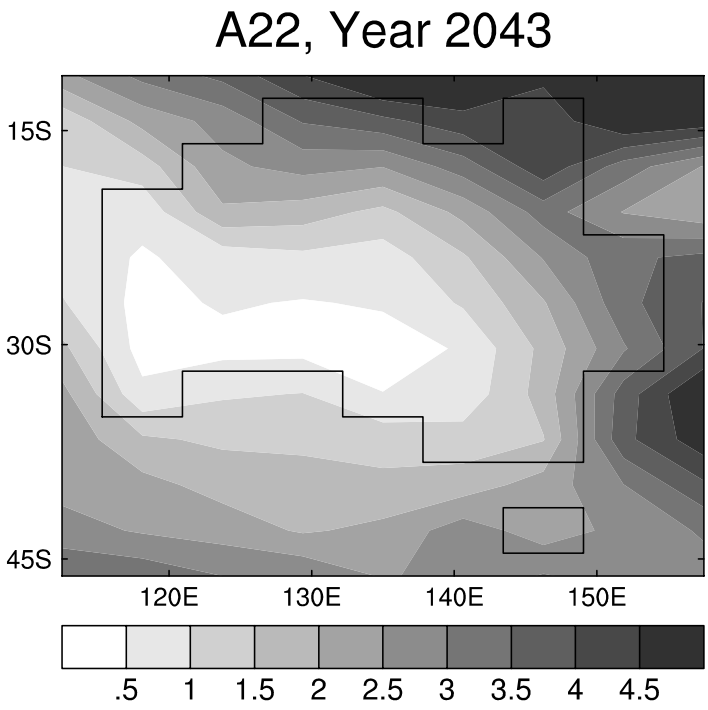

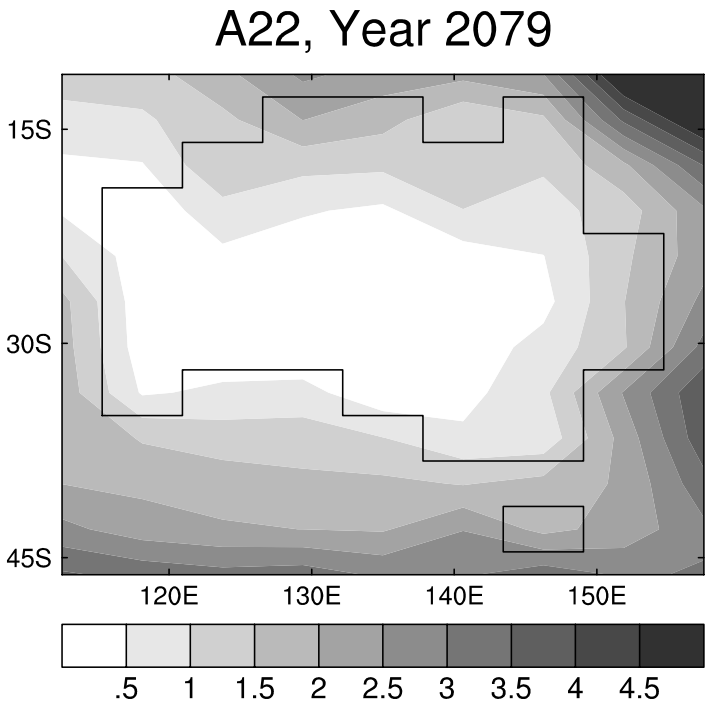

***Figure 5.11**: Annual rainfall simulated for a wet year (2043) top panel and a dry year (2079) bottom panel from one of the A2 scenario runs. (see Figure 5.10 for the corresponding time series over Queensland).*

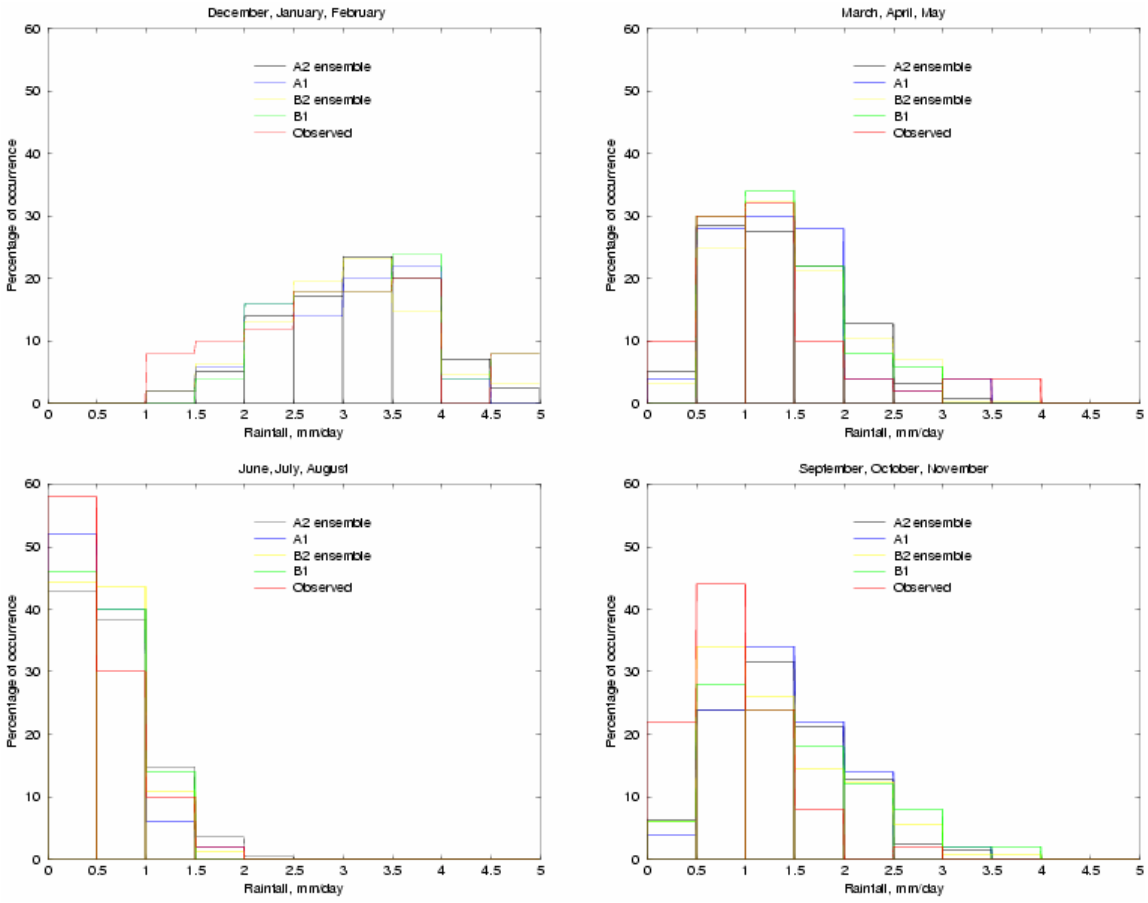

Figure 5.12: *Comparison between observed and simulated frequency distributions of rainfall rates for the Queensland region. Clockwise from top left: summer, autumn, spring and winter. The rainfall rates are based on monthly totals.*

5.2 Chaotic influences on Mark 3 simulations

As part of an informal collaboration with the Queensland DNRM, the Mark 3 atmospheric model has been 'forced' by driving it with observed SST. This is part of an international scientific project involving about ten other research groups.

Two ensembles of simulations were made. The first involved running the model from 1949 to 2000, and the second from 1871 to 2000 using a new version of the gridded SST surface developed by Parker et al. (1995). Both ensembles consisted of five members each one commencing from a different initial atmospheric model condition taken from a previous simulation. Results will be used from both ensembles and also the combined ensemble.

The basic climatology of the Mark 3 model was evaluated by comparing observed and simulated seasonal rainfall over Australia for the period 1949 to 2000. The observed rainfall used was from the Queensland Department of Natural Resources and Mines high resolution dataset (SILO), Figure 5.13. The ensemble mean for the first ensemble from 1949 to 2000 is shown in Figure 5.14. Rainfall in Figure 5.14 is presented for the ocean adjacent to Australia as this illustrates better the rainfall systems to the north of Australia. The model resolution of 1.875° longitude by 1.875° latitude is much coarser than the 1/20° resolution used in the observations, thus much of the detail apparent in Figure 5.13 is missing from Figure 5.14. Nevertheless, the basic seasonal characteristics of Australian rainfall are well-captured by the CSIRO Mark 3 model in atmosphere-only mode.

A broadscale, basic indicator of climatic variability over Australia is the SOI. The SOI is a fairly robust outcome from the Mark 3 model, as shown in Figure 5.15 where the temporal variability of the simulated SOI is illustrated for the five members of the first ensemble together with the ensemble mean. While the presence of chaos is readily discernible in the differences between the various ensemble members, the critical periods where the SOI changes between positive and negative values, associated with either El Niño or La Niña events, is well-defined with a minimum of chaotic variability.

The ensemble mean from Figure 5.15 is compared with observation in Figure 5.16. The observed transition between events is extremely well-captured in the simulation. This feature of the simulation is critically important because of its implications for seasonal prediction. The Mark 3 model is capable of capturing the extreme negative SOI values shown in Figure 5.16 associated with major drought episodes. This is an important feature not realized with earlier versions of the model. More high frequency variability occurs in the observed SOI compared with the ensemble mean in Figure 5.16, especially for small values of the SOI. This difference is partially attributable to the use of the ensemble mean in Figure 5.16 as this smooths out some of the high frequency variability in the simulated SOI. Nevertheless, the month-to-month observed variability has a larger range than that simulated, presumably indicating that finer horizontal resolution is required in the model.

The correlation between the two time series in Figure 5.16 is 0.721, which is significant above the 99.9% level.

A measure of the dispersion between the individual SOI curves in Figures 5.15 and 5.16, and thus of the relative magnitude of the chaos, is provided by the corresponding standard deviation. The temporal variability of this standard deviation is compared in Figure 5.17 with the NINO3.4 (5°S to 5°N, 170°W to 120°W) SST anomalies. Both of these time series have been smoothed with a 10-point running mean in order to eliminate high frequency variability. The resulting correlation between these time series is 0.37, which is significant at 95% confidence level. The significance level suggests that the model is able to produce coherence between SOI and Nino3.4 region, as in the observed.

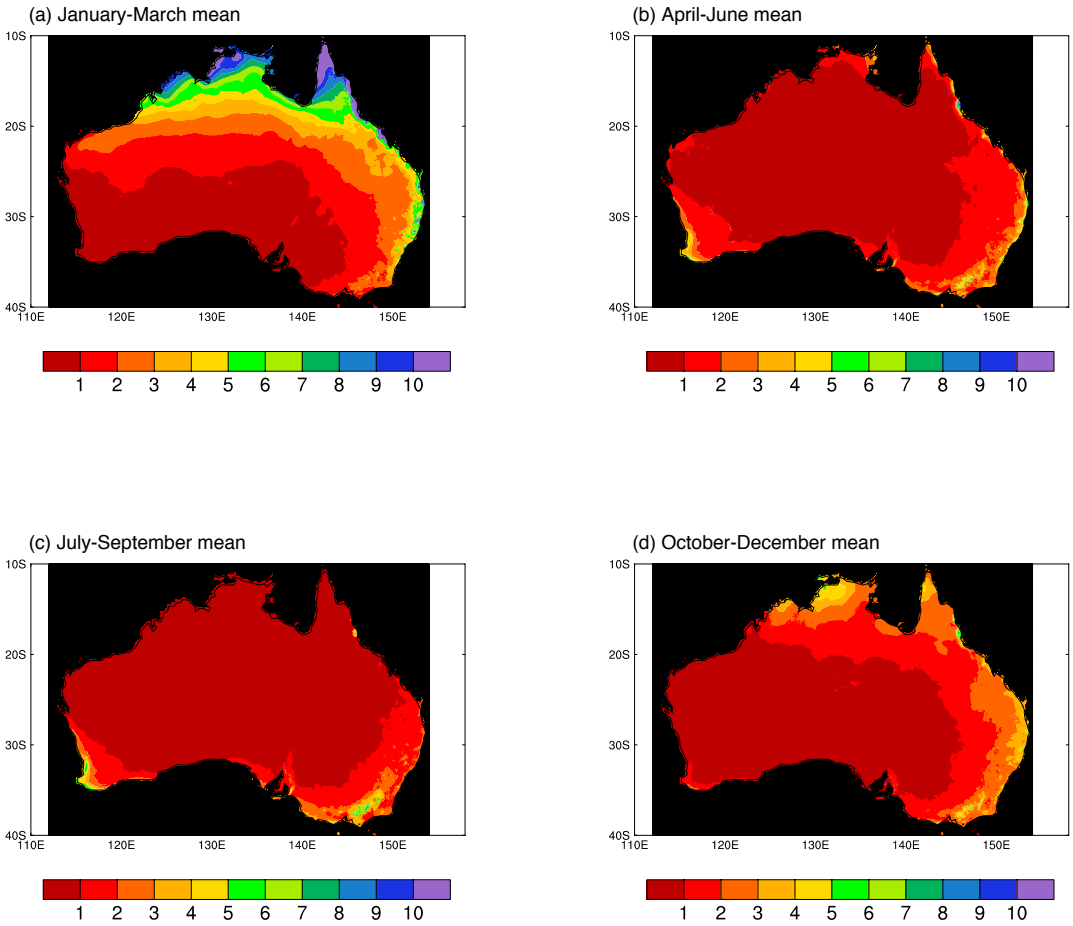

Figure 5.13: *Present day climatological (1949-200) rainfall based on 1/20° resolution dataset of the Queensland Department of Natural Resources and Mines. Rainfall measured in mm per day. Clockwise from top left: summer, autumn, spring and winter.*

Consider now the impact of chaos on the rainfall variability in these simulations. Figure 5.18 illustrates time series of rainfall for a large region of Queensland (27°S to 18°S, 140°E to 150°E) for the five members and ensemble mean of the second ensemble (1871 to 2000). The period 1980 to 2000 only is shown in the figure in order to clearly depict the individual variations. In a number of years (1989, 1993 and 1999) there are distinct outliers associated with individual members of the ensemble. Given the high temporal frequency of typical rainfall variability and the complex physical processes associated with rainfall, such intra-ensemble variability can be readily understood. Generally, years of particularly high or low rainfall in Figure 5.18 have substantial agreement amongst the various ensemble members, suggesting that such situations are associated with effective forcing by the observed SST distributions and that under these circumstances chaotic influences are reduced.

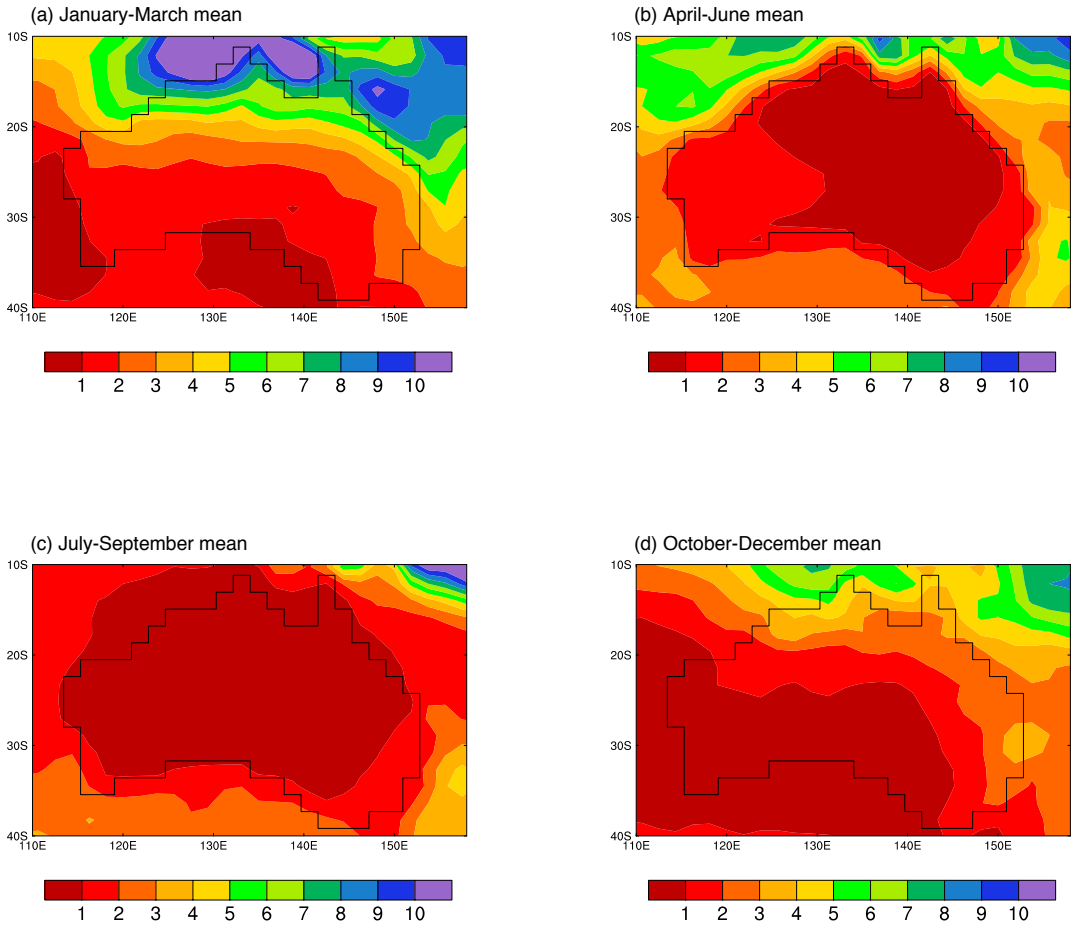

***Figure 5.14**: As for Figure 5.13 but as simulated by the CSIRO Mark 3 atmosphere-only model forced by observed SSTs 1949 to 2000. The climatologies are based on the average of the five member ensemble.*

Comparison of the ensemble means for the common time period of the two ensembles (1949 to 2000) revealed similar temporal variability and amplitudes in most years. Nevertheless, as can be seen in Figure 5.18 an ensemble of five simulations is unlikely to capture the full range of chaotic outcomes. It has been found in various evaluations that ensembles of fifty or more are desirable.

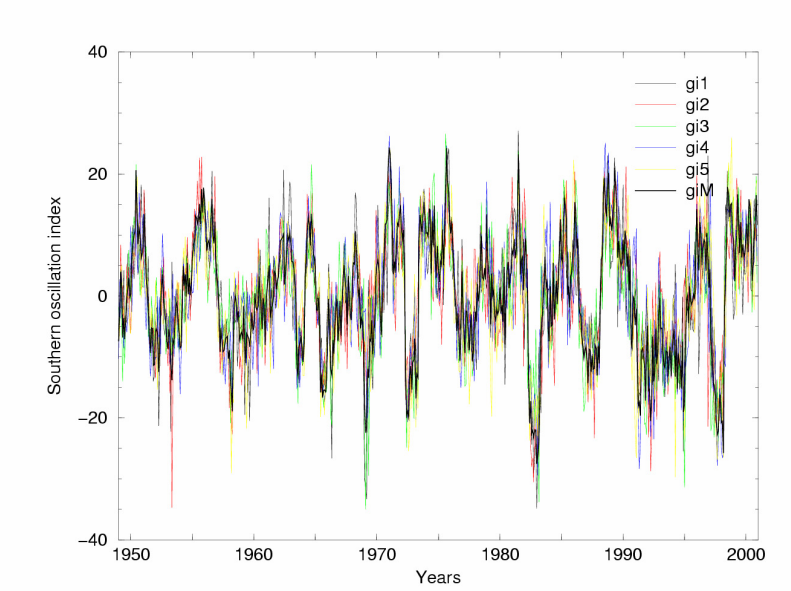

***Figure 5.15**: The Southern Oscillation Index as simulated by the CSIRO Mark 3 atmosphere-only model forced by observed SSTs 1949 to 2000. The results for each ensemble member (g1-g5)are shown together with the ensemble mean result (gM).*

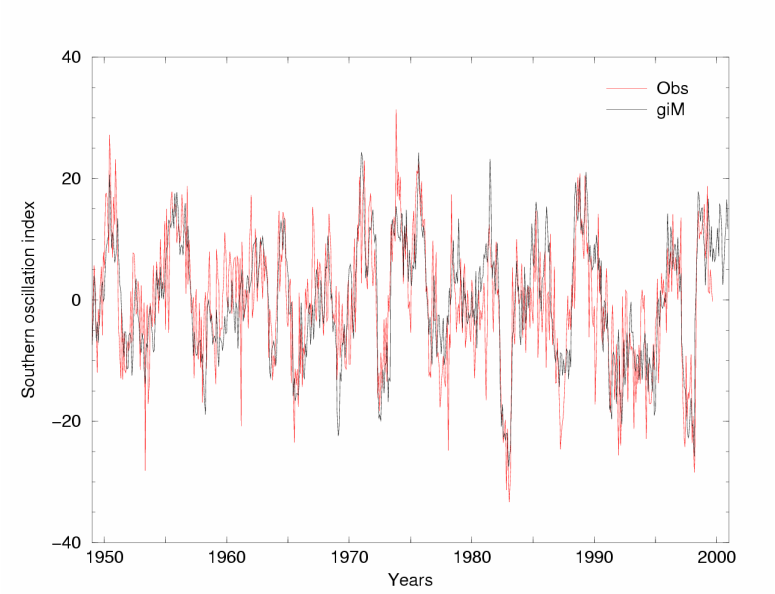

***Figure 5.16**: Comparison of the ensemble mean from Figure 5.15 with the observed SOI for 1949 to 2000.*

For this reason, in Figure 5.19 the average of the two ensembles has been used in the comparison with observed rainfall for the selected Queensland region. The outcome in Figure 5.19 is rather disappointing in that at first inspection the ensemble simulations poorly represent the observed rainfall. This result implies that even when 'correct', i.e. observed SSTs, are used to force the Mark 3 mode it is unable to

reproduce systematically the temporal variability of observed rainfall. This would suggest poor prospects for multi-seasonal predictions with the model.

However, such an assessment would appear to be premature. Other simulations conducted at CSIRO Atmospheric Research, not associated with this Queensland contract, have shown that when global climatic model outputs are used to drive much finer scale regional models then far better agreement with observation is obtained. Thus the discrepancy between the two time series in Figure 5.19 can possibly be resolved by additional simulations using regional models.

The role of chaos versus model deficiencies in accounting for the outcomes in Figure 5.19 is difficult to clarify without a more elaborate series of experiments. It is encouraging to note that on a number of occasions in the late 1950s, middle 1970s and late 1990s the agreement between the amplitudes of the two time series in Figure 5.19 is rather satisfactory. Examination of the corresponding time series for the individual ensemble members shows chaotic variability typical of that given in Figure 5.18, suggesting that the good agreement be obtained despite chaotic influences. The remaining possibility is that the peculiarities of the observed SST distributions for these sequences of years were particularly well captured, resulting in a very appropriate forcing system at these times. Such an outcome could possibly be verified by comparison with other models, which also participated in this scientific study.

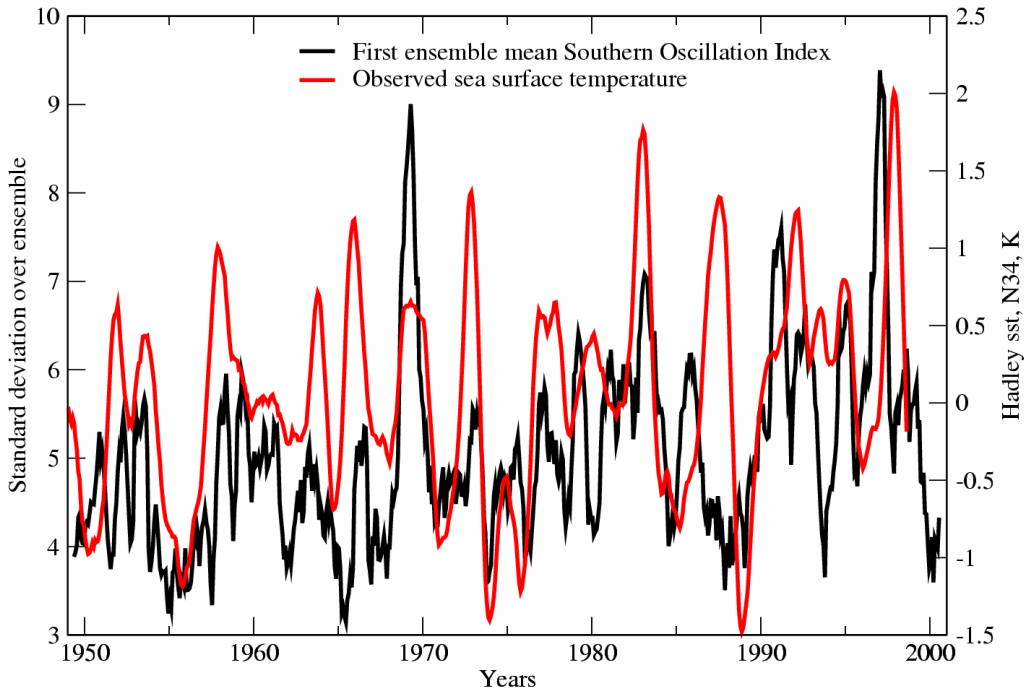

***Figure 5.17**: Standard deviation of the SOI from the 5-member ensemble (black curve) compared with the observed SST anomalies for the NINO3.4 region (red curve).*

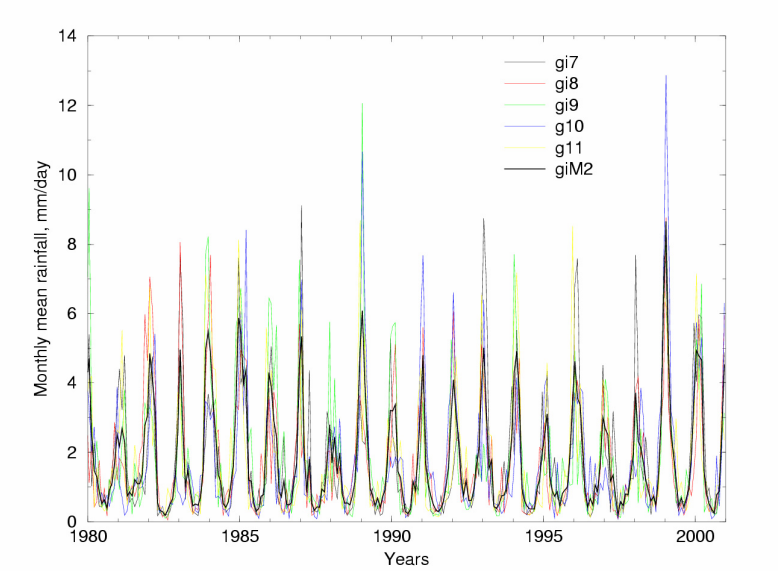

***Figure 5.18**: Time series of monthly rainfall for a large region of Queensland as simulated by the Mark 3 atmosphere-only model (1980-2000). The result from each ensemble member (g7 to g11) is shown together with the ensemble mean result (gM2).*

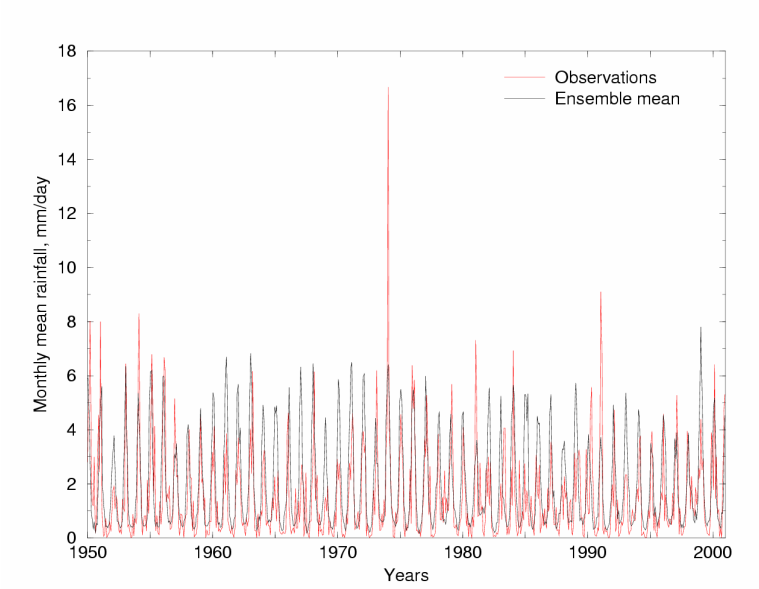

***Figure 5.19**: Time series of monthly rainfall for a large region of Queensland as simulated by the Mark 3 atmosphere-only model (1950-2000). Here the ensemble mean result (green curve) is based on 10 members (g1 to g5 and g7 to g11).Observed monthly rainfall shown as a red curve.*

Two separate case studies were explored: January 1974, which was extremely wet in Queensland, see Figure 5.19, and January 1995, which was dry, see Figure 5.19 also Figure 5.18.

In the case of 1974 there was almost a factor-of-two difference in variability between the January rainfalls for the individual simulations of the second ensemble. For this situation the wettest outlier, identified as the g11 simulation was selected for comparison with observation, Figure 5.20. This provided an indication of the capability of the model to reproduce this very extreme event, see Figure 5.19, even though it was not representative of the ensemble mean. As shown in Figure 5.20 very high rainfall occurred in northern Queensland in January 1974, with low rainfall in southern and especially Western Australia. The model reproduced this basic pattern to the extent of capturing the separate high rainfall areas in Queensland and northwest Australia. The simulated rainfall was much lower than observed over Queensland, but a high intensity region was located off the coast. With a regional model a better outcome over Queensland would be expected.

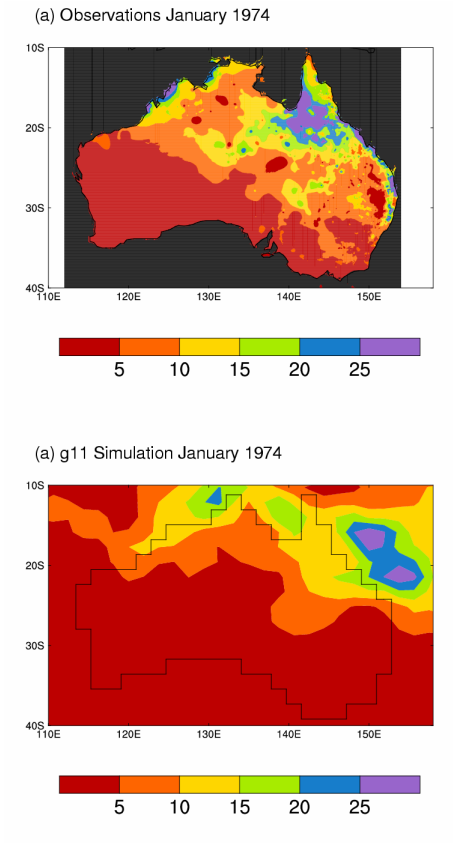

Figure 5.20: *Rainfall for January 1974 as observed (top panel) and as simulated from by an ensemble member (g11) (bottom panel).*

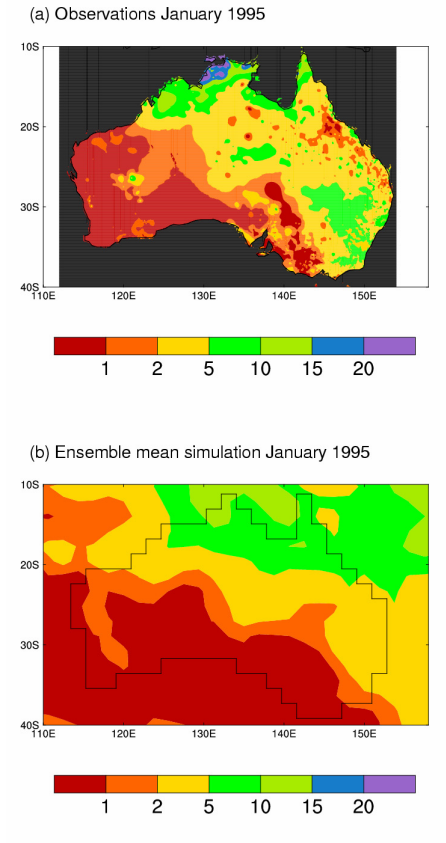

Figure 5.21: Rainfall for January 1995 as observed (top panel) and from a 10-member ensemble (bottom panel)..

The fact that at least one, and probably two, as indicated by an examination of the individual ensemble members, was capable of reproducing the basic characteristics of an extreme rainfall event is considered to be encouraging. Although the g11 simulation was the major outlier of the second ensemble as regards this event, the observed rainfall also represents an outlier, see Figure 5.19. This situation raises a fundamental issue as regards chaos; that is, how can it be determined when an outlier is the most representative of the simulated outcomes? Fortunately, Figure 5.19 suggests that observed outlier situations do not arise very frequently.

January 1995 was a relatively dry year for much of Queensland, a situation reproduced by the ensemble mean as shown in Figure 5.19, and the individual ensemble members in Figure 5.18. The ensemble mean rainfall situation over Australia is compared with observation in Figure 5.21. Again the countrywide rainfall gradient was well simulated. The highest rainfall totals were rather too widely simulated across northern Australia, but this is partially attributed to the relatively large size of the model gridboxes preventing the sharp observed gradients from being captured. Overall the outcome was commendable. Thus, these two specific case studies illustrate that extreme wet and dry conditions can be simulated by the Mark 3 model.

If the simulations for other years can also be improved by combining the present results with a regional model, then expectations for predictions of Queensland rainfall will be encouraging.

For the selected Queensland region (27°S to 18°S, 140°N to 150°E) for the fifty year period 1950 to 1999 the rainfall rate was sampled across all ten ensemble members on a quarterly basis to determine the most likely rainfall categories. The percentage outcomes for the 500 samples are shown in Figure 5.22, together with observations for the same period. For the latter, of course, there is only one sample!

While the simulation reproduces the seasonal variability quite well, the overall comparison with observation is only classified as fair. The model overestimates the rainfall for the highest category in December, January and February, and for the middle categories in March, April and May and also September, October and November. Part of this discrepancy may be attributable to the coarseness of the monthly data, which are summed to produce the quarterly values shown in Figure 5.22. A breakdown into finer time slices would discriminate between the various rainfall categories.

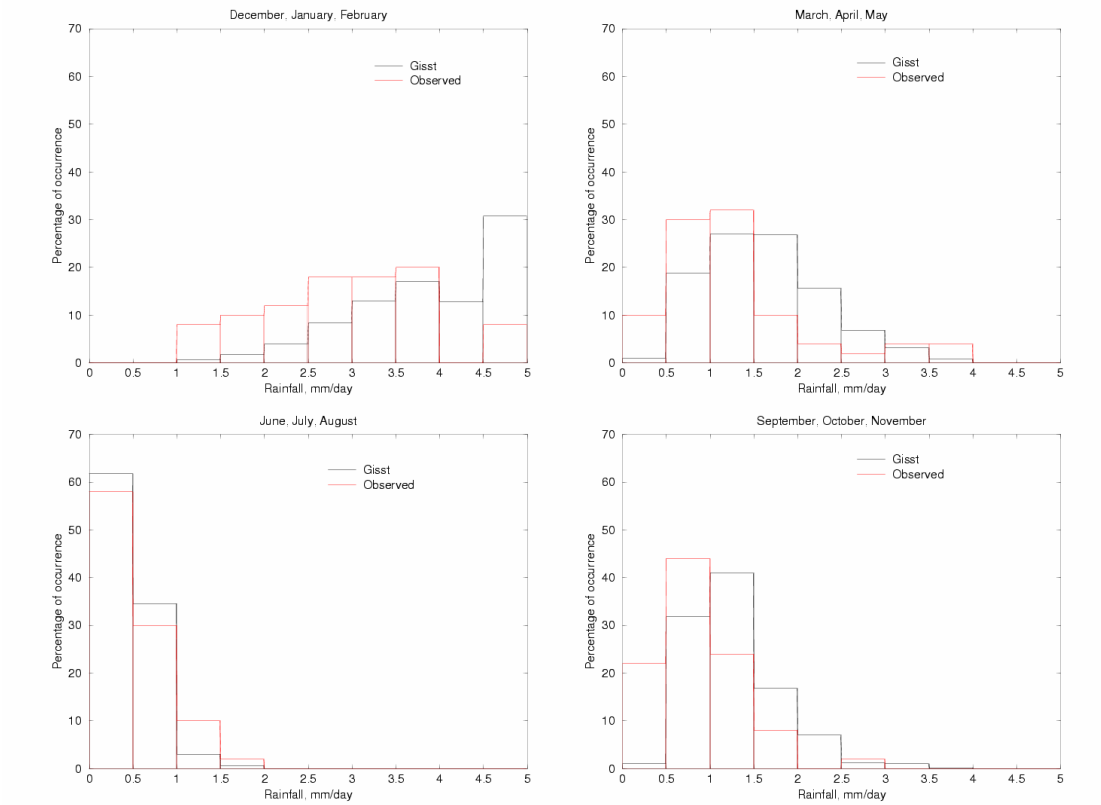

***Figure 5.22**: Comparison between frequency distribution of observed and simulated (calculated using the results of all 10 ensemble members) rainfall rates for the Queensland region. Clockwise from top left: summer, autumn, spring and winter. The rainfall rates are based on monthly totals.*

6 Future work

Over the past five years, with the support of the Queensland Government, CSIRO has continued to develop climate models, which are suitable for conducting Queensland-focused climate research and impact studies. The development proceeds in two fronts. First, a state-of-the art global climate model that examines the large scale circulation and its response to greenhouse warming. Second, a sophisticated regional model that uses the outputs of the global climate model to obtain circulation conditions and climate response on finer scales suitable for regional impact studies. Significant progress has been made in both fronts. Although continued improvements are still needed, for example, on the cold tongue bias, considerable progress has been made during the first year of this consultancy. A significant achievement is that we are now much more confident that rainfall over Queensland as whole will decrease under greenhouse conditions, as supported by the majority of other global climate models.

This achievement represents both opportunities and challenges. It is an opportunity because we can now start to assess its likely impacts. The challenge is to quantify the extent of the reduction on regional scales. This is where regional model comes to play. There is also the need of ensemble strategy so as to suppress chaotic influence, which represents as an element of uncertainty in the assessment. We expect significant ongoing progress in the course of this work agreement.

The progress will enable us to address crucial issues already identified in the work agreement. These include the effects of climate change on tropical cyclones, the impacts of climate change on water resources, energy use, and air quality, and the effect of a greenhouse-induced reduction of soil moisture on agriculture practice, among others. Although these assessments will always contain certain element of uncertainty, the improvement in our model capacity, in particular, the capacity of concerted employment of both the global and the regional models, will certainly lower the level of the uncertainty, and increase the value of these assessments.

7 References

Cai, W. J., Hendon, H. H. and Meyers, G. (2003): An Indian Ocean Dipole in the CSIRO coupled climate model. *J. Climate, to appear.*

Cai, W. J., Whetton, P. H., and Karoly, D. J. (2003): The response of the Antarctic Oscillation to increasing and stabilized atmospheric CO_2. *J. Climate,* **10,** 1525-1538.

Cai, W. J., and Whetton, P. H. (2000): Evidence for a time-varying pattern of greenhouse warming in the Pacific Ocean. *Geophysical Research Letters,* **27**: 2577-2580

Cai, W. J., and Whetton, P. H. (2001). A time-varying greenhouse warming pattern and the tropical-extratropical circulation linkage in the Pacific Ocean. *J. Climate,* **14,** 3337-3355.

Cai, W., Crimp, S. Hennessey, K., and Jones, R. (2003): *Climate change in Queensland under enhanced greenhouse conditions, Stakeholder workshop report*. CSIRO Atmospheric Research, 19 pp.

CSIRO 2001: *Climate change scenarios for the Australian Region*. Climate Impact Group, CSIRO Atmospheric Research, Melbourne, 8pp.

Deser, C., Alexander, M. A., and Timlin, M. S. (1996): Upper ocean thermal variations in the North Pacific during 1970-91. *J. Climate*, **9**, 40-1855.

IPCC 2001. *Climate Change 2001 – The Scientific Basis.* Cambridge University Press, 881 pp.

Gu, D. and Philander S. G. H. (1997): Inter-decadal fluctuations that depend on exchanges between the tropics and the extratropics. *Science*, **275**, 805-807.

Nicholls, N. (2003): The changing nature of Australian droughts. *Climatic Change,* submitted.

Parker, D., Jackson, M. and Horton, E. 1995. *The GISST2.2 sea surface temperature and sea-ice climatology.* Clim. Res. Tech. Notes CRTN63, UK Meteorological Office, Bracknell, Berk.,UK, 35 pp.

Power, S., Casey, T., Folland, C., Colman, A. and Mehta, V.(1999) Inter-decadal modulation of the impact of ENSO on Australia, *Clim. Dyn.*, **15**, 319–324.

Roderick, M. L., and Farquhar, G. D. (2002): The Cause of Decreased Pan Evaporation over the last 50 years, *Science,* **298**, 1410-1411.

Walsh K., Cai, W. J., Hennessy, K., Jones, R., McInnes, K., Nguyen, K., Page, C., and Whetton, P. (2002): *Climate change in Queensland under enhanced greenhouse conditions: Final Report, 1997-2002*. CSIRO Atmospheric Research, 89 pp.